

SCUOLA DI SCIENZE

Corso di Laurea Magistrale in Geologia e Territorio

Dipartimento di Scienze Biologiche, Geologiche ed Ambientali

Tesi di Laurea Magistrale

Mapping the bedrock  $K_2O$ , U and Th  
concentration in Italy – Towards the European  
Atlas of Natural Radiation

Candidato:  
Alessio Nogarotto

Relatore:  
Prof. Roberto Braga

Correlatore:  
Dott.ssa Giorgia Cinelli

# INDEX

1. ABSTRACT .....	1
2. INTRODUCTION .....	2
3. MATERIALS AND METHODS .....	6
3.1 Software and statistical analysis .....	7
3.2 Geological units identification.....	9
3.3 Data research and selection.....	17
4. DATA ANALYSIS .....	20
4.1 Igneous units .....	20
4.1.1 PI – Paleozoic intrusive rocks .....	20
4.1.2 PV – Paleozoic volcanic rocks.....	22
4.1.3 MVI – Mesozoic volcanic and intrusive rocks.....	23
4.1.4 PNI – Paleogene-Neogene intrusive rocks .....	25
4.1.5 PNV – Paleogene-Neogene volcanic rocks .....	26
4.1.6 LTP – Lazio-Tuscany magmatic province .....	28
4.1.7 SAP – Sardinian magmatic province.....	30
4.1.8 CAP – Campanian magmatic province .....	32
4.1.9 SSD – Sicilian strait magmatic district .....	33
4.1.10 AEP – Aeolian magmatic province.....	35
4.1.11 MVP – Mount Vulture magmatic province .....	37
4.1.12 SIP – Sicilian magmatic province .....	39
4.2 Metamorphic and ultramafic units .....	41
4.2.1 PM – Paleozoic metamorphic rocks .....	41
4.2.2 UM – Ultramafic rocks.....	42
4.2.3 TM – Tertiary metamorphic rocks.....	43
4.3 Sedimentary units .....	45
4.3.1 COS – Cambrian-Ordovician-Silurian sedimentary rocks .....	45
4.3.2 DCPS – Devonian-Carboniferous-Permian sedimentary rocks.....	46
4.3.3 TS – Triassic sedimentary rocks.....	47
4.3.4 MC – Mesozoic carbonate rocks .....	48
4.3.5 CdB – “Complessi di base” .....	49
4.3.6 LCPS – Late Cretaceous-Paleogene sedimentary rocks.....	50
4.3.7 EOMS – Eocene-Oligocene-Miocene sedimentary rocks .....	52
4.3.8 ME – Messinian sedimentary rocks.....	53
4.3.9 PLS – Pliocene sedimentary rocks .....	54

4.3.10 Q – Quaternary deposits .....	56
5. DISCUSSION .....	57
5.1 Validation of the GU methodology .....	57
5.2 Results and maps discussion .....	62
6. CONCLUSIONS .....	68
7. BIBLIOGRAPHY.....	70
8. APPENDIX .....	74
8.1 Appendix A – The dose .....	74
8.2 Appendix B – Sardinian samples .....	75
8.3 Appendix C – Statistical graphs .....	76

# 1. ABSTRACT

The Joint Research Center, the European Commission's science and knowledge service, started the European Atlas of Natural Radiation project with the objective of gathering all the data related to natural radioactivity from the European countries. The estimate of the terrestrial natural radioactivity is one of the priority of the project and it includes the realisation of concentration maps of the radioactive elements naturally occurring in the environment, that are the elements of the U and Th families together with  $^{40}\text{K}$ .

The aim of this work is to study the methodology to develop the first complete  $\text{K}_2\text{O}$ , U and Th concentration maps of the bedrock in Italy through the creation of geological units identified on a pre-compiled basis and the collection of geochemical data from scientific literature.

The geological units were determined based on litho-, chrono- and tectono-stratigraphic features of the bedrock. The dataset was created using global open-access database and peer-reviewed articles; the data, more than 15000 in total, was checked for outliers and representativeness and then studied with statistical analysis, in order to evaluate the methodology and to assign an average  $\text{K}_2\text{O}$ , U and Th concentration to the geological units. The results confirm that the methodology is reliable and allows to create  $\text{K}_2\text{O}$ , U and Th concentration maps at 1:1M scale. The main sources of errors come from the high lithological variability of the units, which implies a high variability in the distribution of the concentration values, and from the heterogeneity of the data coverage. Focusing on these problems, it's still possible to improve the methodology, especially by increasing the amount of available geochemical data and, subsequently, by realising more accurate maps on a smaller scale.

## 2. INTRODUCTION

Background ionizing radiation is always present, due to both natural and artificial sources. Natural radioactivity has two main influxes: a cosmic contribution, made by cosmic rays that release secondary radiation when they interact with Earth atmosphere, and a terrestrial contribution, made by the radioactive decay of radionuclides present inside the Earth since its formation.

The man-made sources arise from peaceful (e.g. medical use, energy generation, and associated fuel cycle facilities, radioisotope production and waste management) and military purposes (nuclear tests and their fallout or radioactive release and nuclear explosions).

As can be noticed in *figure 1*, for most individuals the exposure due to natural sources exceeds that from all man-made sources combined. The world average effective dose received by human population is about 3 mSv per year, but large area is known to have values higher than 10 mSv per year (UNSCEAR, 2000; UNSCEAR 2008). See *appendix A* for more information on general concepts of the dose.

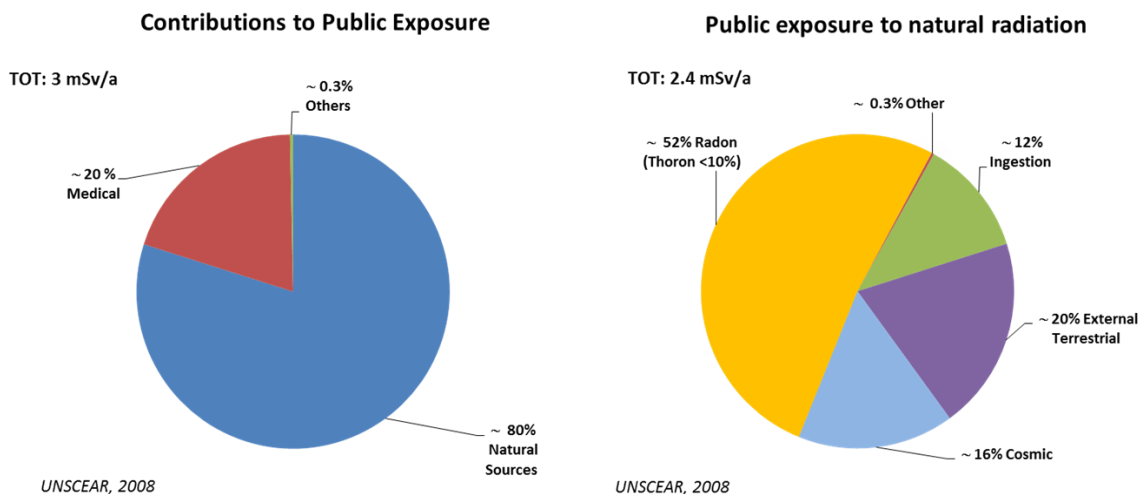


Figure 1: percentage of contributions to the public radiation exposure showing the strong predominance of natural over artificial radioactivity; division of the different natural sources.

Out of the total natural radioactivity, the cosmic contribution represents about 16% of the total exposure which people undergo and its value on a certain zone depends almost entirely on its elevation above sea level (Cinelli *et al.*, 2017); the remaining part is mainly due to terrestrial radionuclides.

The terrestrial contribution is mainly due to potassium (K) and the radioactive families of thorium (Th) and uranium (U), which are the most common natural radioactive elements on Earth and which make up the greatest part of the Naturally-Occurring Radioactive Materials (NORM). They can be found in different concentrations in the Earth's upper continental crust, with an average, expressed with a variability at one sigma level, of  $2.8 \pm 0.2$  wt% of  $K_2O$ ,  $2.7 \pm 0.6$  ppm of U and  $11 \pm 1$  ppm of Th (Rudnick and Gao, 2014). The local values of the three elements vary depending on the site-specific lithology,

geotectonics and geomorphology, which are the controlling factors for estimating natural radioactivity background (Cinelli *et al.*, 2015).

Potassium is the 8<sup>th</sup> most abundant chemical element in the Earth's crust and it's one of the main *rock-forming elements*. It's an essential component of common minerals like feldspars, micas and clay minerals, which can be easily found in different kind of rock.

K has only one radioactive isotope, <sup>40</sup>K, which is 0.01119% of the total potassium and has a half-life of 1.28 Gy (Cicchella *et al.*, 2014). It decays to <sup>40</sup>Ar or <sup>40</sup>Ca, respectively with and without gamma ray emission. Even though its low occurrence as part of the total potassium, it's an important radionuclide due to the high concentration of K in natural materials.

In this work, the K<sub>2</sub>O concentration was preferred to the K content, because the former is commonly used in geosciences. They are correlated by a simple factor:  $wt\%K_2O = 1.2048 \times wt\%K$ .

Uranium and thorium have very low concentration in all the rock-forming minerals. During igneous differentiation processes, both Th and U behave as incompatible lithophile elements and partition into the residual melt during fractional crystallisation. U is the essential constituent of rare ore minerals such as uraninite, while Th forms its own uncommon minerals like thorite, thorianite and huttonite and it is present at wt% level in monazite. Uranium and thorium are found at ppm concentrations in many accessory mineral, the most important being zircon, apatite, allanite and xenotime, found in igneous, metamorphic and siliciclastic sedimentary rocks.

Th and U have comparable geochemical behaviour due to their similarities in ion size and chemical bonding. However, fluid-rock interactions fractionate Th from U, with the latter more readily soluble in water than the former (Taylor and McLennan, 1985). Besides, they can both be found as adsorbed elements in clay rocks, with quite high concentrations.

On average, Th/U ratio goes from 3 to 5 and is quite constant in Earth upper crust, even though the differences in content ratio of different rocks helps to define their genetic conditions.

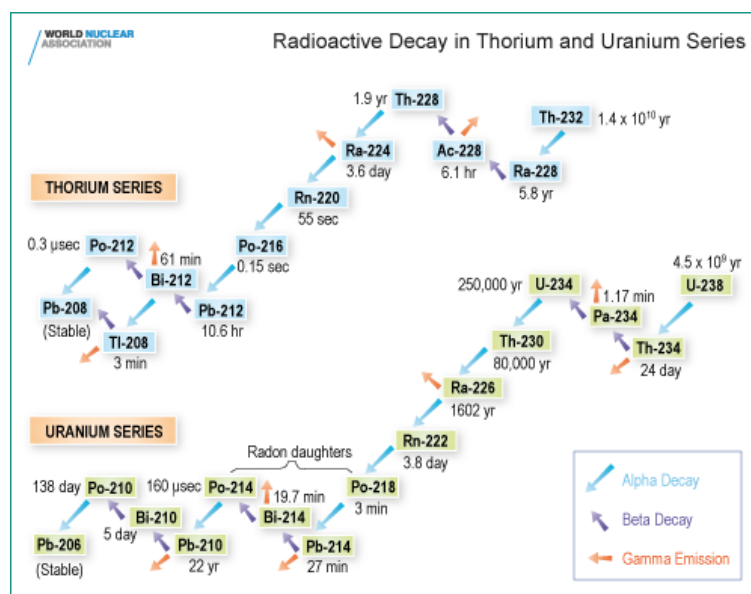


Figure 2: thorium-232 and uranium-238 decay chains.

U has three natural radioactive isotopes ( $^{238}\text{U}$ ,  $^{235}\text{U}$  and  $^{234}\text{U}$ , with the first two making the 99.995% of all uranium present on Earth) that have, respectively, a half-life of 4.5 Gy, 700 My and 269 ky; Th has only one natural isotope,  $^{232}\text{Th}$ , with a half-life of 14 Gy (Cicchella *et al.*, 2014).

The health hazards associated with Th and U are mostly related to some of their daughter radionuclides: radium-226, radium-228, radon-220 and radon-222 (*fig. 2*). Among these, radon is by far the most dangerous: it is a noble gas and therefore very mobile, so once it is created from the decay process, it can easily leave its source material and release in the surroundings; when inhaled, it is considered a carcinogenic substance due to the emission of alpha particles. With its low half-life (55 seconds for  $^{220}\text{Rn}$  and 3.8 days for  $^{222}\text{Rn}$ ) and not so low abundance, it contributes for more than 50% of worldwide total annual exposure to natural radiation per capita (*fig. 1*). Radon concentration in the environment depends on various factors, from bedrock geology to soil geochemistry, from geomorphology to local geotectonic history; only in the last few decades, thanks to the European directives (EC, 1996; EC, 1997; EC, 2013), the problem of natural radioactivity has become an important issue and a growing number of studies have begun to address it (e.g. Callegari *et al.*, 2013; Cinelli *et al.*, 2014).

Studying the natural radioactive background is therefore of primary importance; one of the tasks of the European Commission (EC) under the Euratom Treaty is to collect, validate and provide information about the levels of radioactivity in the environment of the EU Member States (De Cort *et al.*, 2011). So, the project of a European Atlas of Natural Radiation (EANR) came to life in 2006. The Atlas is a collection of maps of Europe displaying the levels of natural radioactivity caused by different sources, from cosmic radiation to terrestrial radionuclides (Cinelli *et al.*, 2018).

Through these maps, the public will be able to: familiarise itself with natural environmental radioactivity; be informed about the levels of natural radioactivity caused by the different sources; have a more balanced view of the annual dose received by the European population, to which natural radioactivity is the largest contributor; and make direct comparisons between doses from natural sources of ionizing radiation and those from man-made (artificial) ones, hence, to better assess the latter (Cinelli *et al.*, 2018).

This project followed the first EC works about collecting, validating and reporting common information about the levels of radioactivity in Europe, like the “Atlas of Caesium deposition on Europe after the Chernobyl accident” (De Cort *et al.*, 1998; De Cort *et al.*, 2011).

As a first task, a European Indoor Radon Map was tackled, since in most cases this is the most important contribution to exposure, and since it could be expected that data collection would take quite some time, because radon surveys have very differently grade of advancement among European countries.

Secondly, the Joint Research Centre (JRC) has undertaken to map a variable, which measures “what earth delivers” in terms of geogenic radon potential (RP), due to heterogeneity of data sources across Europe and the need to develop models for estimating a harmonized quantity that adequately measures or classifies the RP. The European Geogenic Radon Map (EGRM) will give the possibility to characterize areas for

radon risk where indoor radon measurements are not available. The multivariate classification approach to estimate the geogenic radon potential has been developed and proposed to the scientific community during the round-table discussions entitled “*The European Geogenic Radon Map and the European Atlas of Natural Radiation*”, held during the 12<sup>th</sup> International Workshop on the Geological Aspects of Radon Risk Mapping in September 2014 in Prague. In this context, multivariate estimation means to use information from several quantities that are physically related to radon (geochemical data and geological information such as U concentration in bedrock and in soil, terrestrial gamma dose, permeability, geology, etc.) to assess a radon quantity of interest. Some countries, which have several input quantities available, have already been testing this approach. Although work on the geogenic radon map has been under way for several years, it has proven more complicated than initially thought.

For this reason, in the project it has been decided to give priority to the development of those maps that should be part of the EANR but also be used as input parameter in the EGRM, such as the uranium map in soil and bedrock and the terrestrial gamma dose rate. The first version of the European Atlas of Natural Radiation is available in digital format through a web portal (<https://remon.jrc.ec.europa.eu/About/Atlas-of-Natural-Radiation>), in which all the maps are collected and displayed with the related information. However not all the maps are completed yet and the JRC team keeps working for completing and validating the ones in which only data from few countries are available.

The maps of the EANR have been developed using different input data: for some maps data are available at national level (e.g. indoor radon data); for others at European level (e.g. U, Th and K in soil using FOREGS (<http://weppi.gtk.fi/publ/foregsatlas/index.php>) and GEMAS databases (<http://gemas.geolba.ac.at/>)).

Indeed, it seems that there are not easily accessible databases of U, Th and K concentration in bedrock, at European or national level, for developing European maps. Because of this, to create these maps the use of data available in scientific literature has been considered.

In this contest the aim of the present work is to study the methodology to develop the maps of K<sub>2</sub>O, U and Th concentration in bedrock considering Italy as country study. The methodological approach used consists of the following activities:

- identify, starting from OneGeology-Europe data, geological units homogenous in K<sub>2</sub>O, U and Th content using lithostratigraphy, petrology and mineralogy knowledge;
- collect data of K<sub>2</sub>O, U and Th concentration in bedrock (i.e. all the consolidated material that lies under the soil or the loose superficial sediments) using scientific literature source;
- check the quality of the data and the geological units;
- assign K<sub>2</sub>O, U and Th concentration values in bedrock to each geological unit using the collected data;
- map K<sub>2</sub>O, U and Th concentration in bedrock.

### 3. MATERIALS AND METHODS

In order to produce the concentration maps of K<sub>2</sub>O, Th and U in bedrock in Italy we followed this approach:

- 1) Identification of the Geological Units (GU) starting from the available data from OneGeology-Europe. To reduce the number of GUs to a manageable size, we employed an expert judgement approach based on litho-, chrono- and tectono-stratigraphic knowledge. This step was supported by GIS-based tools;
- 2) Assignment of the K<sub>2</sub>O, U and Th data available in the earth science literature, as well as data retrieved from global geochemical/petrological databases (e.g EarthRef), to the GUs;
- 3) Testing the validity of the extrapolation of clustered geochemical data to an entire GU by descriptive statistics of the GUs coupled with ANOVA tests and box plots;
- 4) Creation of the K<sub>2</sub>O, U and Th concentration maps with GIS-based tools, using the statistical results.

The French Institute for Radiological Protection and Nuclear Safety (IRSN) has already used a similar methodology to realise a map of uranium concentration in bedrock in France (Ielsch *et al.*, 2017), implementing geochemical data from literature with specific geological knowledge, e.g. the contributions of the uranium mines and of the enrichment of some sedimentary units in rare elements. The results of the work were then used to study the geogenic radon potential and the environmental radioactivity. The database, though, was not available for the realisation of the French maps of K<sub>2</sub>O, U and Th concentration.

In our work we only considered the data from literature, without implementing them with geological or tectonic features.

### 3.1 Software and statistical analysis

The ESRI software ArcMap (version 10.1 build 3143) was used for the cartographic elaborations.

The StatSoft software STATISTICA version 8.0 and the Microsoft software Excel 2016 were used for the statistical analysis.

For each unit a series of parameters for the descriptive statistic was calculated, separately for  $K_2O$ , U and Th, with: number of samples, mean, median, minimum and maximum values, 25<sup>th</sup> and 75<sup>th</sup> percentiles, standard deviation, skewness and kurtosis.

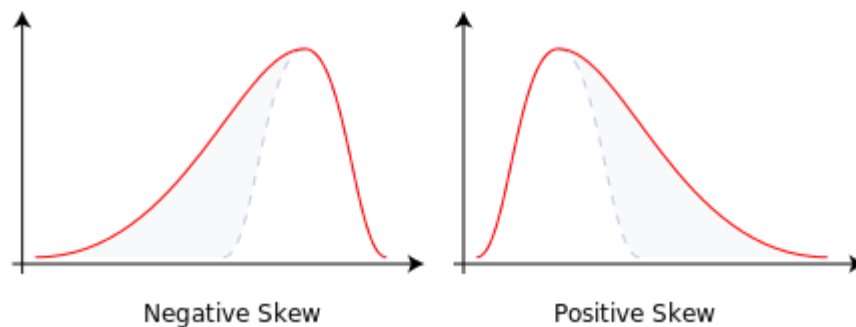


Figure 3: aspect of a distribution depending on the skewness value.

Skewness is a measure of the asymmetry of a distribution of a real variable; it is negative if the distribution has the left tail longer than the right one and vice versa (*fig. 3*). A normal distribution has a skewness value equal to zero.

Kurtosis is a measure of how much a distribution of a real variable differs from a normal one in terms of the form of its tails: a positive kurtosis value indicates a fatter tails distribution, while a negative kurtosis indicates a thinner tails distribution. They are both referred to the normal distribution which has a kurtosis value equal to zero.

In addition to the descriptive statistic, for each GU the dataset of  $K_2O$ , U and Th was examined with the histograms of the distributions, the normal probability plots and the Shapiro-Wilk test, in order to define the characteristics of the data populations and to verify their distribution (e.g. if normal or log-normal).

Together with the histograms, the normal probability plots and the Shapiro-Wilk test were used to analyse the distributions. They have been performed both with the data and with their natural logarithm; the test gives a p-value that indicates the statistical significance with which you can state if the distribution is normal (or log-normal).

The one-way ANOVA test (Analysis of Variance) was used to evaluate the percentage of variation explained by:

- the analytical methods used to estimate  $K_2O$ , U and Th contents;
- the geological units;
- the lithologies.

This test assumes that, when studying a number of groups, there are two kind of variance: one inside the groups and one between them; so you can analyse if these groups are homogeneous between them (so the major variance is within the groups) or in their inside (so the major variance is between the groups). The test also generates a measure of the

effect size, the partial eta-squared value, i.e. an indicator of the percentage of variation of the samples due to the variance between the groups studied.

### 3.2 Geological units identification

For the realisation of the geological map, we used the 1:1M geological cartography available on the OneGeology site (<http://portal.onegeology.org/OnegeologyGlobal/>) as a *shapefile*. This file contains 8909 polygons characterized by the name of the unit to which they belong and a brief description including geological ages and the lithologies present, which are further divided into a main lithology and several minor ones (*table 1*).

Table 1: example of the attribute table of the OneGeology-Europe shapefile.

CODE	ID	name	description		lowerAge	upperAge
IT033	32	GEO1MDB_32	Ophiolites: peridotites, gabbros, basalts, serpentinites and ophiolitic breccias with various grade metamorphism		Jurassic	Jurassic
IT034	33	GEO1MDB_33	Tectonic melanges, locally with low-grade metamorphism. Emplaced during Miocene		Miocene	Miocene
IT035	34	GEO1MDB_34	Limestones and marly limestones with chert, radiolarites, calcareous marls, marls and pelites, locally interbedded turbiditic calcarenites		Cretaceous	Tortonian (Pliocene)
CODE	urn_litho1	urn_litho2	urn_litho3	urn_litho4	urn_litho5	
IT033	Peridotite	Gabbro	Basalt	Serpentinite	missing	
IT034	Clastic sedimentary rock	missing	missing	missing	missing	
IT035	Limestone	Mudstone	Biogenic silica sedimentary rock	missing	missing	

Firstly, the polygons of the *shapefile* were grouped, depending on the name of their belonging unit, using the *dissolve* tool of ArcMap. Then, the original 104 units were reduced by expert judgment to 19 Geological Units, hereafter named GUs (*table 2*).

GUs were chosen based mainly on their litho-, chrono- and tectono-stratigraphic position and their average lithology. As a matter of fact, the aim of creating the GUs was to obtain groups of rocks with similar K<sub>2</sub>O, U and Th concentrations, in order to reduce the number of units to the lowest possible and to simplify the final map, trying to maintain a geological coherence.

For sedimentary and metamorphic rocks, the GUs remained those created in the first place. But igneous rocks required more attention, because of the great variety of Italian volcanic and plutonic rocks, reflected by the thousands of studies about them, especially on the Plio-Quaternary products. So, there were two main reasons to split some of the igneous GUs:

- a) The great lithological variability, even between the products of a single magmatic province (Peccerillo, 2005), implies that grouping igneous rocks from very different areas can lead to great miscalculations in the statistical analysis;

b) The great amount of data available from the scientific literature allows to characterize a lot more units, compared to the units considered for metamorphic and sedimentary rocks.

Table 2: the 19 GUs from the first division of the dataset.

GU	DESCRIPTION	AGE	PREDOMINANT LITHOLOGIES	SUBORDINATE LITHOLOGIES
CdB	"Complessi di Base"	Middle Jurassic - upper Oligocene	Limestone	Mudstone
COS	Cambrian-Ordovician-Silurian sedimentary rocks	Upper Precambrian - lower Carboniferous	Sandstone, conglomerate limestone, pelite	Quartzite, dolostone, mudstone, siltstone
DCPS	Devonian-Carboniferous-Permian sedimentary rocks	Lower Devonian - lower Triassic	Conglomerate, sandstone, limestone	Shale, dolostone
LCPS	Late Cretaceous-Paleogene sedimentary rocks	Middle Cretaceous - lower Miocene	Shale, limestone	Dolostone, mudstone, biogenic silica sedimentary rock
MC	Mesozoic carbonate rocks	Upper Permian - middle Cretaceous	Limestone, dolostone	Sandstone, evaporite
ME	Messinian sedimentary rocks	Upper Miocene (Messinian)	Limestone, sandstone	Mudstone
MVI	Mesozoic volcanic and intrusive rocks	Middle-upper Triassic	Basalt, gabbro, monzonite	Syenite, trachyandesite, diorite
EOMS	Eocene-Oligocene-Miocene sedimentary rocks	Upper Paleocene - upper Miocene	Limestone, sandstone, mudstone	Shale, conglomerate
PNV	Paleogene-Neogene volcanic rocks	Upper Paleocene (Cretaceous) - lower Pleistocene	Rhyolite, andesite	Basalt, trachyte
PNI	Paleogene-Neogene intrusive rocks	Middle Oligocene - lower Pliocene	Granite, tonalite	Granodiorite, quartz-monzonite, diorite, gabbro
PI	Paleozoic intrusive rocks	Carboniferous - Permian	Granite, granodiorite, tonalite, monzonite	Diorite, quartz-diorite, gabbro
PLS	Pliocene sedimentary rocks	Lower-upper Pliocene	Sandstone, mudstone	
PM	Paleozoic metamorphic rocks	Precambrian - Carboniferous (protolith); upper Carboniferous - Permian (metamorphism)	Gneiss, schist, phyllite	Migmatite, granulite, eclogite, amphibolite
PQV	Plio-Quaternary volcanic rocks	Upper Miocene - Holocene	Rhyolite, dacite, trachyte, basalt, andesite, tephrite	Latite, phonolite, foidite
PV	Paleozoic volcanic rocks	Carboniferous - Permian	Rhyolite, dacite	Andesite
Q	Quaternary deposits	Upper Pliocene - Holocene	Clastic sediment	Clay
TM	Tertiary metamorphic rocks	Mesozoic (protolith); Eocene (metamorphism)	Schist	Quartzite
TS	Triassic sedimentary rocks	Lower-middle Triassic	Mudstone	Sandstone, conglomerate
UM	Ultramafic rocks	Paleozoic - Mesozoic	Peridotite, serpentinite	Gabbro, pyroxenite

Initially, only one GU, named PQV, was created to represent the entirety of the Plio-Quaternary volcanic products. This unit was eventually split into 7 new GUs depending on

the geographical location and geotectonic setting: AEP, Aeolian Magmatic Province; CAP, Campanian Magmatic Province; LTP, Lazio-Tuscany Magmatic Province; MVP, Mount Vulture Magmatic Province; SAP, Sardinian Magmatic Province; SIP, Sicilian Magmatic Province; and SSD, Sicilian Strait Magmatic District.

In order to map these units, the PQV feature was separated into its individual 170 polygons using the *Explode Multipart Feature* editing tool of ArcMap; these polygons were then manually merged depending on what was their new corresponding GU.

However, the problem of the high lithological variability of igneous rocks was still present. To reduce this effect even more, some of the igneous units (AEP, SAP, SSD, PNV and PI) were split in two GUs (denoted by m, mafic, and f, felsic; *table 3*), based on the chemical composition of the rocks:

- the mafic term includes basic and intermediate rocks: basalt, trachybasalt, andesite, trachyandesite, latite and their intrusive equivalents, besides of all the halfway terms;
- the felsic term contains acid rocks such as dacite, trachyte, rhyolite and their intrusive equivalents, as well as silica-undersaturated rocks (e.g. tephrite, foidite, phonolite), besides of all the halfway terms.

Intermediate rocks were grouped with the mafic ones due to their geochemical affinity and to the fact that the SIP GU comprises only basaltic and andesitic rocks with very few lithological variations.

Silica-undersaturated rocks are common in central Italy and they have been subject to many geochemical studies and researches. The number of data regarding them often exceeds that of other types of rock. Taking into account their peculiar geochemistry, that includes a high content of alkali and trace elements, often comparable to that of granites (Rudnick and Gao, 2003), they were grouped with the felsic rocks. Only in the PNV unit the slightly silica-undersaturated rocks present (nephelinite and tephrite) were grouped within the mafic unit, because of their low K<sub>2</sub>O, U and Th content.

In order to divide those 5 GUs between felsic and mafic, the descriptions present on the OneGeology-Europe attribute table were used (*table 1*).

There are two reasons why only a few igneous GUs were split between mafic and felsic:

- MVP, SIP, MVI, PNI, PV: the rocks of these units are quite homogeneous and there is not a sharp distinction between two groups;
- CAP, LTP: even though in these two provinces there is evidence of both mafic and felsic products, and the collected data support this fact, the OneGeology-Europe cartography do not make a distinction between them; the only difference reported is made between felsic and silica-undersaturated rocks, that in this work have been grouped together. So, a map that consider felsic and mafic CAP and LTP wasn't possible to realise with OneGeology-Europe 1:1M cartography.

Eventually, 30 GUs were created, as it's possible to see in *table 3* and *figure 4, 5, 6*.

Table 3: complete list of the 30 GUs created for K<sub>2</sub>O, U and Th mapping. The fourth column indicates the percentage of the area covered by the unit without considering the extension of the Q unit, which contains all that we didn't define as bedrock.

GU	AREA (km <sup>2</sup> )	AREA (%)	AREA (% NO Q)	DESCRIPTION	PREDOMINANT LITHOLOGIES	SUBORDINATE LITHOLOGIES
AEPf	43.22	0.01	0.02	Aeolian magmatic province (felsic)	Dacite	Rhyolite, trachyte
AEPm	60.95	0.02	0.03	Aeolian magmatic province (mafic)	Basalt	Andesite
CAP	1800.07	0.60	0.86	Campanian magmatic province	Phonolite, trachyte, tephrite	Latite, rhyolite
CdB	6827.89	2.28	3.28	"Complessi di Base"	Limestone	Mudstone
COS	3495.55	1.17	1.68	Cambrian-Ordovician-Silurian sedimentary rocks	Sandstone, conglomerate, limestone, pelite	Quartzite, dolostone, mudstone, siltstone
DCPS	2632.12	0.88	1.26	Devonian-Carboniferous-Permian sedimentary rocks	Conglomerate, sandstone, limestone	Shale, dolostone
EOMS	59454.80	19.88	28.54	Eocene-Oligocene-Miocene sedimentary rocks	Limestone, sandstone, mudstone	Shale, conglomerate
LCPS	25385.40	8.49	12.19	Late Cretaceous-Paleogene sedimentary rocks	Shale, limestone	Dolostone, mudstone, biogenic silica sedimentary rock
LTP	5967.22	2.00	2.86	Lazio-Tuscany magmatic province	Trachyte, tephrite, phonolite	Rhyolite, trachyandesite, andesite, trachybasalt, leucitite
MC	33681.40	11.26	16.17	Mesozoic carbonate rocks	Limestone, dolostone	Sandstone, evaporite
ME	8601.73	2.88	4.13	Messinian sedimentary rocks	Limestone, sandstone	Mudstone
MVI	267.06	0.09	0.13	Mesozoic volcanic and intrusive rocks	Basalt, gabbro, monzonite	Syenite, trachyandesite, diorite
MVP	193.98	0.06	0.09	Mount Vulture magmatic province	Tephrite, phonolite	Foidite, melilitolite, carbonatite
Pif	8625.38	2.88	4.14	Paleozoic intrusive felsic rocks	Granite	Granodiorite, tonalite
PIm	1066.47	0.36	0.51	Paleozoic intrusive mafic rocks	Monzonite, diorite	Gabbro, quartz-diorite
PLS	13574.70	4.54	6.52	Pliocene sedimentary rocks	Sandstone, mudstone	Marl, limestone
PM	20609.10	6.89	9.89	Paleozoic metamorphic rocks	Gneiss, schist, phyllite	Migmatite, granulite, eclogite, amphibolite

<b>GU</b>	<b>AREA (km<sup>2</sup>)</b>	<b>AREA (%)</b>	<b>AREA (% NO Q)</b>	<b>DESCRIPTION</b>	<b>PREDOMINANT LITHOLOGIES</b>	<b>SUBORDINATE LITHOLOGIES</b>
<b>PNI</b>	929.59	0.31	0.45	Paleogene-Neogene intrusive rocks	Granite, tonalite	Granodiorite, quartz-monzonite, diorite, gabbro
<b>PNVf</b>	2027.43	0.68	0.97	Paleogene-Neogene volcanic felsic rocks	Rhyolite	Andesite, trachyte
<b>PNVm</b>	1562.48	0.52	0.75	Paleogene-Neogene volcanic mafic rocks	Andesite, basalt	Basanite, trachyandesite, trachybasalt
<b>PV</b>	2175.45	0.73	1.04	Paleozoic volcanic rocks	Rhyolite, dacite	Andesite
<b>Q</b>	90689.50	30.33		Quaternary deposits		
<b>SAPf</b>	85.44	0.03	0.04	Sardinian magmatic province (felsic)	Rhyolite, dacite	Trachyte, phonolite
<b>SAPm</b>	1548.19	0.52	0.74	Sardinian magmatic province (mafic)	Basalt, andesite	Trachyandesite
<b>SIP</b>	1168.89	0.39	0.56	Sicilian magmatic province	Basalt, trachybasalt	Andesite, trachyandesite
<b>SSDf</b>	67.78	0.02	0.03	Sicilian Strait magmatic district (felsic)	Trachyte, rhyolite	Missing
<b>SSDm</b>	17.87	0.01	0.01	Sicilian Strait magmatic district (mafic)	Basalt	Andesite
<b>TM</b>	3087.89	1.03	1.48	Tertiary metamorphic rocks	Schist	Quartzite
<b>TS</b>	487.04	0.16	0.23	Triassic sedimentary rocks	Mudstone	Sandstone, conglomerate
<b>UM</b>	2861.06	0.96	1.37	Ultramafic rocks	Peridotite, serpentinite	Gabbro, pyroxenite

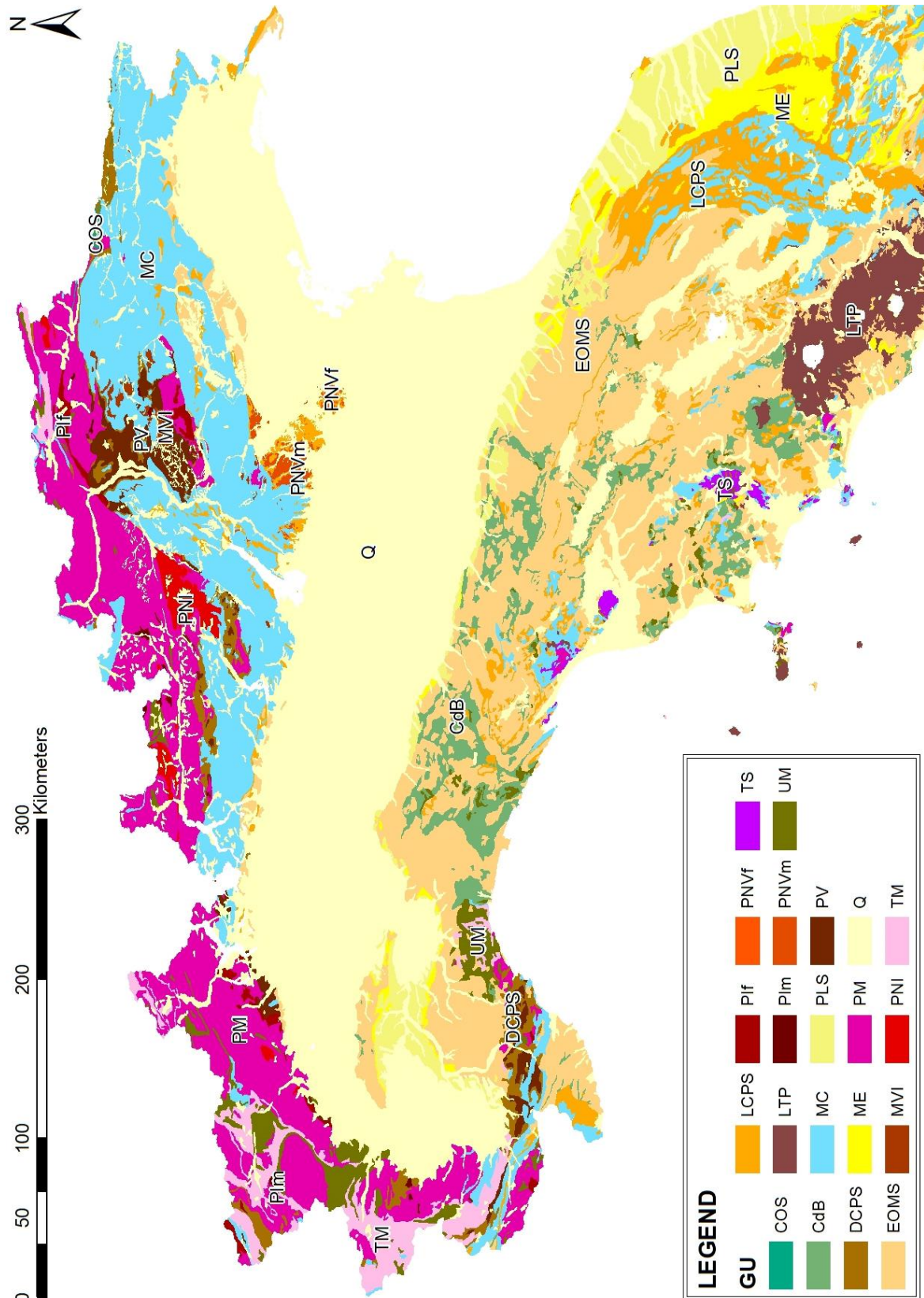


Figure 4: map of northern Italy showing the GUs division.

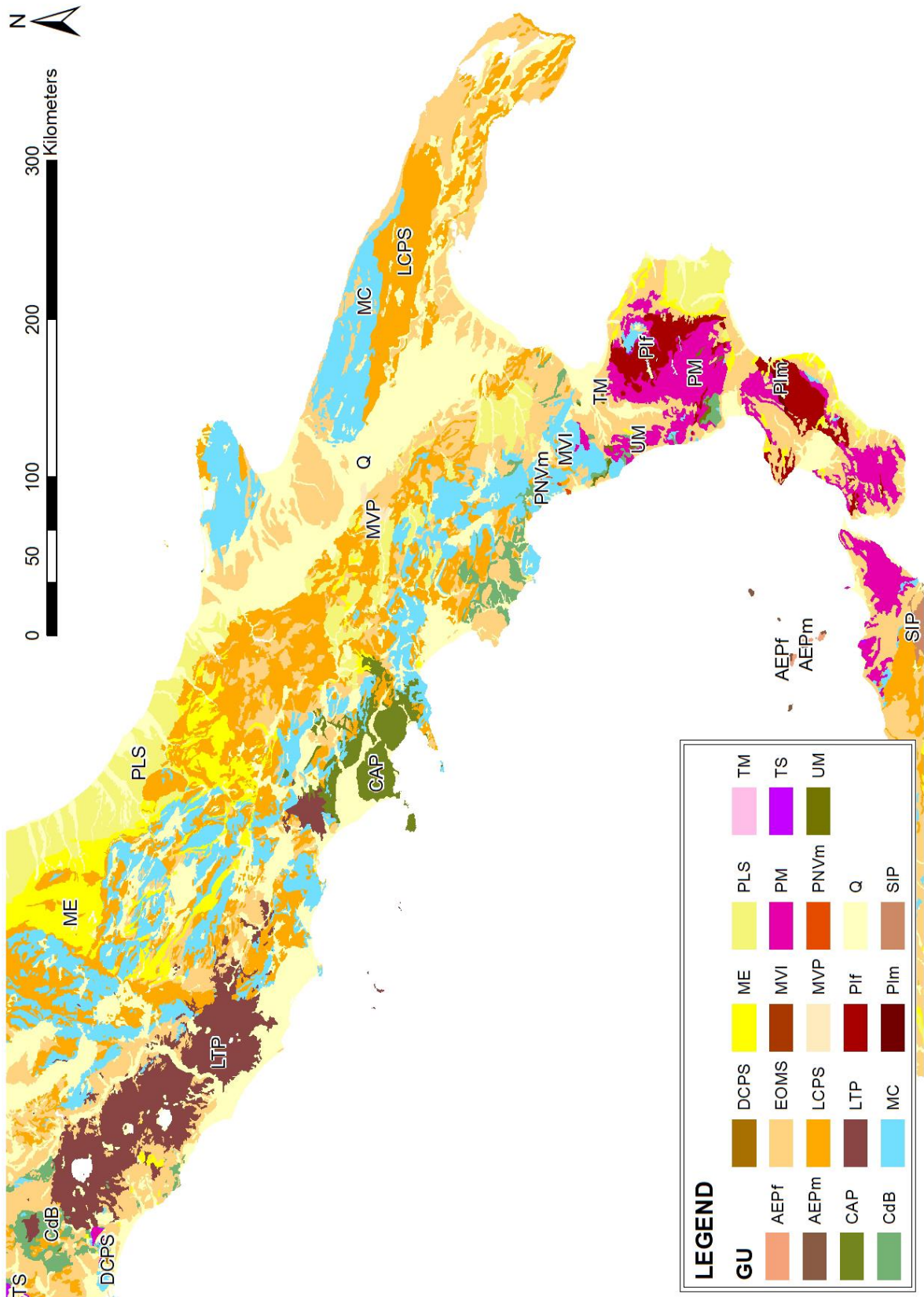


Figure 5: map of southern Italy showing the GUs division.

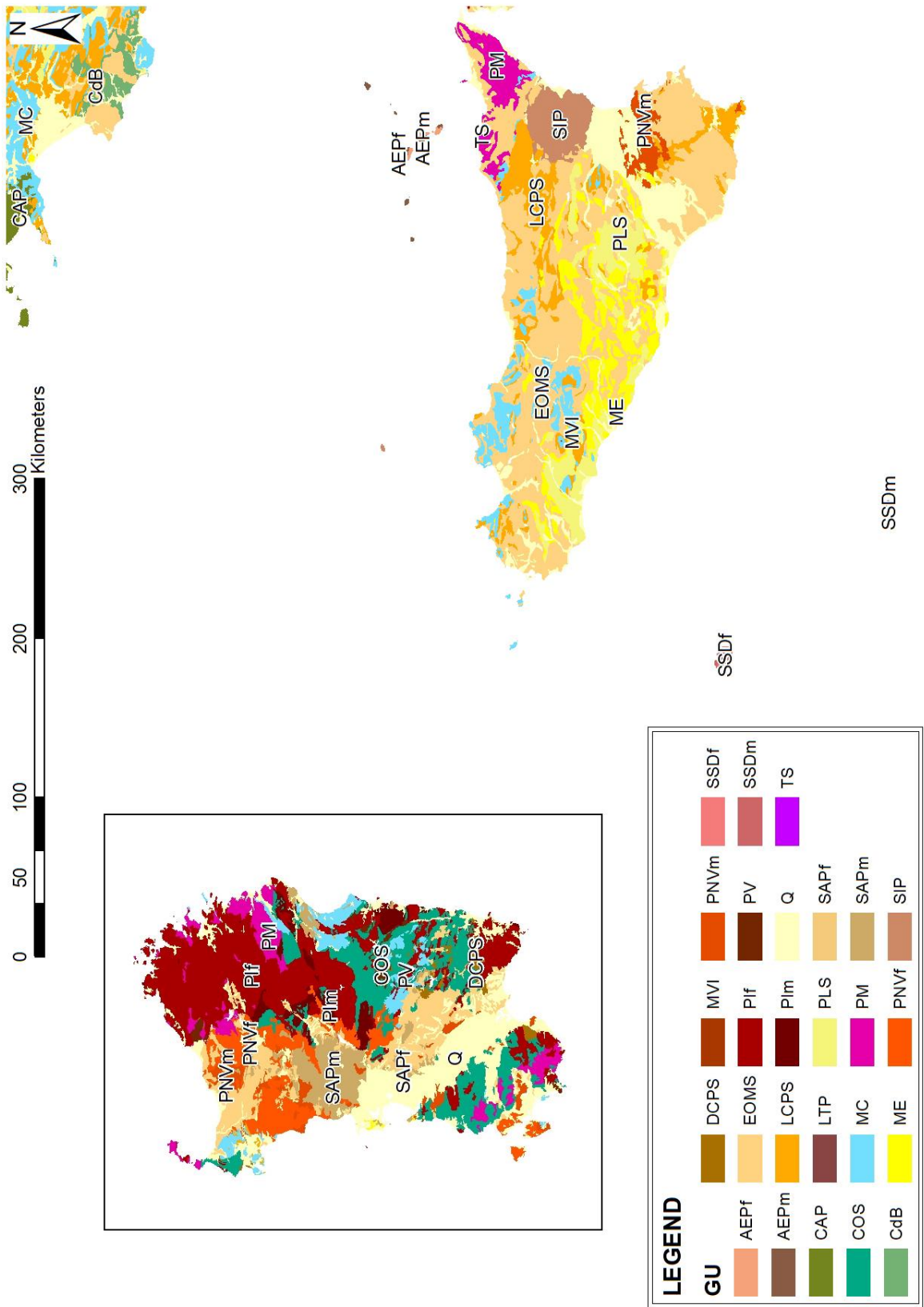


Figure 6: map of the Italian major islands, Sardinia and Sicily, showing the GUs division.

### 3.3 Data research and selection

The data used in this work derive directly from scientific literature and from the EarthChem portal database (<http://www.earthchem.org/portal>), part of the IEDA project, which grants the access to several geoscience databases.

In addition, three samples were collected in central Sardinia and analysed for the K<sub>2</sub>O, Th and U content at Actlabs, Ontario, Canada, with peroxide fusion ICP/ICPMS; this method, which is based on a strong digestion of the sample, was chosen in order to be sure that even the more resilient minerals, such as zircon and monazite (the main hosts of U and Th in common rocks), were destroyed (for more information see <http://www.actlabs.com>). A brief description of the three samples is available in *Appendix B*.

Following the principles of the EU directive INSPIRE (<http://inspire.ec.europa.eu/about-inspire/563>), which aims to create a common spatial data infrastructure for environmental policies and activities with the same standards and criteria in all European countries, these data will be available in the future together with the other datasets of the EANR.

IEDA, which stands for Interdisciplinary Earth Data Alliance, is a project funded by the US National Science Foundation in order to “*support, sustain, and advance the geosciences by providing data services for observational geoscience data from the Ocean, Earth, and Polar Sciences*”. The EarthChem portal gathers thousands of geochemical data from scientific publications, uploaded directly by the authors, in addition to all the analyses available in the greatest world databases, such as the USGS one. All data, besides from the pure geochemical analysis required, have several useful features:

- SAMPLE: the name with which the sample was recorded;
- SOURCE: the database from which the electronic datum derives;
- DOI, TITLE, JOURNAL and AUTHOR: the details of the article in which the datum was described;
- LATITUDE, LONGITUDE and LOC PREC: the geographical coordinates of the sample location with their analytical errors;
- MIN AGE, AGE and MAX AGE: respectively the younger, more probable and older geological age of the rock sample;
- METHOD: the analytical method used to study the sample;
- MATERIAL: the category which the rock sample belongs to (igneous, sedimentary or metamorphic);
- TYPE and COMPOSITION: only for igneous rocks, in order to separate volcanic from plutonic and felsic from mafic;
- ROCK NAME: the lithology of the rock sample.

All these features give the users the possibility to search the database by different constraints, depending on the requirement.

Geochemical data from the scientific literature were copied manually into an electronic table through Microsoft Excel, using the same output of EarthChem data, in order to make them comparable.

After the collection was completed, we performed a quality control of the data based on the following criteria:

- For the Plio-Quaternary volcanic units all data older than 1996 were discarded. For the other GUs, we rejected data older than 1990. Only a few older articles were taken into account for those units with very few data. This was needed in order to reduce uncertainties, since the old analytical techniques, especially for quantifying U and Th concentrations, were less efficient and precise than modern ones;
- Measurements accomplished by electron microprobe (EMP/EMPA) on single crystal were discarded, because of their lack of representativeness, as well as the analyses carried out on enclaves, xenoliths or veins;
- Data referred to soils or highly altered products were discarded too, since their concentrations were not representative of the bedrock;
- Measurements of K content were converted to K<sub>2</sub>O content;
- If no data on the analytical methods and the typology of the sample were available in EarthChem, we took down this information from the article, if publicly available.

After discarding the data that did not meet the above criteria, the accepted data were assigned to their units based on lithology, age, geographical position and geological formation of the samples described in the electronic table. If one or more of these features were not reported, or when the assignment was doubtful, the datum was rejected.

The outliers of each GU were eliminated thanks to a preliminary statistical analysis: all data with a concentration value lower than 1.5 times the interquartile range (IQR) below the 25<sup>th</sup> percentile or higher than 1.5 times the IQR above the 75<sup>th</sup> percentile were defined as outliers and then discarded.

Finally, a database of 15651 analyses, of which 6860 for K<sub>2</sub>O, 3718 for U and 5073 for Th was created (data are available as supplementary material by contacting the author). The distribution of these data among the different GUs is shown in *table 4*: as we can see, the percentage of data and area are uncorrelated.

*Table 4: list of the 29 GUs analysed in this work, with the number of data, the percentage of the total data and the percentage of the total area (without considering the area covered by quaternary deposits) for each unit.*

<b>GU</b>	<b>AEPf</b>	<b>AEPm</b>	<b>CAP</b>	<b>CdB</b>	<b>COS</b>	<b>DCPS</b>	<b>EOMS</b>	<b>LCPS</b>	<b>LTP</b>	<b>MC</b>
<b>N° DATA</b>	408	1370	3452	168	70	14	163	78	2174	69
<b>% DATA</b>	2.61	8.75	22.06	1.07	0.45	0.09	1.04	0.50	13.89	0.44
<b>% AREA</b>	0.02	0.03	0.86	3.28	1.68	1.26	28.54	12.19	2.89	16.17
<b>GU</b>	<b>ME</b>	<b>MVI</b>	<b>MVP</b>	<b>Pif</b>	<b>Plm</b>	<b>PLS</b>	<b>PM</b>	<b>PNI</b>	<b>PNVf</b>	<b>PNVm</b>
<b>N° DATA</b>	120	228	183	384	110	87	1964	325	189	922
<b>% DATA</b>	0.77	1.46	1.17	2.45	0.70	0.56	12.55	2.08	1.21	5.89
<b>% AREA</b>	4.13	0.13	0.09	4.14	0.51	6.52	9.89	0.45	0.97	0.73
<b>GU</b>	<b>PV</b>	<b>SAPf</b>	<b>SAPm</b>	<b>SIP</b>	<b>SSDf</b>	<b>SSDm</b>	<b>TM</b>	<b>TS</b>	<b>UM</b>	
<b>N° DATA</b>	227	95	260	1816	236	114	167	18	240	
<b>% DATA</b>	1.45	0.61	1.66	11.60	1.51	0.73	1.07	0.12	1.53	
<b>% AREA</b>	1.04	0.04	0.74	0.56	0.03	0.01	1.48	0.23	1.37	

Using literature data for mapping has, of course, both pros and cons.

It's very convenient from an economic and quantitative point of view, because a great amount of data is already available, without the need of a sampling campaign. Furthermore, the ongoing growth of geosciences open-access databases in the last decades

is giving everyone the possibility to gather data by simply downloading an electronic table, which is extremely useful for comparing, grouping and analysing different data with ease.

Anyway, there are many problems intrinsic in this methodology:

- Firstly, the sampling is not homogeneous and the sample distribution is not proportional to the values for the area covered by each unit, as it is possible to see in *table 4*. This implies that units and lithologies coverage are not weighted for their extension; actually the GUs with more areal extension are often less represented in the database. This is due to the fact that the number of data for each GU depends on which rocks have been more often object of study and how many of these studies have been published and made available for public use. And so, of course, the number of data does not reflect the unit extents;
- Secondly, geoscientists often dedicate their studies to small-scale features visible in small to meso-scale (from meters to tens of meters) outcrops, rather than to the characterisation of entire units at the km-scale. This means that geochemical studies don't always represent the mean composition of a unit, not even at a large scale;
- Thirdly, geochemical data, especially U and Th, are not routinely acquired from important rock types such as sedimentary rocks;
- Lastly, there is no active control on the real data truthfulness, contrary to what would happen with a planned sampling campaign.

## 4. DATA ANALYSIS

### 4.1 Igneous units

#### 4.1.1 PI – Paleozoic intrusive rocks

##### Description

The PI rocks are Hercynian plutons that form a substantial part of the Sardinian and Calabrian crystalline basement, besides appearing in the Alpine nappes, both in the Southern Alps of Trentino-Alto-Adige (e.g. Cima d'Asta pluton) and in the Alps s.s. (e.g. Graniti dei Laghi). This unit has been divided in two sub-units: mafic and felsic.

Age: Carboniferous – Permian.

Location of the main outcrops: eastern Sardinia; Calabria; central and western Alps.

Lithology/composition: gabbro, monzonite, tonalite, granodiorite, granite.

Genesis/emplacement: the rocks of this GU formed during the latest phase of the Hercynian orogeny. Sardinian and Calabrian intrusive rocks are undeformed or with minor deformation, while in the Alps there are evidences of deformation related to the Alpine orogeny, mostly in the Austroalpine (Matterhorn klippe) and Helvetic domain of the western part of the chain (Bosellini, 2005).

##### Statistical analysis (PIf)

Table 5: descriptive statistic of PIf unit. K<sub>2</sub>O values are expressed in wt%, U and Th values in ppm. N=number of samples. Std.Dev.=standard deviation.

	N	Mean	Median	Minimum	Maximum	25 <sup>th</sup> Percentile	75 <sup>th</sup> Percentile	Std.Dev.	Skewness	Kurtosis
K <sub>2</sub> O	166	3.6	3.6	1.5	6.1	2.9	4.4	1.0	0.0	-0.6
U	81	2.4	2.0	0.4	8.7	1.3	2.9	1.6	1.6	2.6
Th	137	11.7	12.0	1.3	25.0	9.0	15.2	5.9	0.0	-0.5

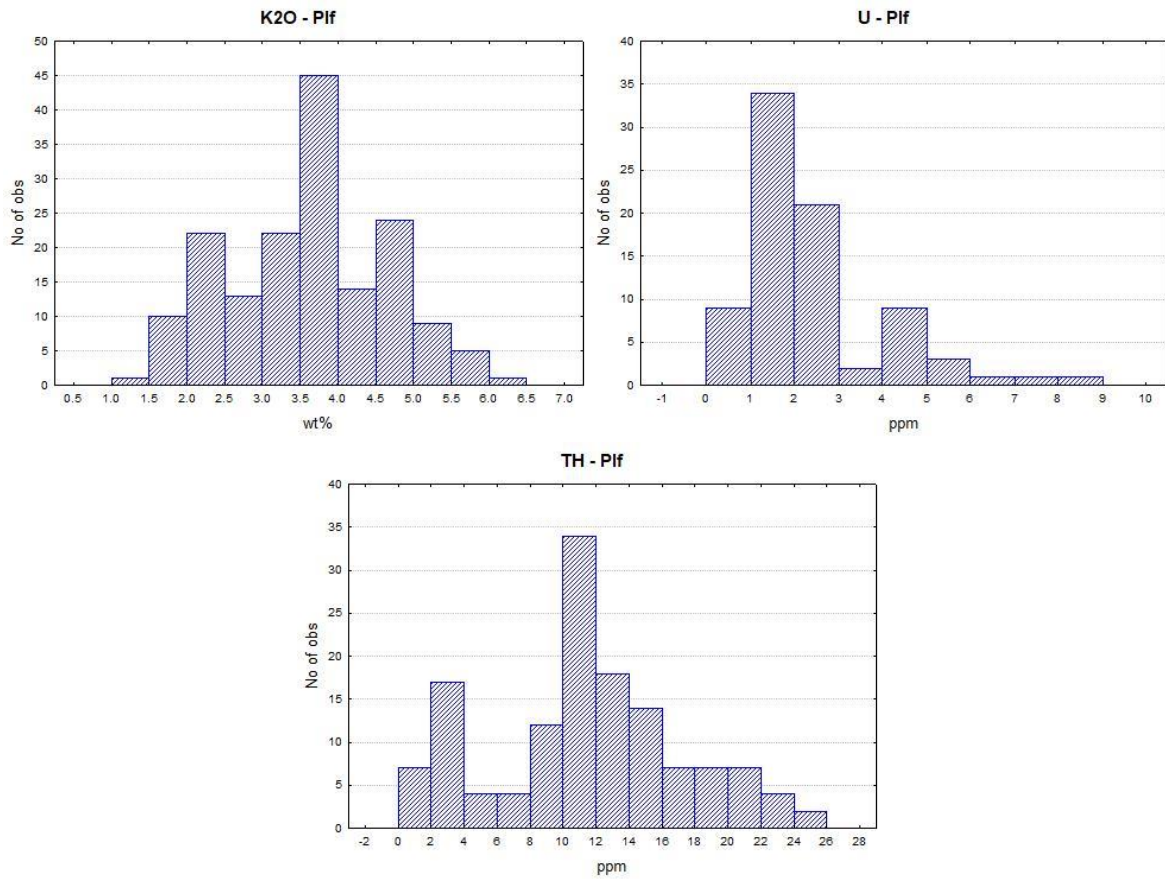


Figure 7: histograms of the  $K_2O$ , U and Th distribution of the Pif unit.

The Pif unit represents a part of the crystalline basement, which make up for a large portion of the upper crust, and its  $K_2O$ , U and Th concentration (table 5) are comparable to those of the estimate of Rudnick and Gao (2014) for similar materials.

The  $K_2O$  and Th distributions are rather symmetrical, while the U data don't fit well in a normal distribution (fig. 7) and have high skewness and kurtosis values.

### Statistical analysis (Plm)

Table 6: descriptive statistic of Plm unit.  $K_2O$  values are expressed in wt%, U and Th values in ppm. N=number of samples. Std.Dev.=standard deviation.

	N	Mean	Median	Minimum	Maximum	25 <sup>th</sup> Percentile	75 <sup>th</sup> Percentile	Std.Dev.	Skewness	Kurtosis
$K_2O$	53	1.0	1.0	0.1	2.2	0.6	1.2	0.5	0.4	-0.2
U	15	2.1	2.0	0.1	3.3	1.8	3.0	0.9	-0.7	0.3
Th	42	2.6	2.5	0.5	7.1	1.4	3.6	1.6	0.6	0.2

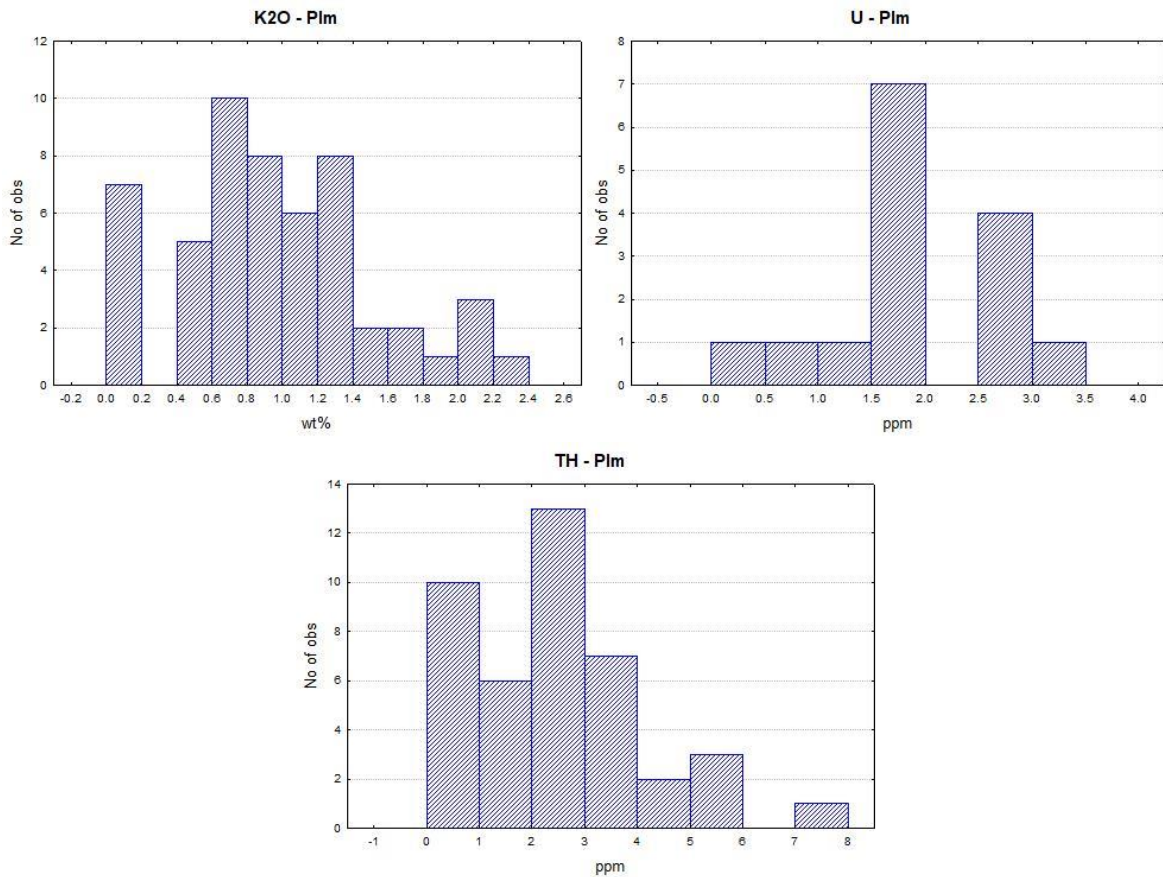


Figure 8: histograms of the K<sub>2</sub>O, U and Th distribution of the Plm unit.

The Plm unit shows lower K<sub>2</sub>O, U and Th concentrations (*table 6*) than the Plf unit, due to its mafic composition.

The form of the U distribution (*fig. 8*) highly depends on the low number of samples. The bodies of the K<sub>2</sub>O and Th distributions can be considered normal, even though they are asymmetrical due to the absence of negative values, as for every natural distribution.

#### 4.1.2 PV – Paleozoic volcanic rocks

##### Description

Volcanic rocks associated with PI unit.

Age: Carboniferous – Permian.

Location of the main outcrops: Southern Alps of Trentino-Alto-Adige; western Liguria, near the border with Piedmont; central and northern Sardinia.

Lithology/composition: felsic and intermediate volcanic rocks with calcalkaline or K-alkaline affinity, ranging from andesite and trachy-andesite to rhyolite and dacite (Cortesogno *et al.*, 1998).

Genesis/emplacement: the rocks of this unit formed during the latest phase of the Hercynian orogeny. Although most of the Hercynian volcanic product did not survive the erosional processes, there are still large outcrop of them in Trentino-Alto-Adige (e.g. the Lower Permian Athesian Volcanic Group), near the border between Liguria and Piedmont (e.g. Melogno porphyry) and in Sardinia, often associated to plutonic rocks.

## Statistical analysis

Table 7: descriptive statistic of PV unit.  $K_2O$  values are expressed in wt%, U and Th values in ppm. N=number of samples. Std.Dev.=standard deviation.

	N	Mean	Median	Minimum	Maximum	25 <sup>th</sup> Percentile	25 <sup>th</sup> Percentile	Std.Dev.	Skewness	Kurtosis
$K_2O$	97	3.6	3.5	0.1	7.4	2.1	5.2	1.9	0.1	-0.9
U	56	3.4	3.5	1.6	6.2	2.5	4.0	1.1	0.4	-0.3
Th	74	16.9	17.8	7.0	26.0	14.0	20.5	5.2	-0.2	-0.8

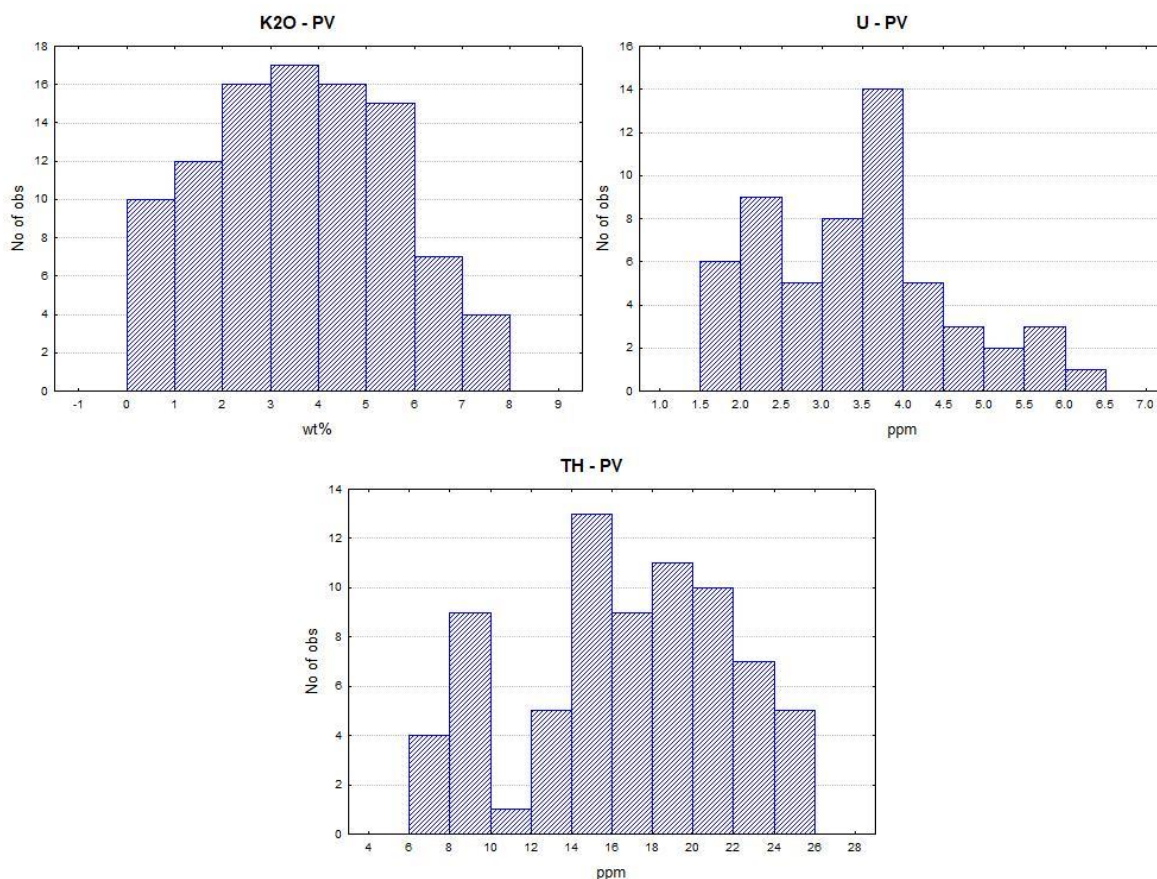


Figure 9: histograms of the  $K_2O$ , U and Th distribution of the PV unit.

The  $K_2O$ , U and Th concentrations of the PV unit (table 7) are comparable to those of the P1f unit, as the former includes the volcanic terms of the latter. U and Th concentrations, however, show higher values in this unit, even though it comprehends andesitic products that should be more mafic than the average P1f sample.

The distributions (fig. 9) are quite symmetrical; the high negative kurtosis value indicates that the tails are not well represented.

### 4.1.3 MVI – Mesozoic volcanic and intrusive rocks

#### Description

Mesozoic intrusive rocks and volcanic submarine products associated with MC successions.

Age: middle Triassic (Cretaceous).

Location of the main outcrops: Dolomites; Alpine foothills of Lombardy and Veneto; northern Carnia; western Sicily.

Lithology/composition: basalt, andesite, latite and intrusive mafic and felsic rocks with tholeiitic and shoshonitic affinity; rare rhyodacitic lava flows and ignimbritic tuffs.

**Genesis/emplacement:** the Triassic period was characterized by extensional/strike slip tectonic due to the breaking up of the supercontinent Pangea and this led to the formation of a large number of volcanic centres related to lithospheric thinning. The largest outcropping portion of these products is formed by the Predazzo-Monzoni complex, a series of magmatic bodies that intruded the forming MC succession during middle Triassic: it hosts shoshonitic mafic and felsic rocks, from pyroxenite to granite; its precise origin is still debated (Filipponi, 2018).

The other volcanic products that survived until now are mostly lava flows, pillow lavas and hyaloclastites that are found inside Southern Alps carbonate successions and in Sicily (Bronzi *et al.*, 1977, Cirrincione *et al.*, 2014). There is evidence of the presence of Cretaceous lamprophyre in Tuscany (Stoppa *et al.*, 2014).

### Statistical analysis

Table 8: descriptive statistic of MVI unit. K<sub>2</sub>O values are expressed in wt%, U and Th values in ppm. N=number of samples. Std.Dev.=standard deviation.

	N	Mean	Median	Minimum	Maximum	25 <sup>th</sup> Percentile	75 <sup>th</sup> Percentile	Std.Dev.	Skewness	Kurtosis
K <sub>2</sub> O	130	3.0	3.0	0.0	8.2	1.5	4.3	1.9	0.4	-0.4
U	24	1.5	1.6	0.5	3.0	1.1	2.0	0.7	-0.1	-0.3
Th	74	5.3	5.0	0.1	17.0	3.0	6.5	3.1	1.4	2.5

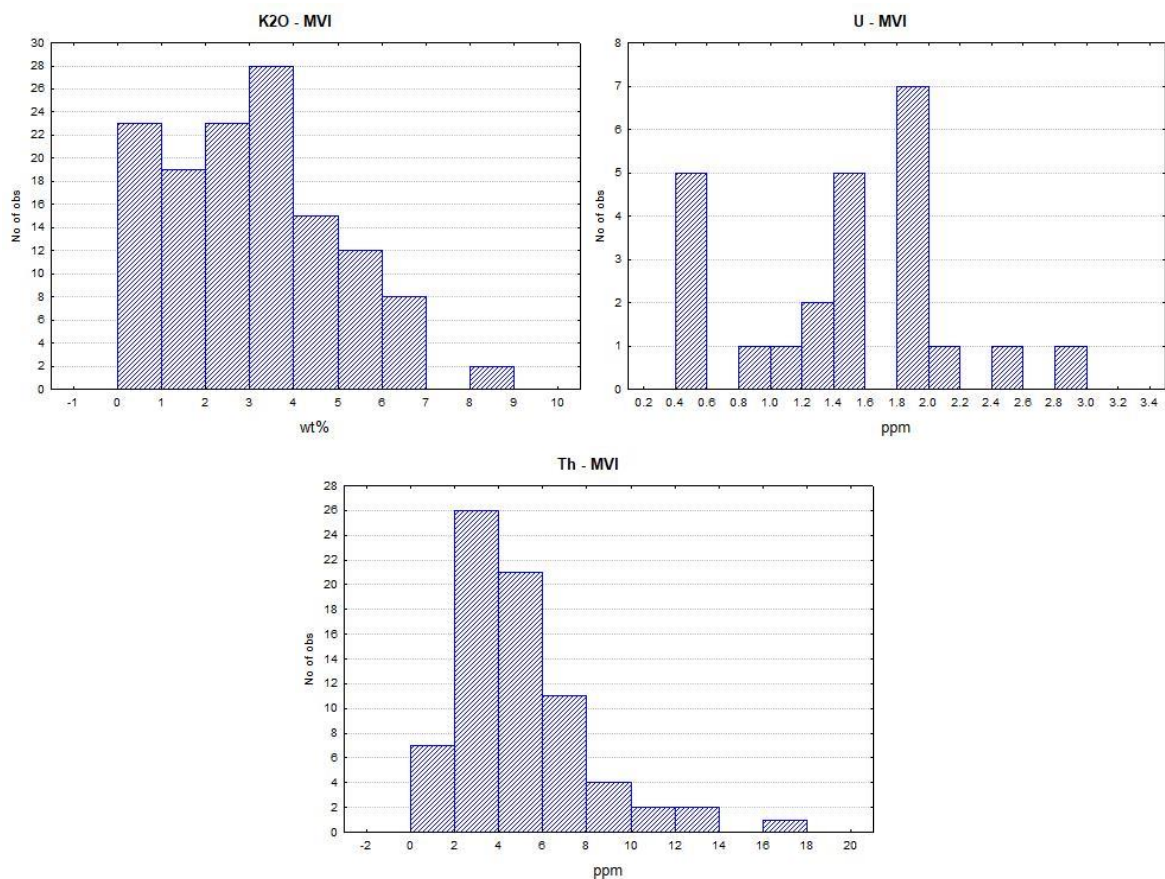


Figure 10: histograms of the K<sub>2</sub>O, U and Th distribution of the MVI unit.

The MVI unit shows low K<sub>2</sub>O, U and Th concentrations (*table 8*), though the values are strongly influenced by samples of lamprophyre and pyroxenite that are not entirely representative of the unit's lithology.

The data don't fit in normal distributions (*fig. 10*), mainly because of the large lithological heterogeneity.

#### 4.1.4 PNI – Paleogene-Neogene intrusive rocks

##### Description

Oligocene-Miocene syn-collisional plutonic rocks.

Age: middle-upper Oligocene.

Location of the main outcrops: central and western Alps.

Lithology/composition: granite, granodiorite, tonalite, gabbro, quartz-monzonite.

Genesis/emplacement: middle to upper Oligocene igneous bodies of the Alps located along the Periadriatic Fault System. Their formation is related to the slab breakoff during the Alpine continental collision (von Blanckenburg and Davies, 1995), that led to an enhanced heat flow from the upwelling asthenospheric mantle. The upwelling mantle caused the partial melting of the overriding upper mantle and lower crust. The outcrops are essentially made of differentiated plutonic felsic rocks, while volcanic products (e.g. the Biella Volcanic Suite; Kapferer *et al.*, 2012) are less represented.

##### Statistical analysis

Table 9: descriptive statistic of PNI unit.  $K_2O$  values are expressed in wt%, U and Th values in ppm. N=number of samples. Std.Dev.=standard deviation.

	N	Mean	Median	Minimum	Maximum	25 <sup>th</sup> Percentile	75 <sup>th</sup> Percentile	Std.Dev.	Skewness	Kurtosis
$K_2O$	120	1.8	2.0	0.2	3.7	1.3	2.4	0.8	-0.4	-0.5
U	101	3.1	2.9	0.3	7.7	1.8	4.2	1.7	0.3	-0.3
Th	104	11.1	11.3	0.3	28.1	5.0	16.0	6.6	0.2	-0.6

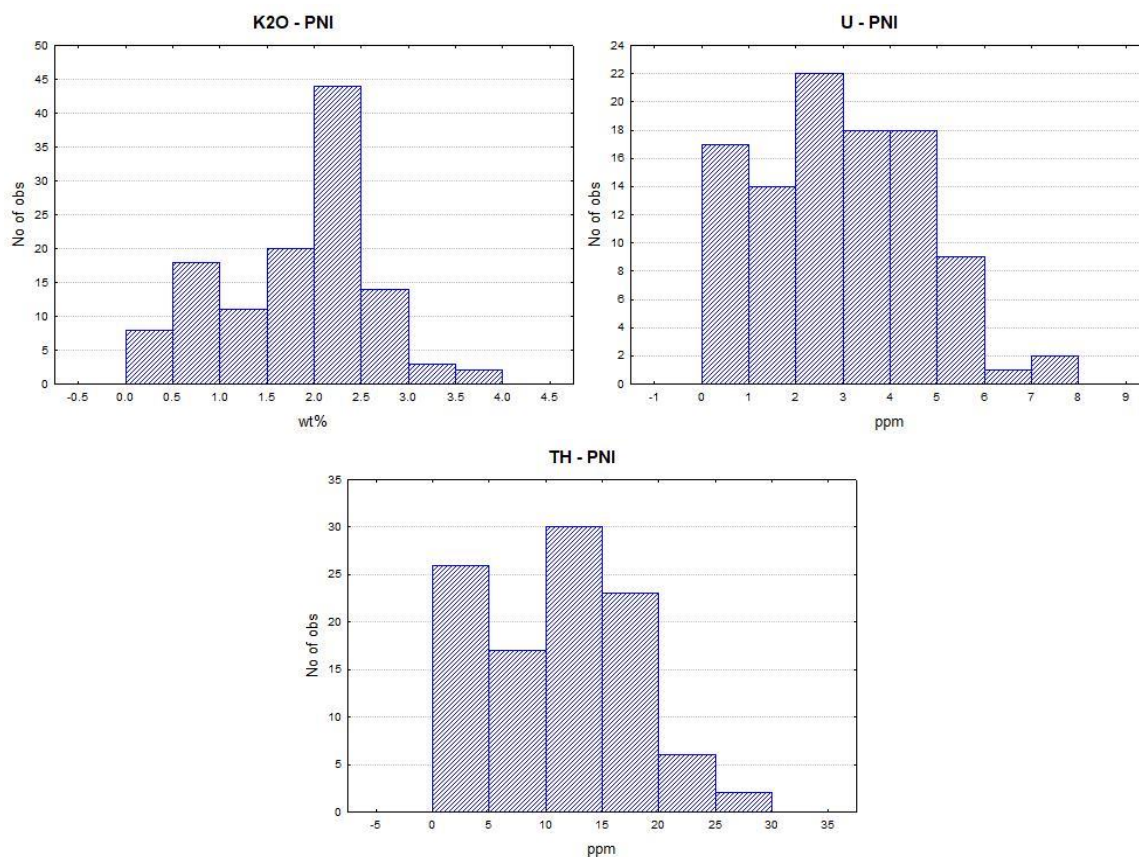


Figure 11: histograms of the  $K_2O$ , U and Th distribution of the PNI unit.

The PNI unit shows U and Th concentrations similar to the previous felsic units, but K<sub>2</sub>O content is definitely lower (*table 9*).

The distributions (*fig. 11*) are quite symmetrical, but they are affected by the absence of negative values; as like the PV unit, the tails are poorly represented.

#### 4.1.5 PNv – Paleogene-Neogene volcanic rocks

##### Description

Paleogene and Neogene volcanic and sub-volcanic products related to extensional tectonics or subduction. This unit has been divided in two sub-units: mafic and felsic.

Age: Cretaceous – lower Pleistocene.

Location of the main outcrops: Euganean Hills; Hyblean plateau; western Sardinia.

Lithology/composition: basalt, andesite, latite, dacite, trachyte, rhyolite.

Genesis/emplacement: the volcanic districts of the Euganean Hills, the Monti Lessini, the Adige valley and the area of Marostica (Veneto) formed between upper Paleocene and upper Oligocene due to extensional tectonics, as a reaction to the compression on the N-S axis that was caused by Alpine orogeny. The products of the Euganean Hills follow the alkaline magmatic series, evolving from K-basalt to latite, trachyte and rhyolite (Tositti *et al.*, 2017). The rocks from the other zones have tholeiitic affinity and they have few compositional differences: they consist of basalt, basaltic andesite and nephelinite (Beccaluva *et al.*, 2007).

The Hyblean Plateau volcanism date back to early Cretaceous (even though some cut drillings recovered from commercial wells indicate it was already active during Triassic) and it correlates to the Pietre Nere (Puglia) Mesozoic volcanic activity, as they both are a kind of intraplate magmatism, due to a regime of passive rifting (Beccaluva *et al.*, 1998). The oldest products, in the Pachino-Capo Passero zone (Sicily), are the result of submarine activity that formed basaltic pillow lavas and hyaloclastites; the main phase of activity started in lower Pliocene with mostly basaltic lava flows with tholeiitic or Na-alkaline affinity (Carbone, 2011).

The Oligocene-Miocene activity in Sardinia resulted from the development of a volcanic arc above a subducting slab: it formed when the Corsica-Sardinia block began to separate from Europe, first sliding and then rotating anticlockwise towards its current position, causing the subduction of the Alpine Tethys (Bosellini, 2005). The volcanic products show a calcalkaline affinity and all terms, from mafic to felsic ones, are represented.

##### Statistical analysis (PNVf)

*Table 10: descriptive statistic of PNVf unit. K<sub>2</sub>O values are expressed in wt%, U and Th values in ppm. N=number of samples. Std.Dev.=standard deviation.*

	N	Mean	Median	Minimum	Maximum	25 <sup>th</sup> Percentile	75 <sup>th</sup> Percentile	Std.Dev.	Skewness	Kurtosis
K <sub>2</sub> O	135	4.6	4.8	1.6	7.7	3.7	5.4	1.2	0.0	-0.1
U	23	5.7	5.6	1.2	9.8	4.8	6.7	2.0	0.0	0.6
Th	31	23.3	22.2	8.0	38.8	20.0	27.0	7.4	0.1	0.2

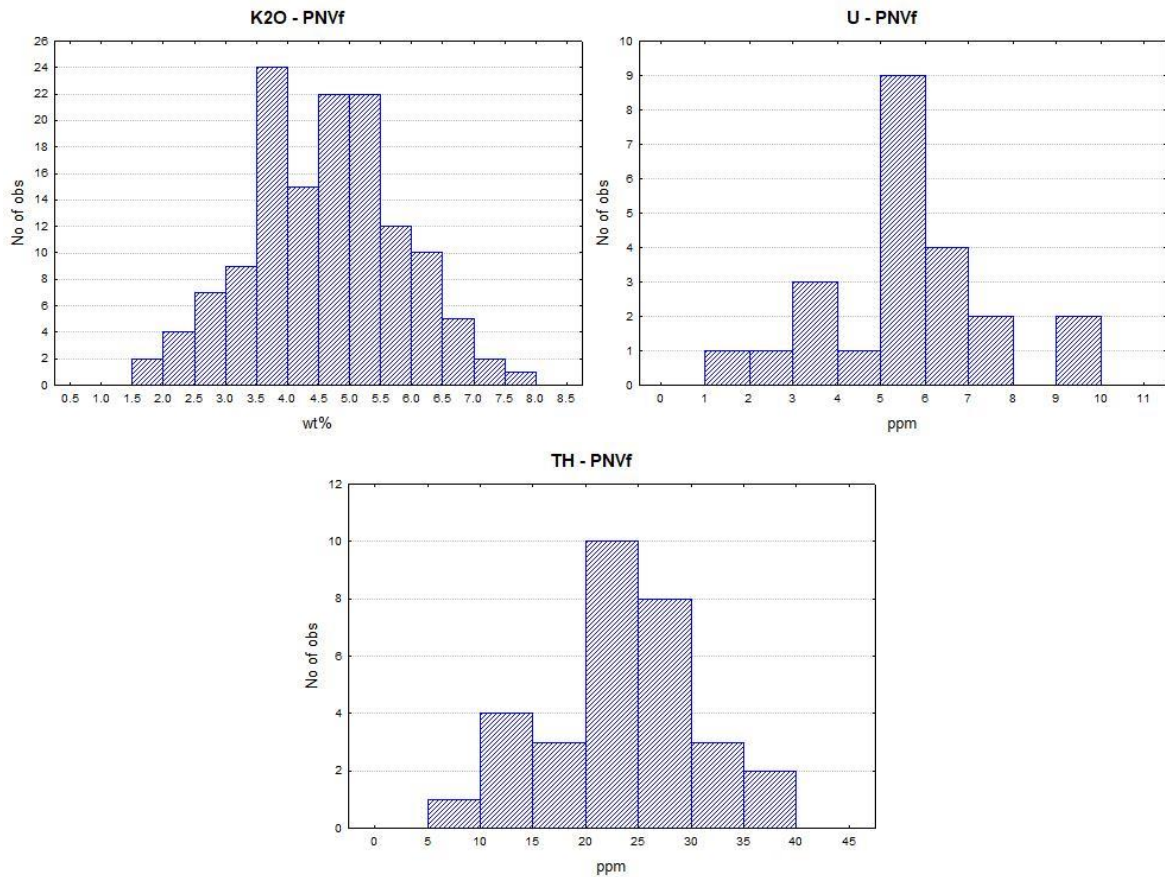


Figure 12: histograms of the  $K_2O$ , U and Th distribution of the PNVf unit.

The  $K_2O$ , U and Th concentrations of the PNVf unit are rather high (*table 10*); this is strongly related to the alkaline affinity of the products of the Veneto Volcanic Province, which also make up the majority of the samples.

The data fit well in a normal distribution (*fig. 12*), even though the kurtosis value for U indicates that the tails are overdeveloped.

### Statistical analysis (PNVm)

Table 11: descriptive statistic of PNVm unit.  $K_2O$  values are expressed in wt%, U and Th values in ppm. N=number of samples. Std.Dev.=standard deviation.

	N	Mean	Median	Minimum	Maximum	25 <sup>th</sup> Percentile	75 <sup>th</sup> Percentile	Std.Dev.	Skewness	Kurtosis
$K_2O$	439	1.2	1.1	0.0	3.0	0.8	1.6	0.7	0.6	-0.1
U	158	1.4	1.1	0.2	4.5	0.6	1.9	1.0	1.0	0.3
Th	325	6.4	5.3	0.5	17.0	3.6	8.1	3.8	0.9	0.0

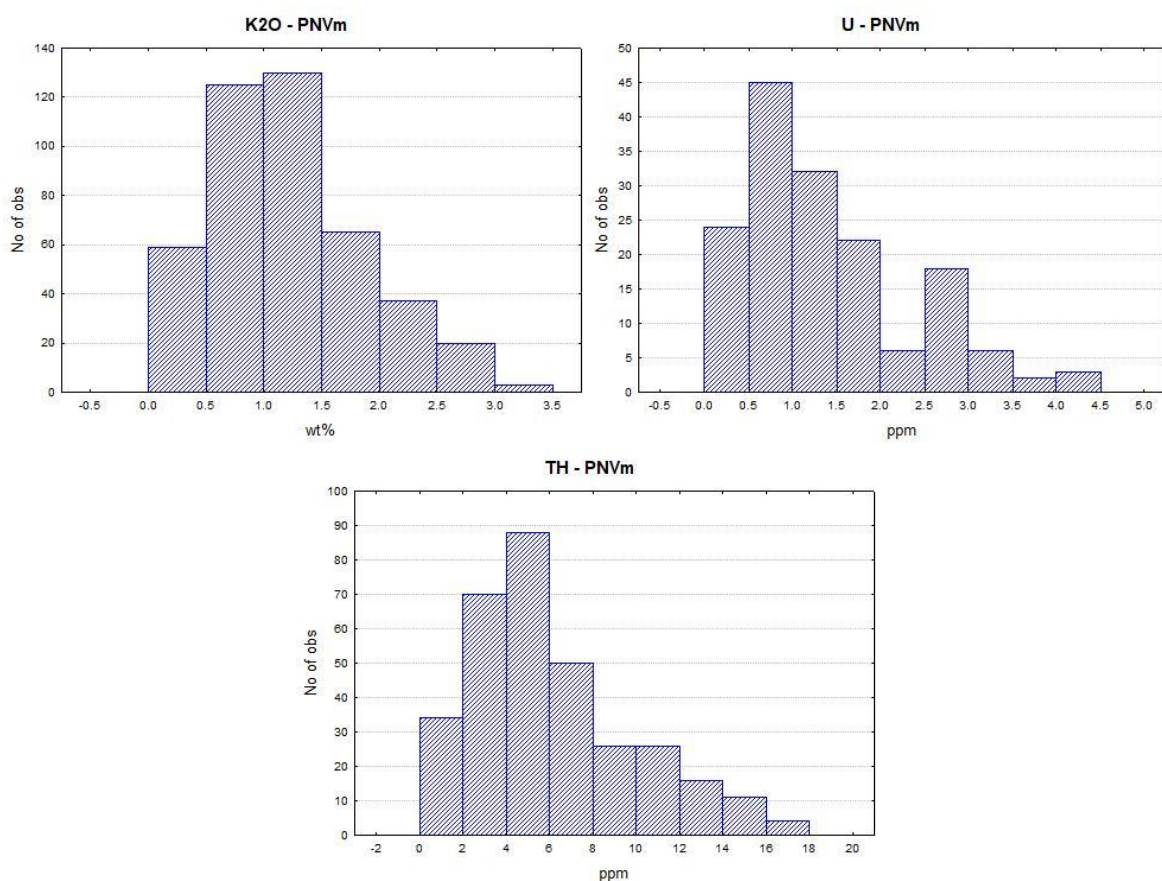


Figure 13: histograms of the  $K_2O$ , U and Th distribution of the PNVm unit.

The PNVm unit shows  $K_2O$  and U concentrations typical of mafic rocks, while Th concentrations are higher than average (*table 11*).

The high number of samples indicates that the result should be representative; as a matter of fact, the distributions are normal-shaped (*fig. 13*). The high skewness values are due to the impossibility to have negative numbers in a natural distribution.

#### 4.1.6 LTP – Lazio-Tuscany magmatic province

##### Description

Plio-Quaternary plutonic and volcanic products of central Italy, from Lazio, Tuscany, Abruzzo and Umbria region.

Age: late Miocene – Holocene.

Location of the main outcrops: southern Tuscany; Elba island; Lazio; northernmost Campania; little and sporadic outcrops in Umbria and Abruzzo (ULUD: Umbria-Lazio Ultrapotassic District; Lavecchia and Stoppa, 1996).

Lithology/composition: mainly ultrapotassic and silica-undersaturated products, usually with kamafugitic and carbonatitic affinity in Umbria and Abruzzo (Peccerillo, 1998). Shoshonitic, calcalkaline and high-K calcalkaline products are present in the Tuscan area (Chelazzi *et al.*, 2006). The main lithologies consist in trachyandesite, tephrite, phonolite, trachyte and rhyolite.

Genesis/emplacement: the magmatism of central Italy developed within the extensional basins caused by the opening of the Tyrrhenian Sea (Bosellini, 2005). It is composed of several volcanic centres spread across the Tyrrhenian side of central Italy, of which the

most important are Elba island, Mount Amiata, Cimini Hills, Vico, Vulcini, Monti Sabatini, Alban Hills, Monti Ernici and Roccamonfina. The only one still considered active, though quiescent, is the Alban Hills volcanic centre, which probably erupted during Holocene (Peccerillo, 2005).

The activity has been mostly explosive, with few effusive events. Intrusive rocks are limited to the Tuscan archipelago (Elba, Giglio and Montecristo islands) and near the town of Gavorrano (Livorno); the main compositions are felsic or intermediate, and their origin is due to an interaction between mantle and crustal melts (Principi *et al.*, 2010).

### Statistical analysis

Table 12: descriptive statistic of LTP unit.  $K_2O$  values are expressed in wt%, U and Th values in ppm. N=number of samples. Std.Dev.=standard deviation.

	N	Mean	Median	Minimum	Maximum	25 <sup>th</sup> Percentile	75 <sup>th</sup> Percentile	Std.Dev.	Skewness	Kurtosis
$K_2O$	900	5.8	5.8	0.2	14.0	3.8	8.0	2.8	-0.1	-0.8
U	478	11.4	9.1	0.8	37.0	6.1	15.9	7.5	1.1	0.4
Th	798	56.6	46.1	2.4	175.0	27.6	80.0	38.5	0.9	0.0

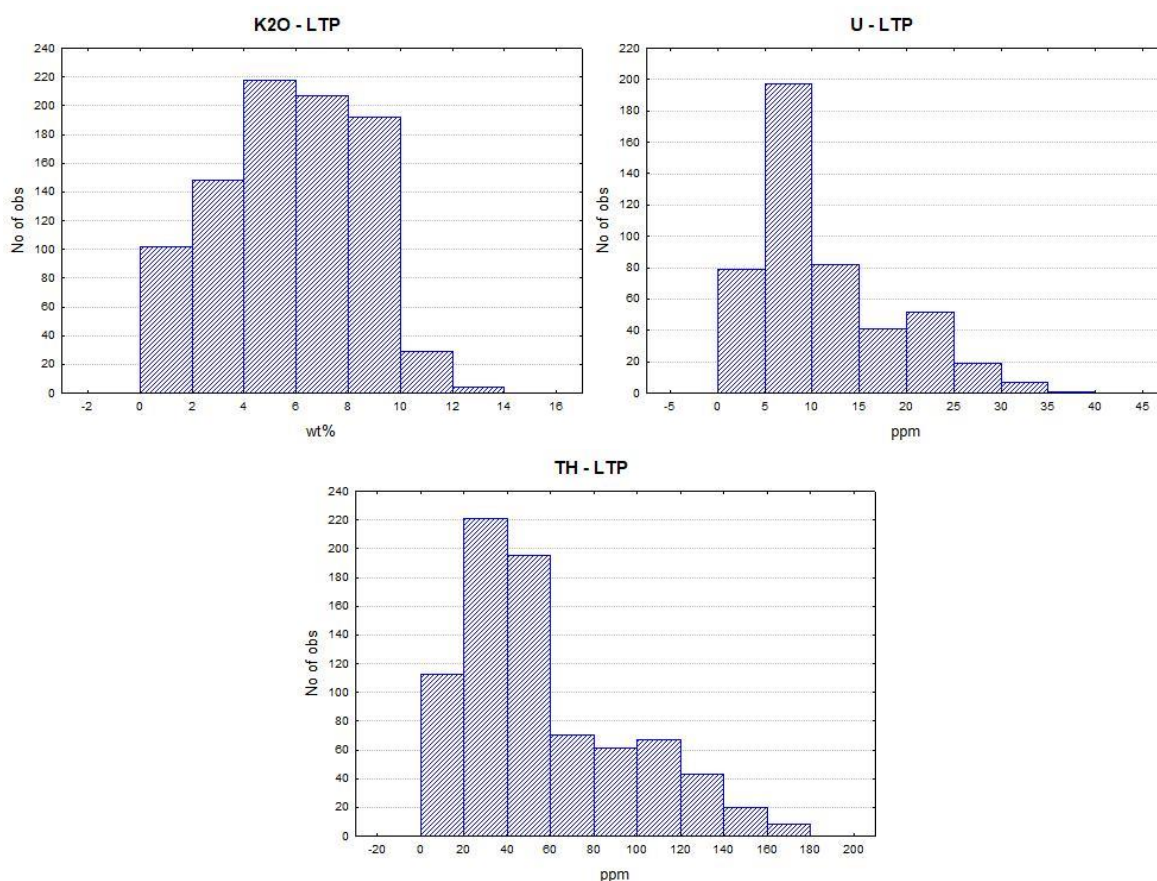


Figure 14: histograms of the  $K_2O$ , U and Th distribution of the LTP unit.

The LTP unit shows the highest  $K_2O$ , U and Th concentrations (table 12), considering the three of them together, as it is already known from literature (Peccerillo, 2005). This is due to the presence of large bodies formed by potassic and ultrapotassic rocks, which are always enriched in rare elements like U and Th.

The K<sub>2</sub>O distribution has high symmetry, but its tails are almost non-existent; the U and Th distributions, on the other hand, have well-developed tails (*fig. 14*), but they are asymmetrical due to the absence of negative values.

#### 4.1.7 SAP – Sardinian magmatic province

##### Description

Plio-Quaternary volcanic products of Sardinia. This unit has been divided in two sub-units: mafic and felsic.

Age: lower Pliocene – upper Pleistocene.

Location of the main outcrops: central Sardinia.

Lithology/composition: basalt, trachyandesite, trachyte, dacite, rhyolite with tholeiitic or alkaline affinity and geochemical characteristics of intraplate magmatism (Lustrino *et al.*, 2004).

Genesis/emplacement: the Plio-Quaternary volcanism in Sardinia developed within the extensional regime due to the opening of the Tyrrhenian Sea. The main eruptive centres are Capo Ferrato, Logudoro, Montiferru, Monte Arci, Central Sardinia and Orosei-Dorgali. Even though the geotectonic setting is the same for all the districts, the rock composition is extremely heterogeneous and the affinity varies from subalkaline to highly alkaline; furthermore, there is evidence of silica-undersaturated products (Peccerillo, 2005).

The activity has been mainly effusive, with sporadic explosive events.

##### Statistical analysis (SAPf)

Table 13: descriptive statistic of SAPf unit. K<sub>2</sub>O values are expressed in wt%, U and Th values in ppm. N=number of samples. Std.Dev.=standard deviation.

	N	Mean	Median	Minimum	Maximum	25 <sup>th</sup> Percentile	75 <sup>th</sup> Percentile	Std.Dev.	Skewness	Kurtosis
K <sub>2</sub> O	41	5.5	5.4	3.6	8.0	4.5	7.2	1.4	0.4	-1.2
U	22	4.4	4.4	2.3	6.8	3.5	5.0	1.2	0.1	-0.6
Th	32	21.4	21.0	9.0	37.3	15.5	25.0	7.9	0.3	-0.6

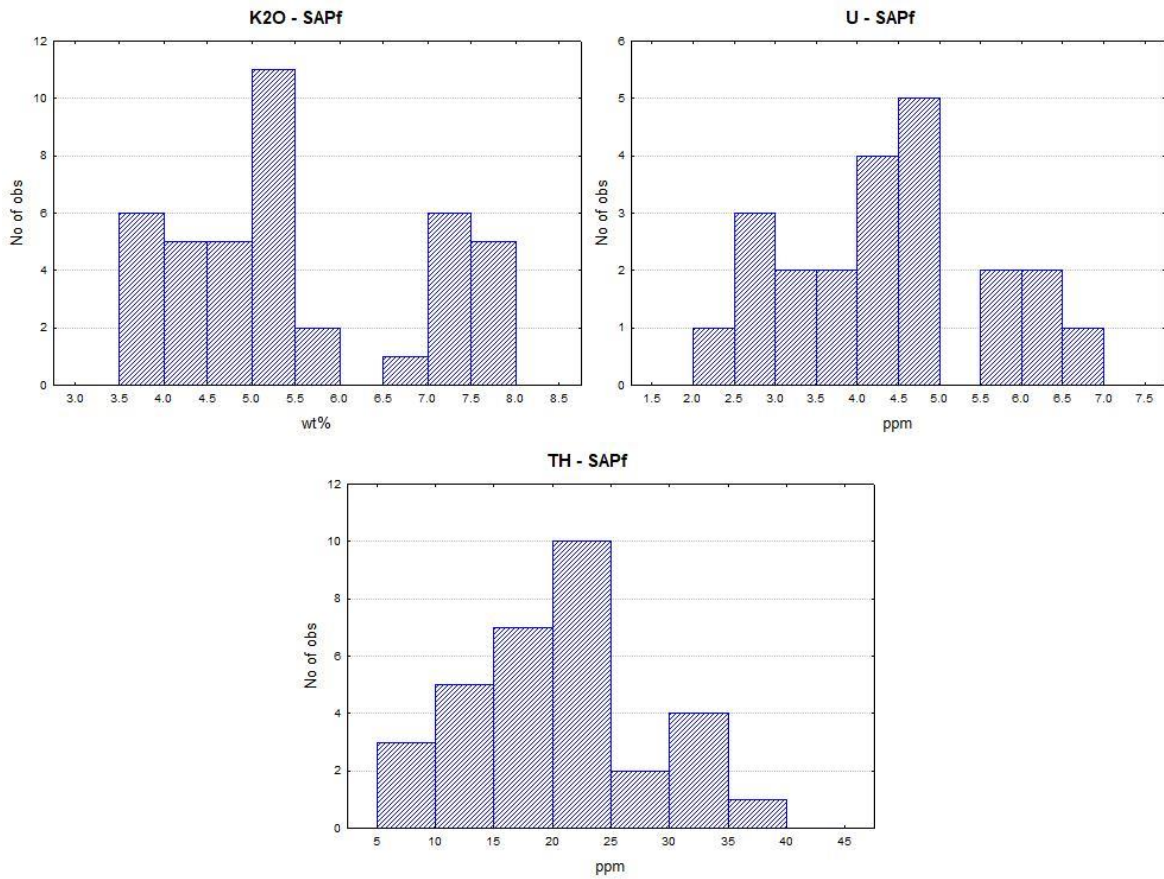


Figure 15: histograms of the  $K_2O$ , U and Th distribution of the SAPf unit.

The  $K_2O$ , U and Th concentrations for the SAPf unit (table 13) are higher than the average composition of the upper crust.

The distributions seem bimodal (fig. 15), even though this could be an effect of the low number of samples.

#### Statistical analysis (SAPm)

Table 14: descriptive statistic of SAPm unit.  $K_2O$  values are expressed in wt%, U and Th values in ppm. N=number of samples. Std.Dev.=standard deviation.

	N	Mean	Median	Minimum	Maximum	25 <sup>th</sup> Percentile	75 <sup>th</sup> Percentile	Std.Dev.	Skewness	Kurtosis
$K_2O$	116	1.8	1.9	0.5	4.2	1.1	2.4	0.8	0.4	-0.3
U	71	0.9	0.8	0.3	2.2	0.6	1.2	0.5	0.8	0.0
Th	73	4.5	4.5	1.5	9.9	2.9	5.8	2.1	0.5	-0.4

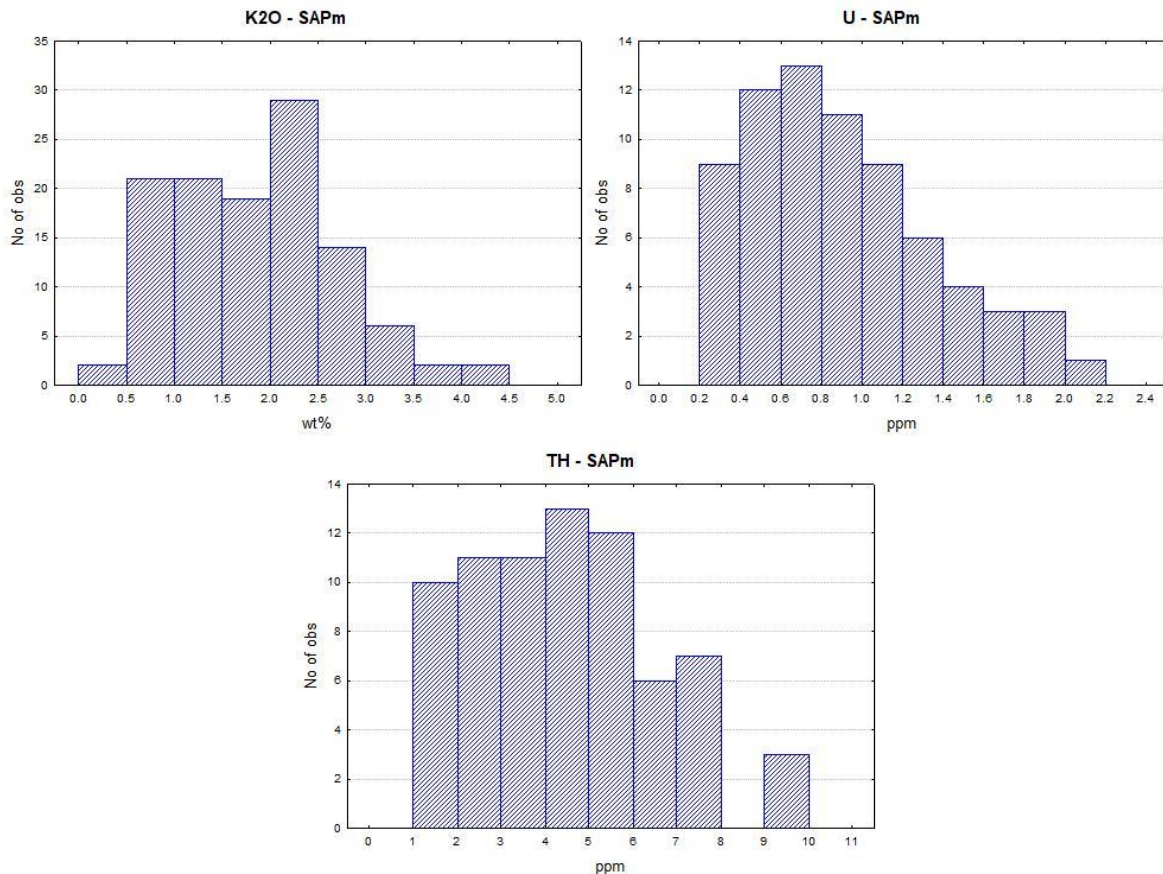


Figure 16: histograms of the K<sub>2</sub>O, U and Th distribution of the SAPm unit.

The SAPm unit shows low values for K<sub>2</sub>O, U and Th concentration (*table 14*) like the others mafic GU.

The distributions are quite asymmetrical (*fig. 16*), partly due to the absence of negative values, especially for U.

#### 4.1.8 CAP – Campanian magmatic province

##### Description

Potassic and ultrapotassic volcanic rocks formed during Plio-Quaternary. This unit has been divided in two sub-units: mafic and felsic.

Age: upper Pliocene – present.

Location of the main outcrops: central Campania and gulf of Naples archipelago.

Lithology/composition: basalt, trachybasalt, tephrite, phonolite and trachyte showing alkaline affinity, with high-K content and commonly silica-undersaturated.

Genesis/emplacement: the products originated from 5 main volcanic centres: Mount Vesuvius, Phlegraean Fields, Ischia, Procida and Vivara. They all formed in extensional basins along the Tyrrhenian Sea border and two of them, Mount Vesuvius and Phlegraean Fields, are still active today (Bosellini, 2005).

The activity has been mostly explosive, with the generation of a great amount of pyroclastic rocks.

## Statistical analysis

Table 15: descriptive statistic of CAP unit.  $K_2O$  values are expressed in wt%, U and Th values in ppm. N=number of samples. Std.Dev.=standard deviation.

	N	Mean	Median	Minimum	Maximum	25 <sup>th</sup> Percentile	75 <sup>th</sup> Percentile	Std.Dev.	Skewness	Kurtosis
$K_2O$	1836	7.5	7.4	4.9	10.0	6.9	8.1	1.0	0.1	-0.1
U	665	8.7	7.2	0.9	20.9	5.9	10.9	4.3	0.9	0.2
Th	951	29.1	26.6	1.5	73.4	19.7	35.9	14.3	0.7	0.4

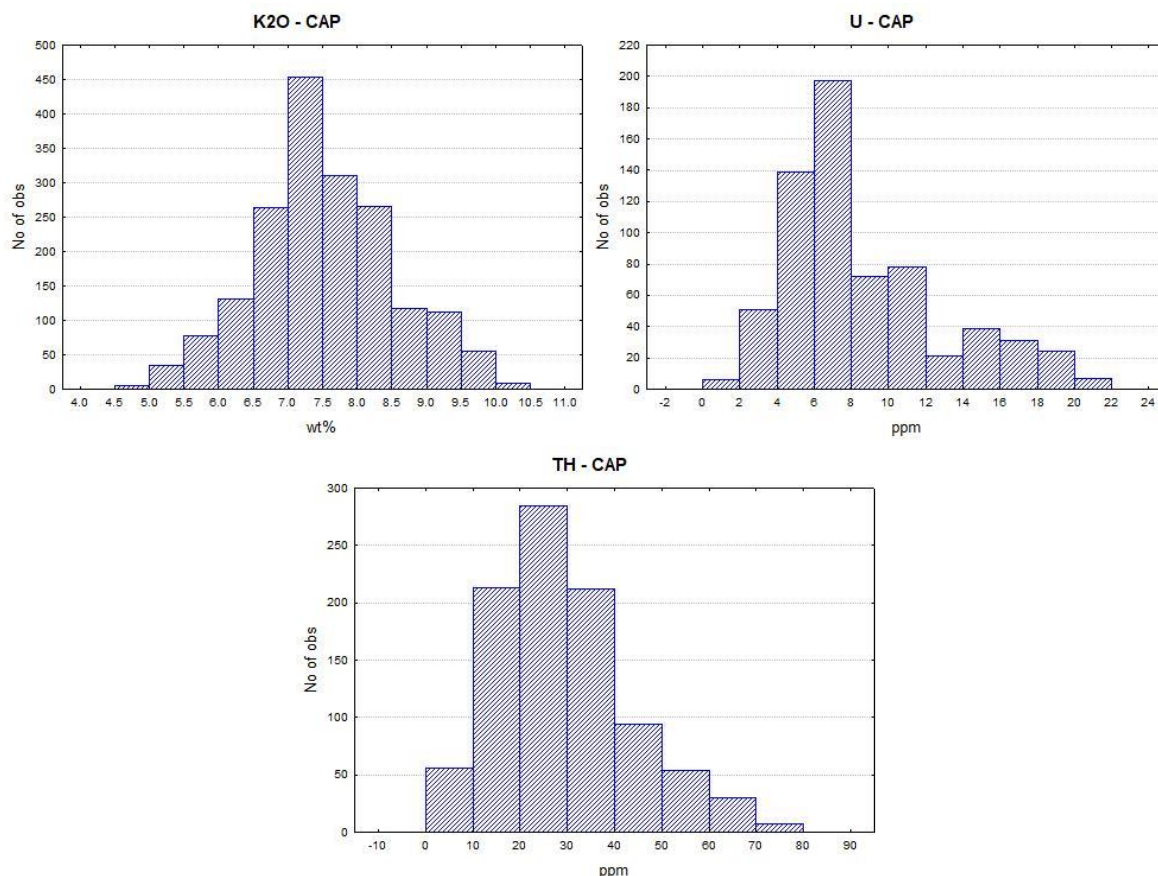


Figure 17: histograms of the  $K_2O$ , U and Th distribution of the CAP unit.

The CAP unit has the largest pool of data and its  $K_2O$ , U and Th concentrations are among the highest ones (table 15), due to the common presence of alkaline and ultra-alkaline silica-undersaturated rocks.

The  $K_2O$  data fit well in a normal distribution, while U and Th are affected by the absence of negative values (fig. 17).

### 4.1.9 SSD – Sicilian strait magmatic district

#### Description

Plio-Quaternary volcanic products of the Sicilian Strait. This unit has been divided in two sub-units: mafic and felsic.

Age: lower Pleistocene – Holocene.

Location of the main outcrops: Pantelleria and Linosa islands.

Lithology/composition: basalt, andesite, trachyte, rhyolite (pantellerite and comendite) with alkaline and peralkaline affinity.

**Genesis/emplacement:** the magmatism of the Sicilian strait developed inside the continental rifting system that interest the northern part of African plate (Peccerillo, 2005) and that formed the two islands of Pantelleria and Linosa. It has an important intraplate volcanism signature, with a great amount of alkaline and peralkaline products. The first magmatic stage was characterized by hydromagmatic, strombolian and explosive activity, while the last events was almost purely effusive.

**Statistical analysis (SSDf)**

Table 16: descriptive statistic of SSDf unit. K<sub>2</sub>O values are expressed in wt%, U and Th values in ppm. N=number of samples. Std.Dev.=standard deviation.

	N	Mean	Median	Minimum	Maximum	25 <sup>th</sup> Percentile	75 <sup>th</sup> Percentile	Std.Dev.	Skewness	Kurtosis
K <sub>2</sub> O	129	4.5	4.5	3.9	5.0	4.3	4.6	0.2	-0.1	0.1
U	30	9.6	9.8	1.9	17.2	4.9	13.1	4.4	-0.1	-1.0
Th	77	33.2	33.0	10.5	57.0	28.7	40.0	10.0	-0.2	0.4

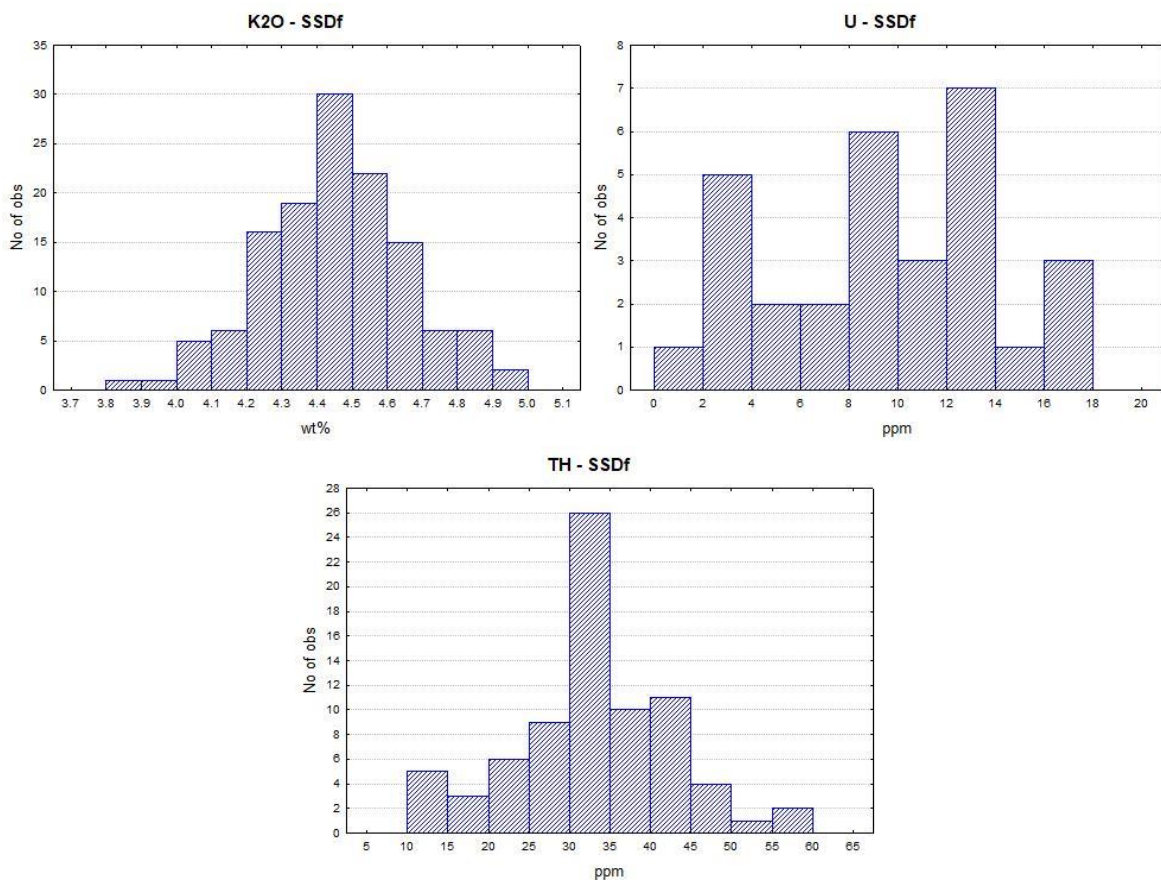


Figure 18: histograms of the K<sub>2</sub>O, U and Th distribution of the SSDf unit.

The SSDf unit has high K<sub>2</sub>O, U and Th contents (table 16), due to the alkaline and peralkaline affinity of the rocks and the enrichment in rare elements that occurs in pantellerite, the typical peralkaline rhyolite of this GU.

The distributions are symmetrical (fig. 18), but U distribution has really high kurtosis value due to the absence of the tails.

## Statistical analysis (SSDm)

Table 17: descriptive statistic of SSDm unit.  $K_2O$  values are expressed in wt%, U and Th values in ppm. N=number of samples. Std.Dev.=standard deviation.

	N	Mean	Median	Minimum	Maximum	25 <sup>th</sup> Percentile	75 <sup>th</sup> Percentile	Std.Dev.	Skewness	Kurtosis
$K_2O$	31	1.1	1.0	0.8	2.0	0.9	1.4	0.3	1.4	1.3
U	38	1.3	1.1	0.6	3.1	0.7	1.9	0.7	0.8	-0.4
Th	45	3.9	2.6	2.0	8.4	2.4	4.8	2.1	1.0	-0.4

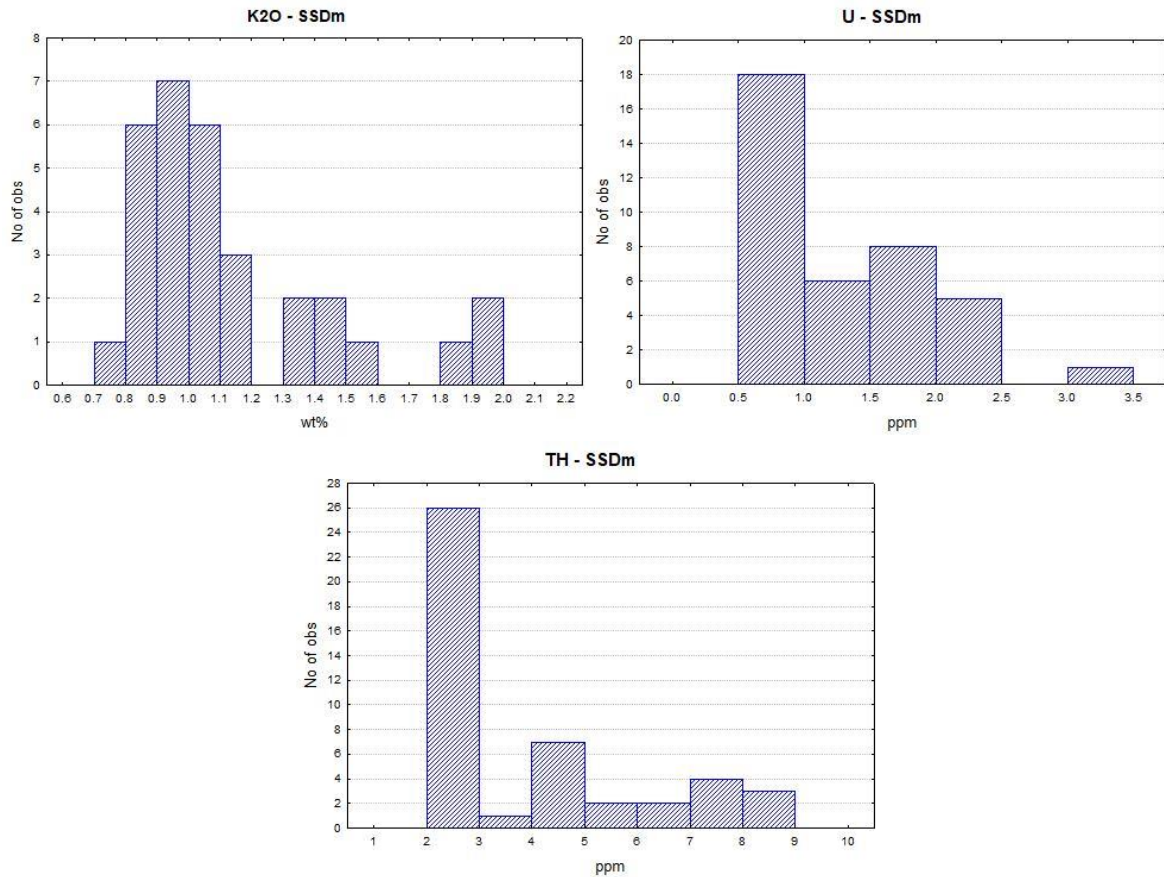


Figure 19: histograms of the  $K_2O$ , U and Th distribution of the SSDm unit.

The SSDm unit shows low values for  $K_2O$ , U and Th concentration (table 17) like the others mafic GU.

The SSDm distributions are among the worst (fig. 19). The problem seems to be the presence of rocks with very different  $K_2O$ , U and Th contents scattered in a low number of data.

### 4.1.10 AEP – Aeolian magmatic province

#### Description

Products of the volcanic arc of the Aeolian Islands, north of Sicily. This unit has been divided in two sub-units: mafic and felsic.

Age: middle Pleistocene – present.

Location of the main outcrops: Aeolian archipelago.

Lithology/composition: basalt, andesite, latite, dacite, rhyolite with calcalkaline, high-K calcalkaline and shoshonitic affinity.

**Genesis/emplacement:** the Aeolian volcanic arc formed in Pleistocene due to the subduction of the Ionian Sea under the Calabrian-Peloritan arc. It's composed of 7 islands: Stromboli, Panarea, Vulcano, Lipari, Salina, Filicudi, Alicudi; among these, Lipari, Vulcano and Stromboli are still active volcanoes, but Lipari and Vulcano are quiescent.

Taking into consideration the complex tectonic background of the area, the volcanic products don't always have pure calcalkaline affinity and their chemical composition shows considerable variations (Peccerillo, 2005).

The activity has been both effusive and explosive.

### Statistical analysis (AEPf)

Table 18: descriptive statistic of AEPf unit.  $K_2O$  values are expressed in wt%, U and Th values in ppm. N=number of samples. Std.Dev.=standard deviation.

	N	Mean	Median	Minimum	Maximum	25 <sup>th</sup> Percentile	75 <sup>th</sup> Percentile	Std.Dev.	Skewness	Kurtosis
$K_2O$	200	4.5	4.9	1.3	7.3	4.1	5.1	1.0	-0.8	0.3
U	101	8.9	9.1	2.3	16.6	5.6	11.9	3.9	0.1	-1.1
Th	107	29.0	30.0	0.1	58.2	17.9	39.1	14.6	0.1	-1.0

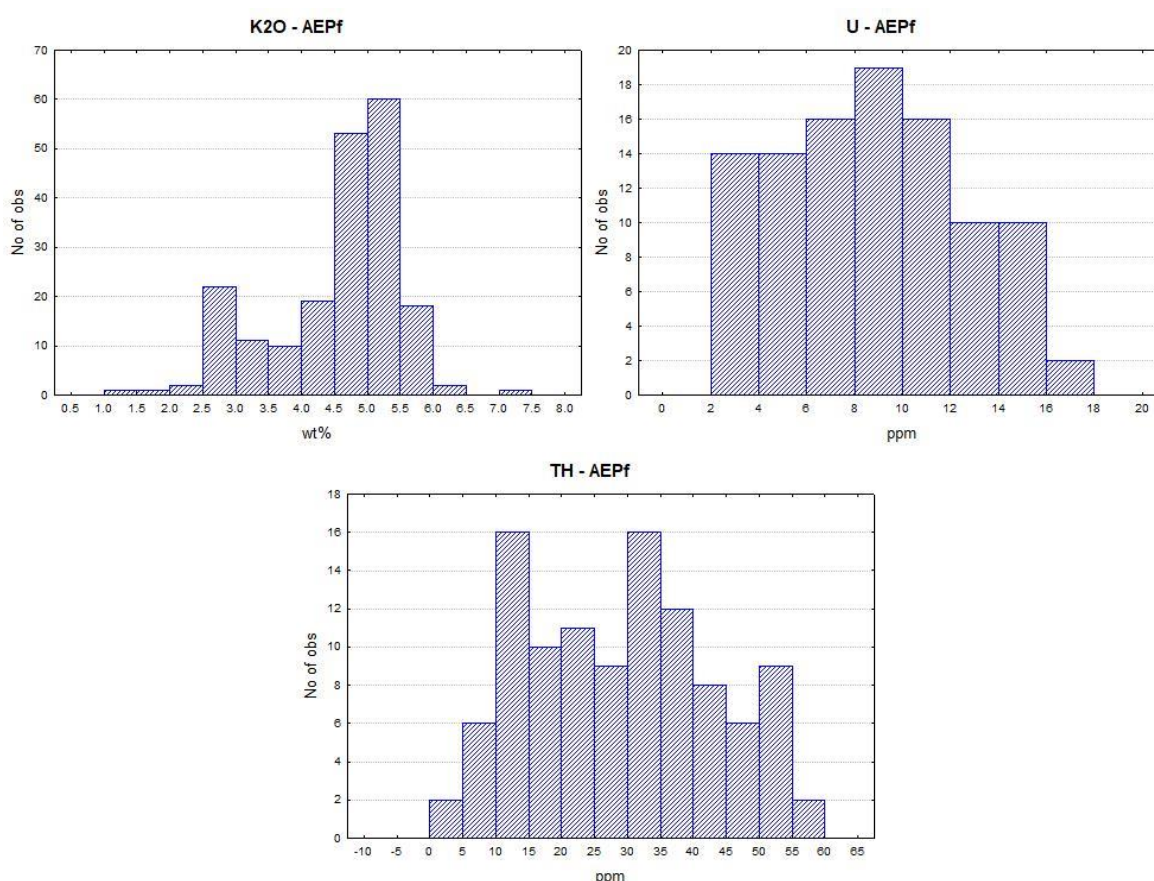


Figure 20: histograms of the  $K_2O$ , U and Th distribution of the AEPf unit.

The AEPf unit has high  $K_2O$ , U and Th concentrations (table 18), although the affinity varies from calcalkaline to shoshonitic.

The  $K_2O$  distribution is asymmetrical; the U and Th distributions, while being symmetrical, have low represented tails (fig. 20).

## Statistical analysis (AEPm)

Table 19: descriptive statistic of AEPm unit.  $K_2O$  values are expressed in wt%, U and Th values in ppm. N=number of samples. Std.Dev.=standard deviation.

	N	Mean	Median	Minimum	Maximum	25 <sup>th</sup> Percentile	75 <sup>th</sup> Percentile	Std.Dev.	Skewness	Kurtosis
$K_2O$	528	2.5	2.1	0.6	5.5	1.8	3.2	1.1	0.8	-0.1
U	380	3.9	3.9	0.2	7.8	3.0	4.8	1.6	0.1	0.1
Th	462	14.4	15.0	1.1	32.1	9.4	18.2	6.4	0.0	-0.3

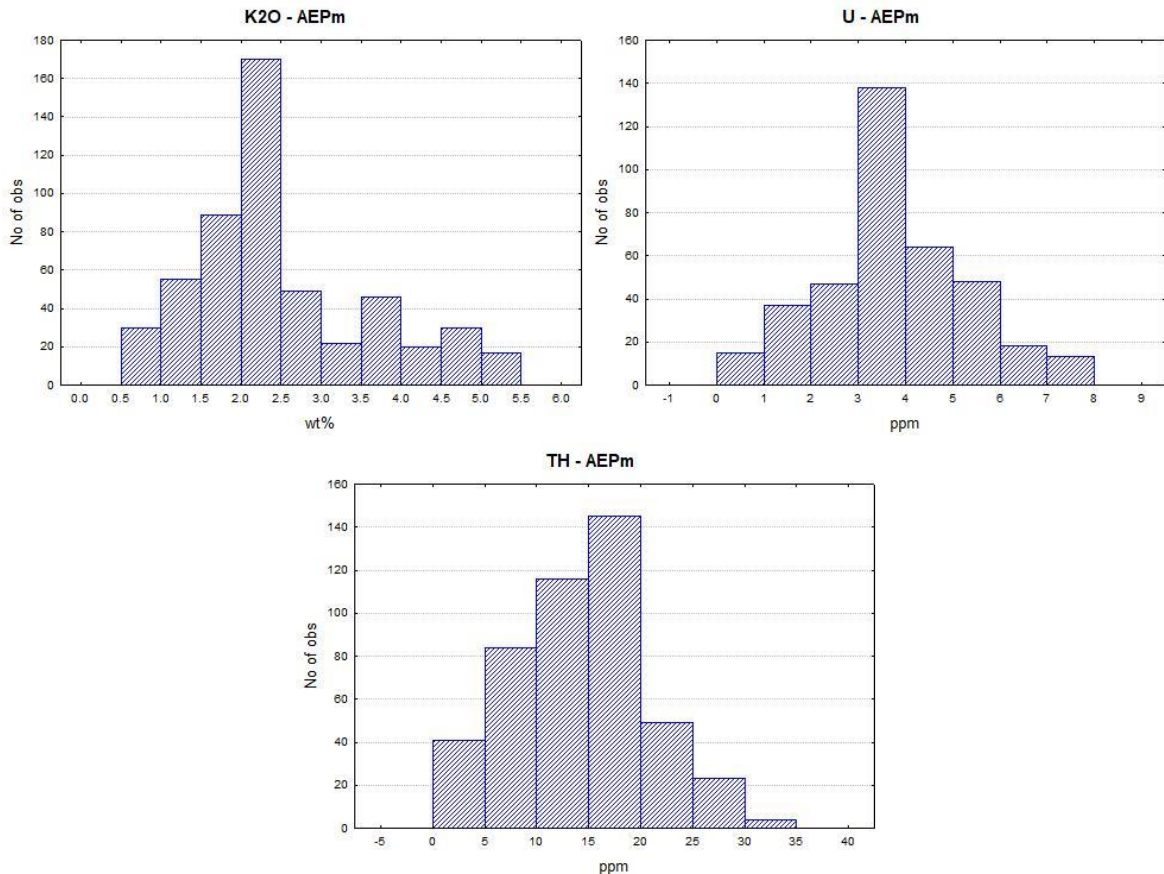


Figure 21: histograms of the  $K_2O$ , U and Th distribution of the AEPm unit.

The AEPm unit has very high  $K_2O$ , U and Th concentrations for a mafic GU (table 19); this is due to the common presence of rocks with trachyandesitic and trachybasaltic composition. The data fit quite well in a normal distribution (fig. 21), apart from the asymmetry of  $K_2O$  distribution.

### 4.1.11 MVP – Mount Vulture magmatic province

#### Description

Plio-Quaternary volcanic products of Mount Vulture (Basilicata).

Age: middle-upper Pleistocene.

Location of the main outcrops: Mount Vulture.

Lithology/composition: tephrite, basanite, foidite and phonolite with high alkaline affinity. Evidence of carbonatitic pyroclasts.

Genesis/emplacement: Mount Vulture volcano shares the same origin of the other volcanoes of central Italy, even though its position is quite isolated: it's located at the front

of the Apennines, on the margin of the Apulian foreland, far from the rest of the magmatic districts (Peccerillo, 2005).

The activity of Mount Vulture has been mostly explosive, with the formation of great amount of pyroclastic rocks and some dome structures; several lava flows are also recognizable on the eastern flank of the volcano.

### Statistical analysis

Table 20: descriptive statistic of MVP unit.  $K_2O$  values are expressed in wt%, U and Th values in ppm. N=number of samples. Std.Dev.=standard deviation.

	N	Mean	Median	Minimum	Maximum	25 <sup>th</sup> Percentile	75 <sup>th</sup> Percentile	Std.Dev.	Skewness	Kurtosis
$K_2O$	57	1.1	0.4	0.2	4.6	0.3	1.3	1.4	1.7	1.5
U	59	36.8	42.5	3.5	63.0	12.8	56.0	20.6	-0.4	-1.6
Th	67	69.0	72.0	15.0	118.0	47.4	87.9	25.1	-0.2	-1.0

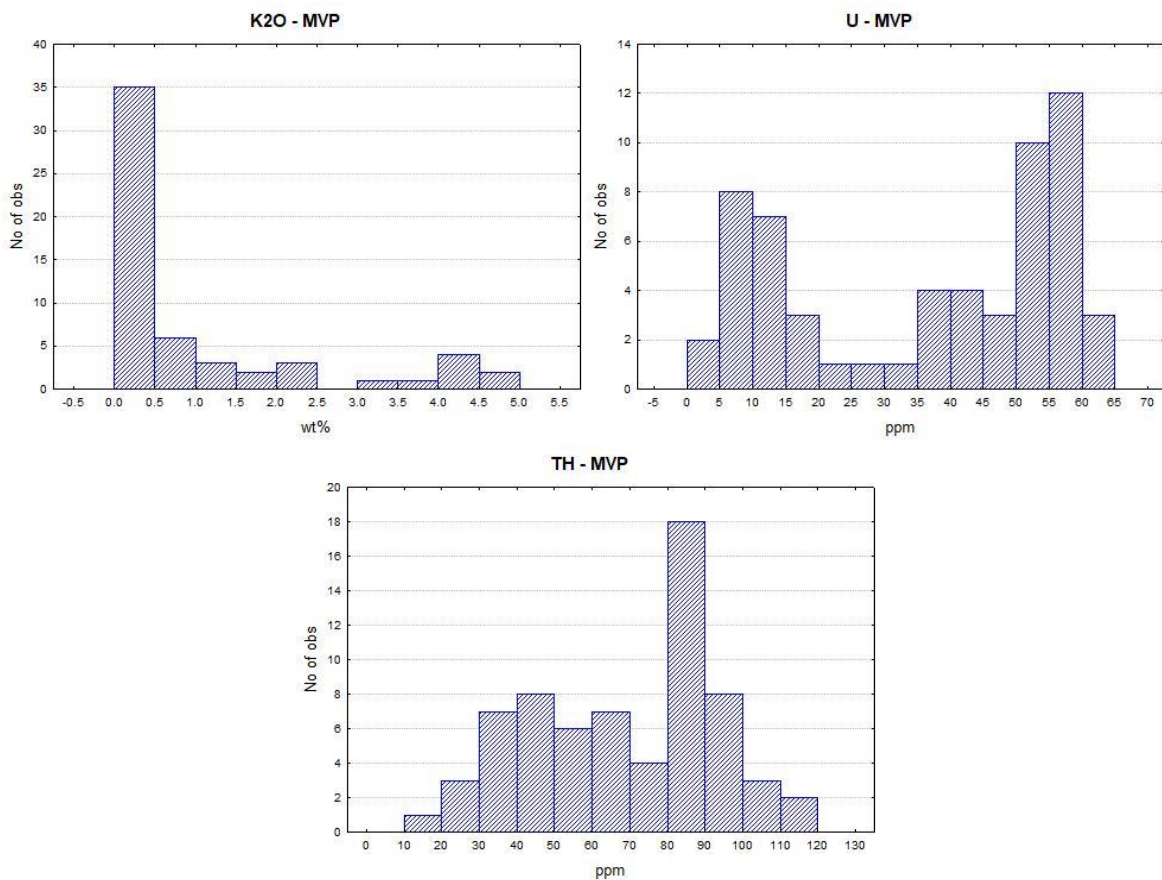


Figure 22: histograms of the  $K_2O$ , U and Th distribution of the MVP unit.

The  $K_2O$  and U concentrations of the MVP unit are underestimated and overestimated, respectively, due to the high percentage of works regarding Mt. Vulture carbonatitic products, which have very low  $K_2O$  content and extremely high U content. The Th concentration is more likely representative (table 20), because its content is more comparable between carbonatite and other products.

The distributions show the same trend (fig. 22): most of the  $K_2O$  data are very low (carbonatites) and U data are divided between high values (carbonatites) and intermediate values (other rocks).

#### 4.1.12 SIP – Sicilian magmatic province

##### Description

Plio-Quaternary volcanic products of eastern Sicily and Ustica island.

Age: middle Pleistocene – present.

Location of the main outcrops: Mount Etna; Ustica island.

Lithology/composition: basalt, trachybasalt, trachyandesite (mugearite and benmoreite) with tholeiitic affinity in the oldest products and Na-alkaline in the recent ones (Branca *et al.*, 2004).

Genesis/emplacement: Mount Etna and Ustica island formed in a complex geotectonic system and the source of their magma has always been debated. Although the geochemical features of their products differ from one another, some authors assert that they both derive from a mantle plume present beneath the southern Tyrrhenian Sea (Gasparini *et al.*, 2002).

The activity of Mount Etna has been both effusive and Strombolian, with rare explosive events; the activity of Ustica island, on the other hand, was strongly characterized by hydromagmatic events.

##### Statistical analysis

Table 21: descriptive statistic of SIP unit. K<sub>2</sub>O values are expressed in wt%, U and Th values in ppm. N=number of samples. Std.Dev.=standard deviation.

	N	Mean	Median	Minimum	Maximum	25 <sup>th</sup> Percentile	75 <sup>th</sup> Percentile	Std.Dev.	Skewness	Kurtosis
K <sub>2</sub> O	741	1.9	2.0	1.3	2.5	1.9	2.1	0.2	-0.8	0.6
U	510	2.4	2.4	1.3	3.5	2.2	2.7	0.4	0.5	0.9
Th	565	8.5	8.2	3.4	14.2	7.4	9.6	1.8	0.4	0.9

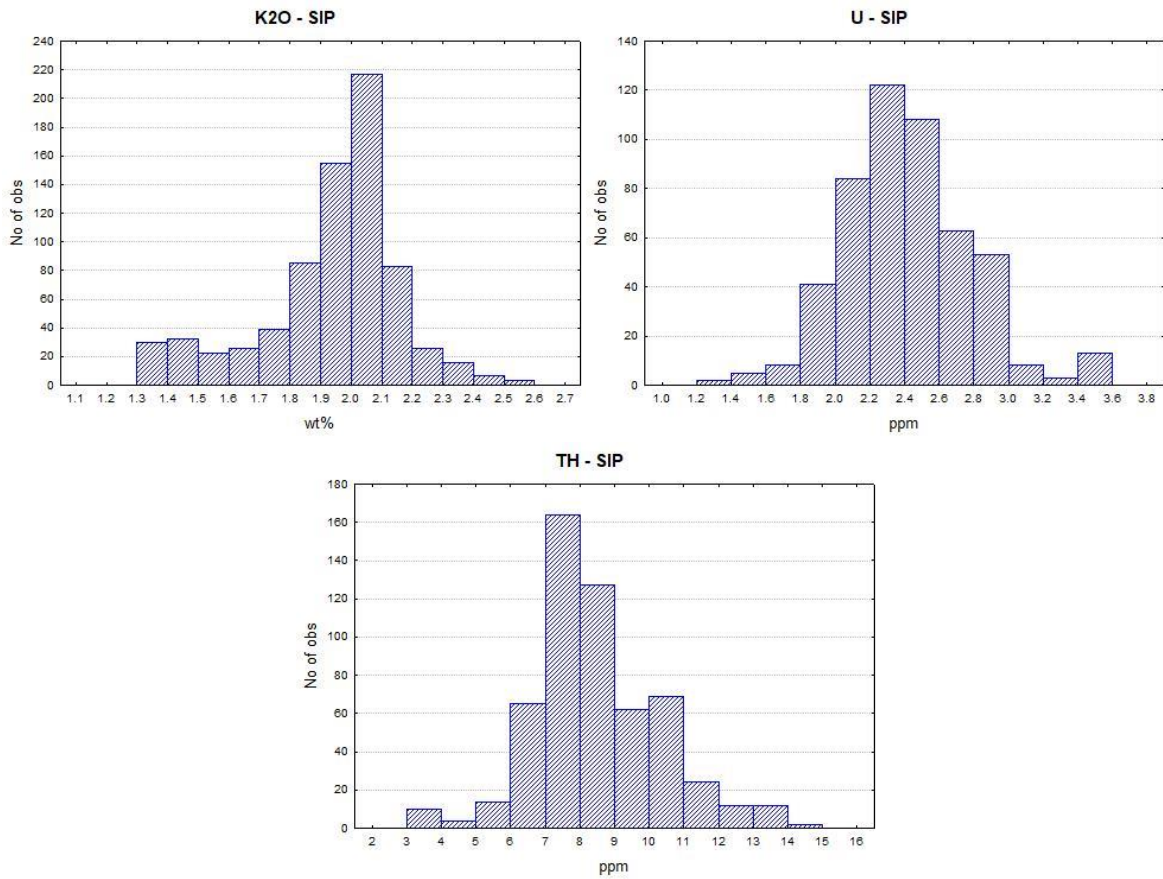


Figure 23: histograms of the  $K_2O$ , U and Th distribution of the SIP unit.

The SIP unit has low  $K_2O$  and U concentrations, while Th content is slightly higher (*table 21*) than that of the average mafic units.

The distributions have high skewness and kurtosis values, but the central bodies can be assimilated to normal distribution (*fig. 23*).

## 4.2 Metamorphic and ultramafic units

### 4.2.1 PM – Paleozoic metamorphic rocks

#### Description

Metamorphic rocks composing the Italian crystalline basement with PI and PV units.

Age: Precambrian – Carboniferous (protolith); upper Carboniferous – Permian (metamorphism).

Location of the main outcrops: tectonic units of the Alpine belt; Ligurian Alps; Tuscan metamorphic ridge (Punta Bianca, Apuan Alps, Monti Pisani, Monticiano-Monti Leoni); Calabrian-Peloritan arc; northern and south-western Sardinia.

Lithology/composition: mafic and felsic metamorphic rocks, mostly consisting of phyllite, schist, gneiss and migmatite. To a lesser extent, in the Alpine nappes, amphibolite, granulite, eclogite and quartzite are also present.

Genesis/emplacement: the protoliths were sedimentary and volcano-sedimentary successions, plutonic/volcanic rocks and rocks from the lower crust; they all underwent metamorphism during the Hercynian orogeny. The rocks of this unit were heterogeneously overprinted by the Alpine metamorphism during Eocene or by the Apennine one during Miocene (Bosellini, 2005), except those forming the Sardinian basement.

#### Statistical analysis

Table 22: descriptive statistic of PM unit.  $K_2O$  values are expressed in wt%, U and Th values in ppm. N=number of samples. Std.Dev.=standard deviation.

	N	Mean	Median	Minimum	Maximum	25 <sup>th</sup> Percentile	75 <sup>th</sup> Percentile	Std.Dev.	Skewness	Kurtosis
$K_2O$	745	2.9	3.1	0.0	7.8	1.5	4.0	1.7	0.1	-0.6
U	560	2.5	2.6	0.0	6.3	1.5	3.4	1.3	0.0	-0.5
Th	659	10.8	11.0	0.0	29.2	6.0	15.0	6.3	0.2	-0.4

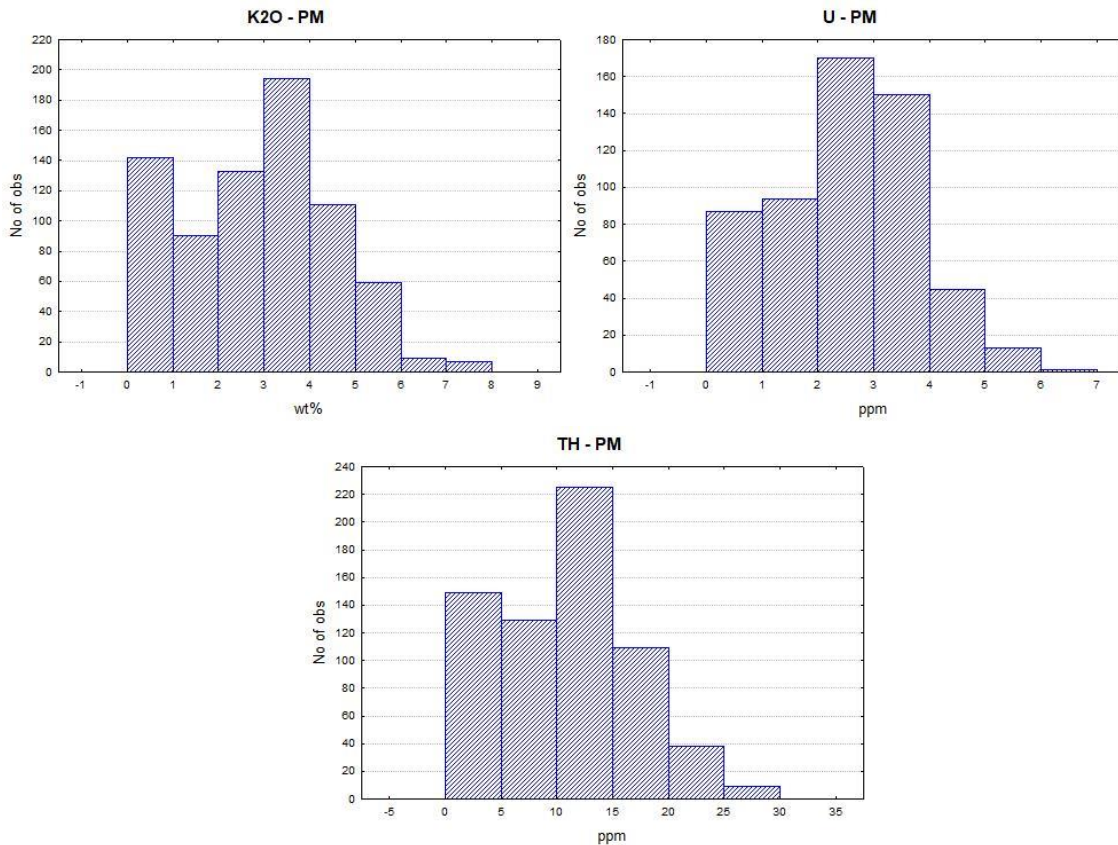


Figure 24: histograms of the K<sub>2</sub>O, U and Th distribution of the PM unit.

The PM unit has lower K<sub>2</sub>O, U and Th concentrations (*table 22*) than the felsic units; it is formed by both mafic and felsic terms because often they were not discernible, so the total average is not representative of the felsic metamorphic part of the upper crust, that should have higher values.

The distributions are quite symmetrical but lack tails (*fig. 24*).

#### 4.2.2 UM – Ultramafic rocks

##### Description

Plutonic and metamorphic ultramafic rocks from Alps and Apennines.

Age: Paleozoic - Mesozoic.

Location of the main outcrops: Alps, north of the Periadriatic Fault System; Liguria; northern Apennine; Tuscany and Elba island; northern Calabria.

Lithology/composition: peridotite, serpentinite, gabbro and ultramafic with cumulus texture (e.g. troctolite, pyroxenite).

Genesis/emplacement: this unit consists of two types of ultramafic rocks:

- the magmatic and heavily weathered portions of Alpine and Apennine Jurassic oceanic lithosphere forming the Valais and Alpine Tethys oceans;
- the upper mantle slices that has been exhumed by Alpine orogeny.

Regardless their origin, all ultramafic rocks were grouped in the same unit because of their extremely low K<sub>2</sub>O, Th and U concentrations.

## Statistical analysis

Table 23: descriptive statistic of UM unit.  $K_2O$  values are expressed in wt%, U and Th values in ppm. N=number of samples. Std.Dev.=standard deviation.

	N	Mean	Median	Minimum	Maximum	25 <sup>th</sup> Percentile	75 <sup>th</sup> Percentile	Std.Dev.	Skewness	Kurtosis
$K_2O$	62	0.1	0.1	0.0	0.5	0.0	0.2	0.1	1.1	0.5
U	84	0.1	0.0	0.0	0.3	0.0	0.1	0.1	1.5	1.5
Th	94	0.1	0.0	0.0	0.5	0.0	0.1	0.1	1.9	2.6

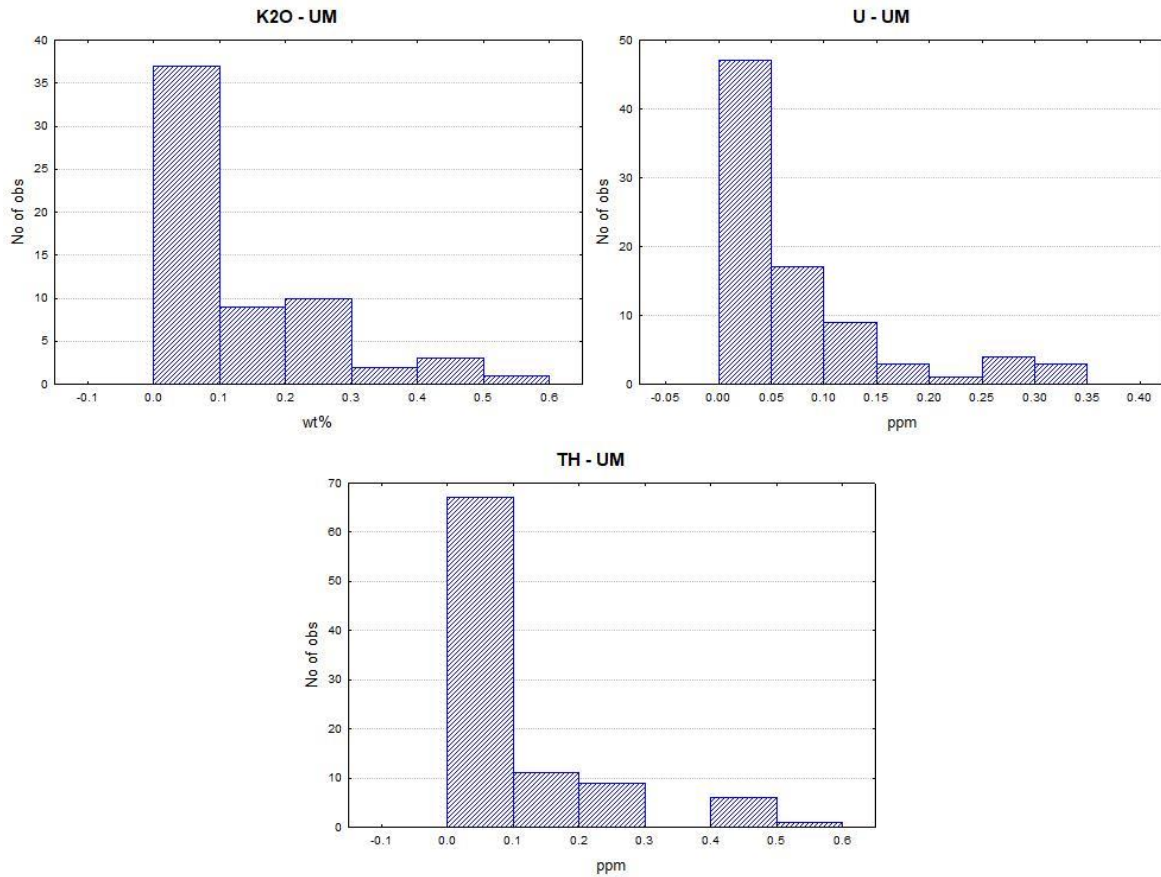


Figure 25: histograms of the  $K_2O$ , U and Th distribution of the UM unit.

The UM unit has the lowest  $K_2O$ , U and Th concentrations (table 23), as it was expected. In many samples the  $K_2O$ , U and Th content is lower or at most slightly higher than the detection limit of the measuring instrument; this leads to great analytical errors that usually occur in situation like this one. Both the descriptive statistic and the histograms (fig. 25) are highly affected by this phenomenon.

### 4.2.3 TM – Tertiary metamorphic rocks

#### Description

Low to medium grade metamorphic rocks that form a considerable volume of the tectonic units of the Alpine belt.

Age: Mesozoic (protolith); Eocene (metamorphism).

Location of the main outcrops: western Alps and Liguria; South Tyrol, near the border with Austria; northern Calabria; little outcrops in Tuscany and Elba island.

Lithology/composition: calcshist (i.e. Bündner schist), phyllite, quartzite and marble.

**Genesis/emplacement:** these metamorphic rocks derive from the Jurassic-Cretaceous oceanic sediments of two basins, the Valais ocean and the Alpine Tethys ocean, which underwent subduction under the Adria plate during the Alpine continental collision: their sedimentary cover (mostly made of micritic limestone and marl with chert intercalations) became part of the Alpine accretionary prism and there it was heavily deformed and metamorphosed (Bosellini, 2005); now they are part of the Penninic domain.

**Statistical analysis**

Table 24: descriptive statistic of TM unit. K<sub>2</sub>O values are expressed in wt%, U and Th values in ppm. N=number of samples. Std.Dev.=standard deviation.

	N	Mean	Median	Minimum	Maximum	25 <sup>th</sup> Percentile	75 <sup>th</sup> Percentile	Std.Dev.	Skewness	Kurtosis
K <sub>2</sub> O	66	1.9	1.6	0.1	4.3	1.0	2.8	1.2	0.6	-0.7
U	39	2.0	2.0	0.3	5.2	1.1	2.7	1.2	0.7	0.1
Th	62	7.2	6.0	0.7	16.8	5.0	9.2	3.9	0.8	-0.1

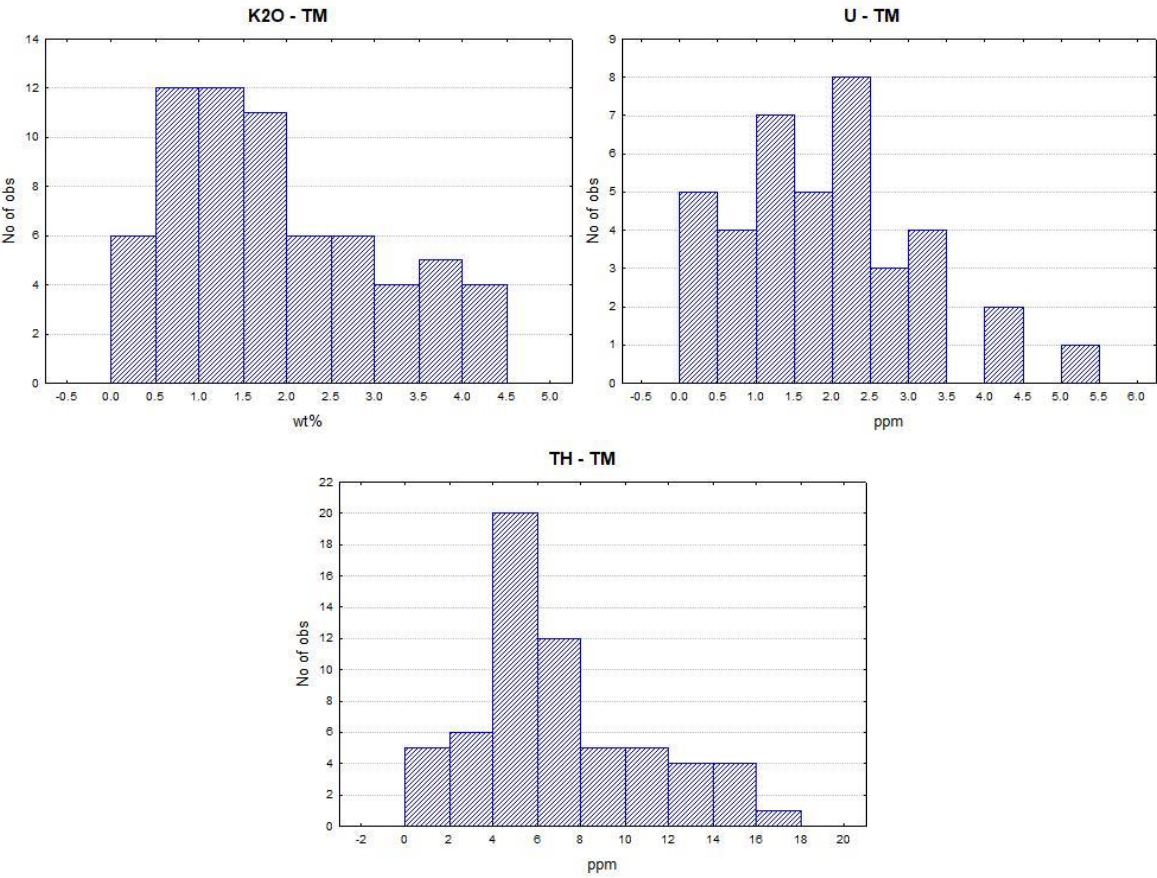


Figure 26: histograms of the K<sub>2</sub>O, U and Th distribution of the TM unit.

The TM unit has low K<sub>2</sub>O, U and Th concentrations (table 24), due to the occurrence of calcschist as the main lithology.

The distributions are asymmetrical (fig. 26), but only K<sub>2</sub>O distribution completely lacks the tails.

## 4.3 Sedimentary units

### 4.3.1 COS – Cambrian-Ordovician-Silurian sedimentary rocks

#### Description

Early Paleozoic marine and continental sedimentary sequences.

Age: upper Precambrian – lower Carboniferous.

Location of the main outcrops: Sardinia; northernmost Carnia.

Lithology/composition: shale, sandstone, conglomerate, limestone.

Genesis/emplacement: these rocks derive from sediments that formed on the northern margin of Gondwana, from different environments: open sea, platform, sabhka, carbonate platform, coast and floodplain, with presence of Ordovician volcanic activity (Pertusati *et al.*, 2000; Pasci *et al.*, 2011; Venturini, 2009). These successions were partly deformed and metamorphosed during Hercynian orogeny.

#### Statistical analysis

Table 25: descriptive statistic of COS unit.  $K_2O$  values are expressed in wt%, U and Th values in ppm. N=number of samples. Std.Dev.=standard deviation.

	N	Mean	Median	Minimum	Maximum	25 <sup>th</sup> Percentile	75 <sup>th</sup> Percentile	Std.Dev.	Skewness	Kurtosis
$K_2O$	24	2.7	2.9	0.0	4.9	1.5	3.9	1.5	-0.3	-1.0
U	23	2.6	2.4	1.3	4.5	2.1	3.1	0.8	0.5	0.5
Th	23	13.1	12.8	8.7	20.5	10.2	15.1	3.2	0.6	-0.1

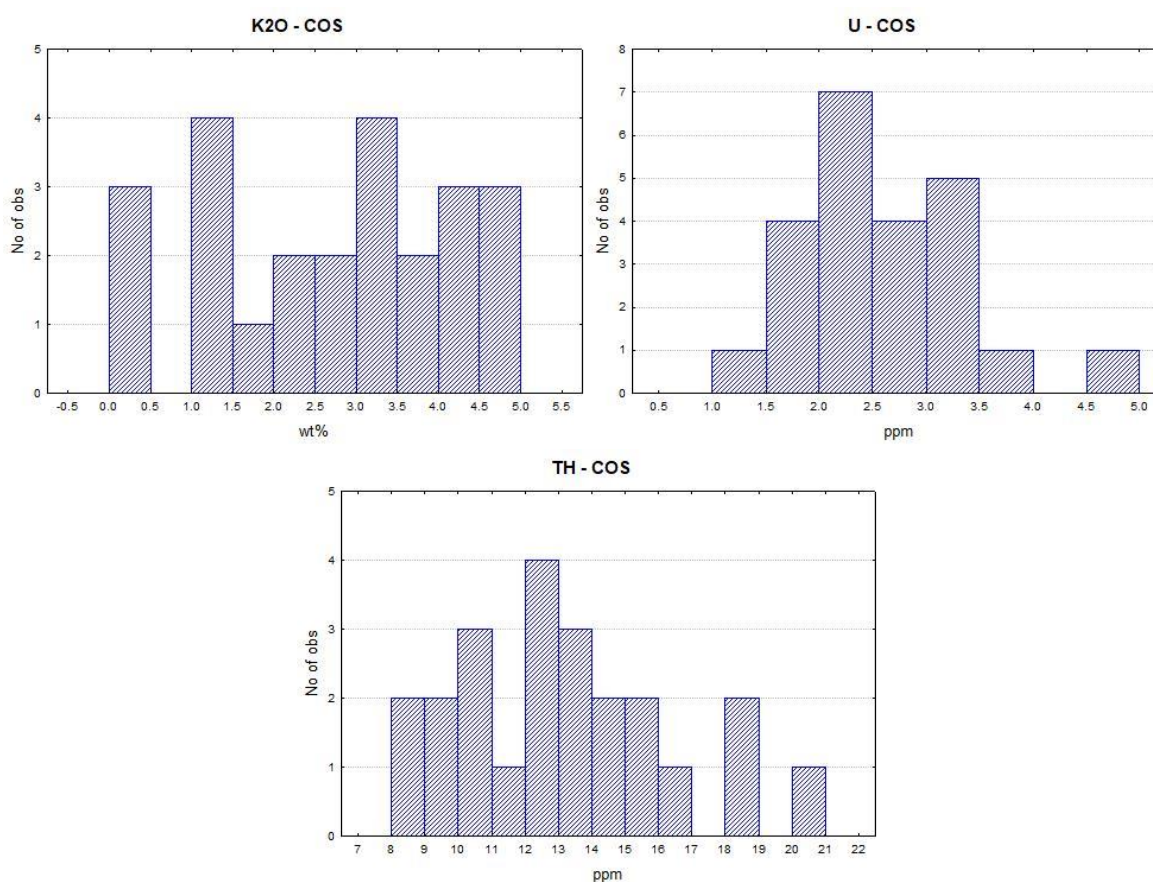


Figure 27: histograms of the  $K_2O$ , U and Th distribution of the COS unit.

The COS unit has intermediate  $K_2O$ , U and Th concentrations (table 25).

The distributions (*fig. 27*) are highly affected by the low number of data, but their body can still be assimilated to a normal distribution.

### 4.3.2 DCPS – Devonian-Carboniferous-Permian sedimentary rocks

#### Description

Late Paleozoic marine and continental sedimentary sequences.

Age: lower Devonian – lower Triassic.

Location of the main outcrops: Sardinia; northern Carnia; middle-eastern Alps; Tuscany.

Lithology/composition: shale, sandstone, conglomerate, limestone.

Genesis/emplacement: first marine and then continental successions which lay in conformity or paraconformity on the COS unit. Sardinian and Carnic DCPS follow the COS unit showing a shallowing upward trend, starting with Devonian-Carboniferous pelagic sediments up to Permian volcanoclastic subaerial sandstones (Funedda *et al.*, 2011); in the Alpine succession there is evidence of a new incoming transgression at the end of Permian, when evaporitic and bioclastic sedimentation begins (Venturini, 2009), due to the fragmentation of Pangea. The few outcrops of DCPS conglomerates in Tuscany form a nonconformity with the Hercynian basement, from which they have formed during Permian (Morini, 2006).

These rocks have been partly deformed and metamorphosed during Hercynian and Alpine orogeny.

#### Statistical analysis

Table 26: descriptive statistic of DCPS unit.  $K_2O$  values are expressed in wt%, Th values in ppm. The U data are missing. N=number of samples. Std.Dev.=standard deviation.

	N	Mean	Median	Minimum	Maximum	25 <sup>th</sup> Percentile	75 <sup>th</sup> Percentile	Std.Dev.	Skewness	Kurtosis
$K_2O$	10	4.7	4.5	3.3	6.5	3.7	5.7	1.2	0.6	-1.1
Th	4	23.5	22.5	21.0	28.0	21.0	26.0	3.3	1.1	0.0

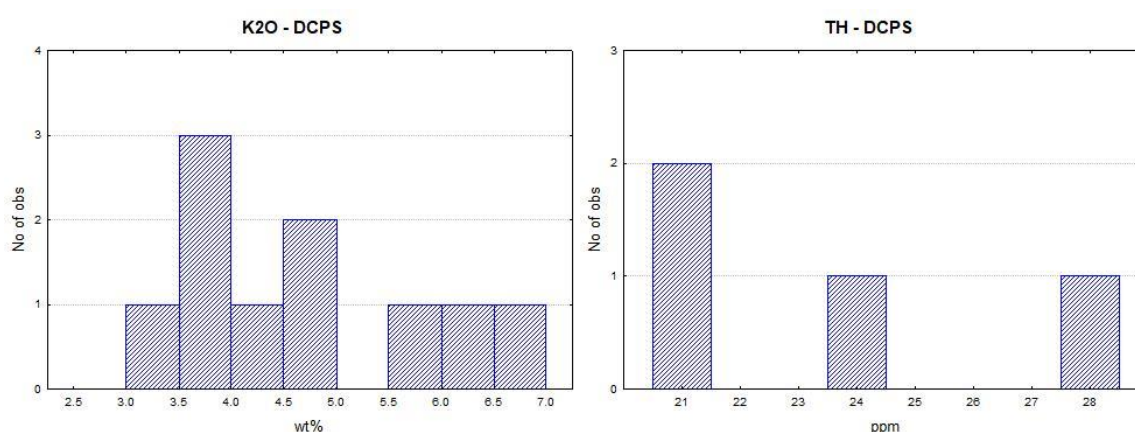


Figure 28: histograms of the  $K_2O$  and Th distribution of the DCPS unit. The U data are missing.

The DCPS unit has high  $K_2O$  and Th concentrations (*table 26*); these average values could be unrepresentative of the entire unit, due to the low number of samples. The U are unavailable.

The small sample population (less than 10 samples per element) prevents the study of the data distribution (*fig. 28*).

### 4.3.3 TS – Triassic sedimentary rocks

#### Description

Early Triassic sedimentary continental succession of Tuscany.

Age: lower-middle Triassic.

Location of the main outcrops: Tuscany.

Lithology/composition: continental sandstone, conglomerate (anagenite) and shale with volcanic and metamorphic clasts, with intercalations of basaltic and andesitic lavas (Abbate *et al.*, 2005).

Genesis/emplacement: this unit consists of the so called “Verrucano”, a succession of continental clastic rocks which originated from the subaerial weathering and erosion of the Hercynian basement, over which they lay in nonconformity.

Both the anchimetamorphic succession, deformed during the Apennine orogeny, and the undeformed one are present: the former is exposed in the Apuan Alps, the latter in other zones such as Elba island and Monte Argentario (Principi *et al.*, 2010).

#### Statistical analysis

Table 27: descriptive statistic of TS unit.  $K_2O$  values are expressed in wt%, U and Th values in ppm. N=number of samples. Std.Dev.=standard deviation.

	N	Mean	Median	Minimum	Maximum	25 <sup>th</sup> Percentile	75 <sup>th</sup> Percentile	Std.Dev.	Skewness	Kurtosis
$K_2O$	6	1.8	0.5	0.1	4.7	0.2	4.6	2.2	0.9	-1.9
U	6	2.2	2.4	0.4	3.6	1.6	2.7	1.1	-0.5	0.5
Th	6	12.4	13.7	2.3	18.3	8.7	17.8	6.1	-1.0	0.3

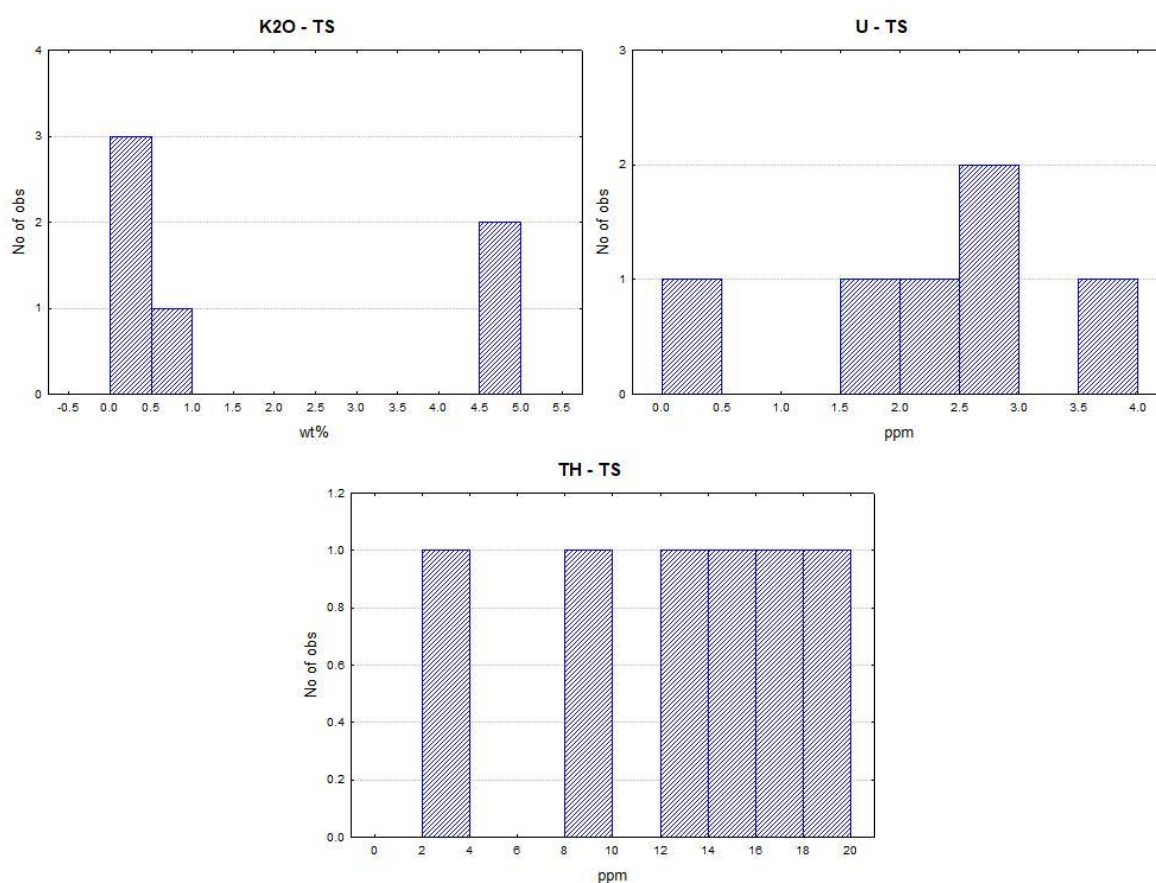


Figure 29: histograms of the  $K_2O$ , U and Th distribution of the TS unit.

The TS unit has intermediate K<sub>2</sub>O, U and Th concentrations (*table 27*); these average values could be unrepresentative of the entire unit, due to the low number of samples and the lithological heterogeneity.

With less than 10 samples per element, it's impossible to study the data distribution (*fig. 29*).

#### 4.3.4 MC – Mesozoic carbonate rocks

##### Description

Successions of biogenic, detrital and, to a lesser extent, clastic sedimentary rocks of mainly carbonate composition, commonly subject to dolomitization.

Age: upper Permian – middle Cretaceous.

Location of the main outcrops: Alps, especially in the Southern Alps domain; central and southern Apennines; middle-eastern and north-western Sardinia; northern part of the Maghreb chain in Sicily; Apulian foreland.

Lithology/composition: limestone, dolostone, evaporite, sandstone.

Genesis/emplacement: during the Mesozoic era the terrains now belonging to the Southern Alps domain were mostly submerged under a shallow sea at an almost tropical latitude; this setting enabled the formation and evolution of several large carbonate platforms and the associated environments. The only place in Italy where this unit is undeformed is Sardinia, where it lays in nonconformity directly upon the Hercynian basement (Bosellini, 2005).

Besides, this unit comprises the Jurassic deep-sea sedimentary members of the ophiolitic successions from Alps and Apennines, formed in the Alpine Tethys.

##### Statistical analysis

*Table 28: descriptive statistic of MC unit. K<sub>2</sub>O values are expressed in wt%, U and Th values in ppm. N=number of samples. Std.Dev.=standard deviation.*

	N	Mean	Median	Minimum	Maximum	25 <sup>th</sup> Percentile	75 <sup>th</sup> Percentile	Std.Dev.	Skewness	Kurtosis
K <sub>2</sub> O	19	1.4	1.3	0.0	3.2	0.3	2.1	1.1	0.5	-0.8
U	19	1.0	0.5	0.1	3.9	0.2	1.4	1.1	1.5	1.7
Th	31	3.1	3.3	0.0	11.0	0.2	5.0	2.7	0.7	0.5

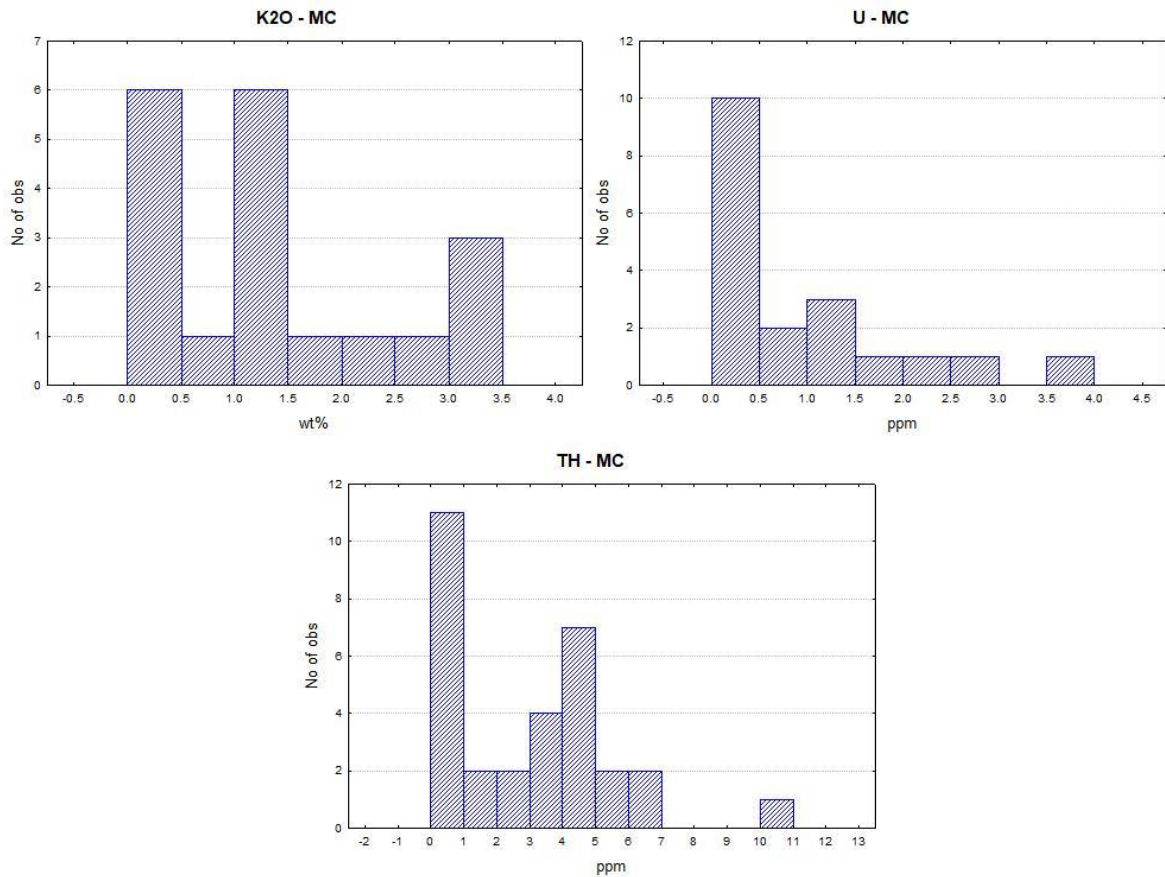


Figure 30: histograms of the K<sub>2</sub>O, U and Th distribution of the MC unit.

The MC unit has very low K<sub>2</sub>O, U and Th concentrations (*table 28*), due to the predominance of carbonate rocks. The K<sub>2</sub>O content is probably overestimated, since a third of the samples collected are biogenic silica rocks, that has higher K<sub>2</sub>O content than limestone and dolostone.

The distributions (*fig. 30*) are highly affected by the low number of data and by the values close to the detection limit.

#### 4.3.5 CdB – “Complissi di base”

##### Description

Chaotic and deformed terrains of the Ligurian Nappe of the Apennines, which are part of the allochthonous ophiolite-bearing units with clayey matrix and blocks/clasts of large dimension of older and contemporary sedimentary formations.

Age: middle Jurassic – upper Oligocene.

Location of the main outcrops: northern and southern Apennines; Tyrrhenian side of Calabria.

Lithology/composition: clayey matrix supported breccia, shale, sandstone.

Genesis/emplacement: these rocks are formed by seafloor sediments of the Alpine Tethys, a branch of the Atlantic Ocean expanding towards east during Jurassic and Cretaceous. The Alpine Tethys divided Eurasian and African plate and therefore began to close at the end of Mesozoic, when the two continents began to collide. The ocean was completely consumed by subduction by the Oligocene-Miocene boundary. This GU overthrusts the

foreland units (Tuscan and Umbria-Marche nappes) during Apennine orogeny and is now the highest tectonic unit of the chain (Elter *et al.*, 2005).

### Statistical analysis

Table 29: descriptive statistic of CdB unit. K<sub>2</sub>O values are expressed in wt%, U and Th values in ppm. N=number of samples. Std.Dev.=standard deviation.

	N	Mean	Median	Minimum	Maximum	25 <sup>th</sup> Percentile	75 <sup>th</sup> Percentile	Std.Dev.	Skewness	Kurtosis
K <sub>2</sub> O	57	3.2	3.1	1.3	5.2	2.6	3.8	1.0	-0.2	-0.4
U	53	2.1	1.9	0.6	5.6	1.2	2.9	1.0	0.8	0.8
Th	58	9.9	9.5	1.7	19.4	6.5	13.2	4.4	0.2	-0.9

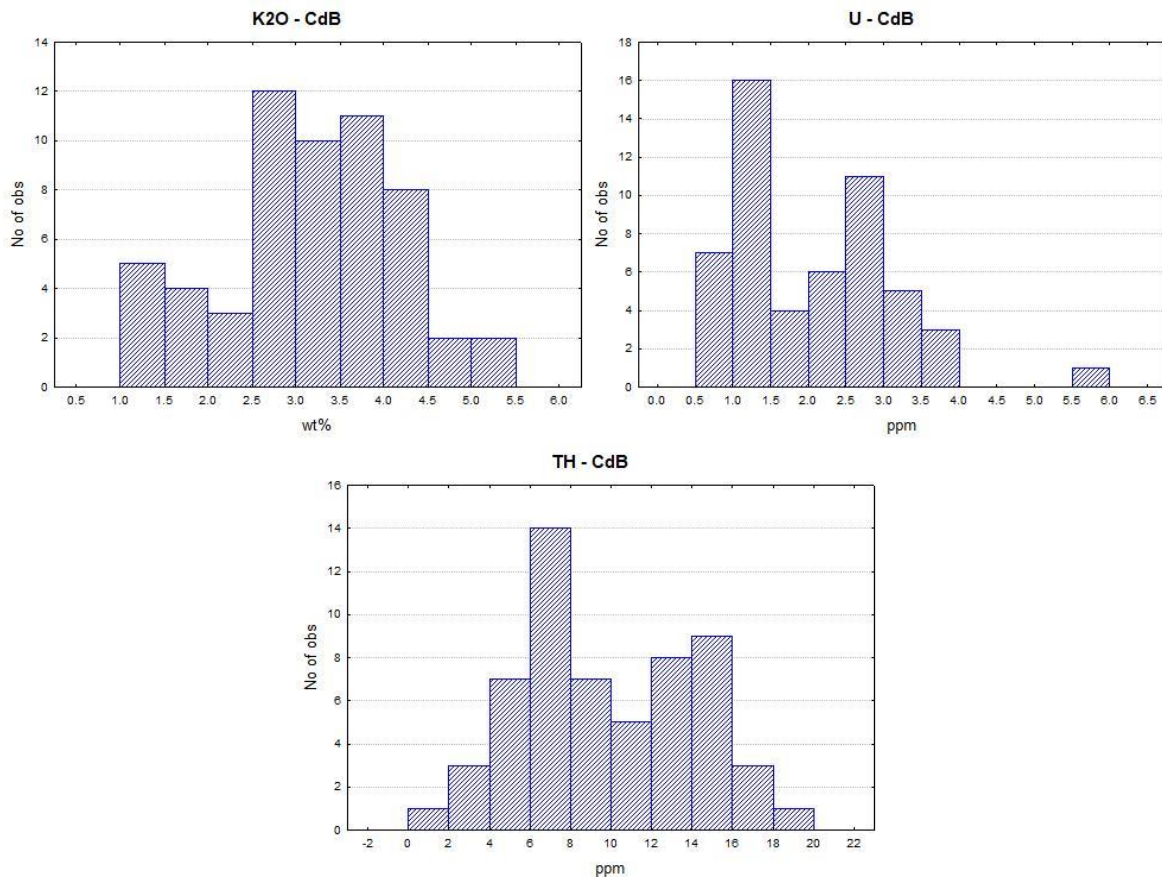


Figure 31: histograms of the K<sub>2</sub>O, U and Th distribution of the CdB unit.

The CdB unit has intermediate K<sub>2</sub>O, U and Th concentrations (*table 29*); usually pelitic sediments show higher U and Th content.

The K<sub>2</sub>O and Th distribution (*fig. 31*) are quite symmetrical but their tails are not well represented; the U distribution seems to be asymmetric due to the absence of negative values.

### 4.3.6 LCPS – Late Cretaceous-Paleogene sedimentary rocks

#### Description

Successions of Adria foreland formed by homogeneous pelagic sedimentation with both siliciclastic and carbonaceous components or torbiditic contribution, without strong influence of the Alpine orogeny. They lay in continuity above the MC sequences.

Age: middle Cretaceous – lower Miocene.

Location of the main outcrops: Apennine-Maghrebian chain; Apulian and Hyblean forelands; north-western Sardinia; western Alps; central and eastern Alpine foothills.

Lithology/composition: mudstone, shale, limestone and biogenic silica sedimentary rocks, mostly of pelagic environment.

Genesis/emplacement: at the end of Mesozoic the relative sea-level on Adria foreland began to rise due to extensional tectonic; the large biohermes construction of the MC unit ceased and pelagic sedimentation began (e.g. Scaglia Fms.); this environment remained stable, for the most part, until Oligocene-Miocene boundary (Damiani, 2011). Areas with topographic lows were characterized by deep sea sedimentation, in a turbidite-like environment; on the contrary, few areas with topographic highs were characterized by shallow water deposition.

### Statistical analysis

Table 30: descriptive statistic of LCPS unit.  $K_2O$  values are expressed in wt%, U and Th values in ppm. N=number of samples. Std.Dev.=standard deviation.

	N	Mean	Median	Minimum	Maximum	25 <sup>th</sup> Percentile	75 <sup>th</sup> Percentile	Std.Dev.	Skewness	Kurtosis
$K_2O$	23	2.7	2.8	0.0	5.1	1.2	4.3	1.7	-0.2	-1.3
U	28	3.9	2.5	0.1	13.0	1.0	6.8	3.8	1.0	-0.2
Th	27	3.5	1.8	0.0	15.0	0.4	5.4	4.2	1.5	1.1

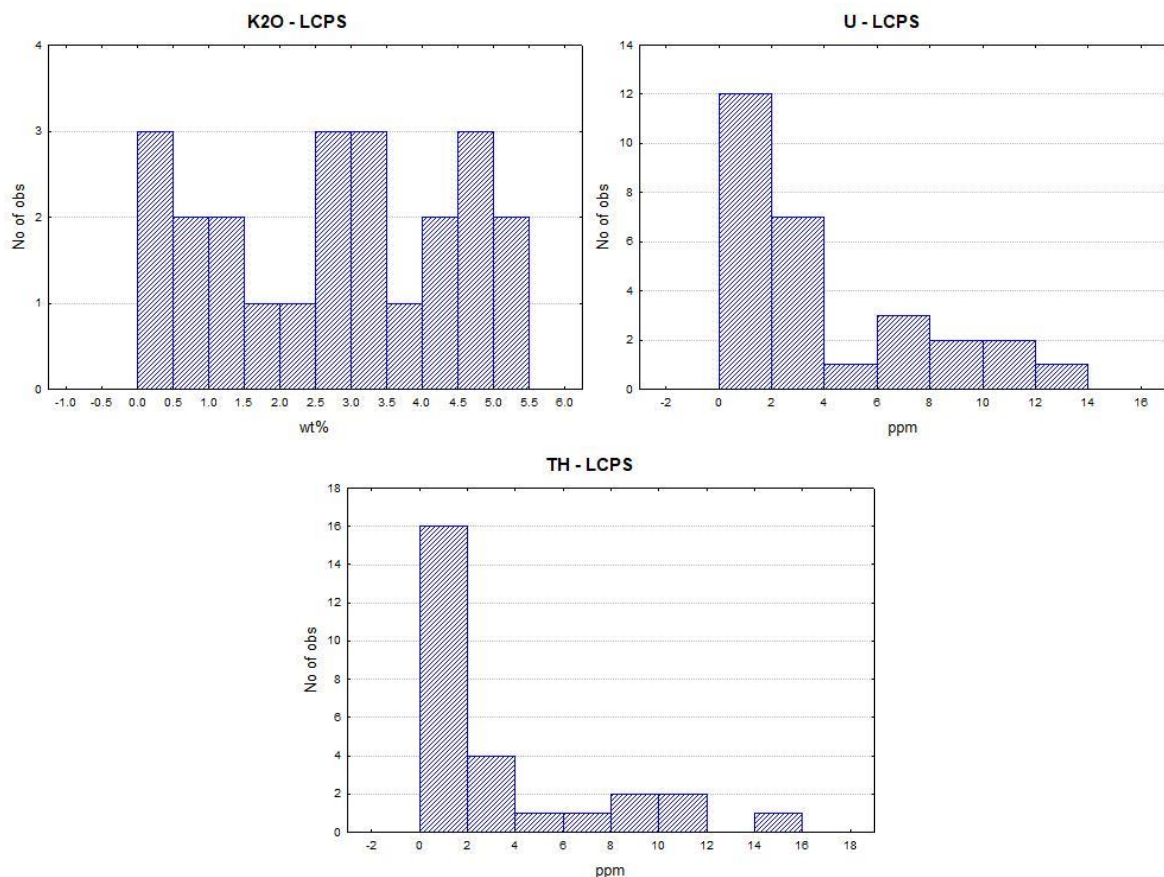


Figure 32: histograms of the  $K_2O$ , U and Th distribution of the LCPS unit.

The LCPS unit has intermediate  $K_2O$  concentration but low U and Th content (table 30). The distributions (fig. 32) are strongly affected by the various different rock types that constitute this GU and by the low number of data.

### 4.3.7 EOMS – Eocene-Oligocene-Miocene sedimentary rocks

#### Description

Sedimentary rocks, both marine and continental, formed during the Alpine orogeny and the beginning of the Apennine one. The greatest contribution to this unit derives from coarse-grained terrigenous sediments of basin-floor and foretrough generating from the new orogenic belts.

Age: upper Paleocene – upper Miocene.

Location of the main outcrops: Alpine foothills; Langhe and western Liguria; Apennine-Maghrebian chain; Sardinia; Apulian and Hyblean foreland.

Lithology/composition: mudstone, sandstone, conglomerates, limestone.

Genesis/emplacement: from early Oligocene to upper Miocene a thick turbiditic succession formed in the Alpine-Apennine foretrough (Gelati *et al.*, 2010); this succession forms large outcrops throughout the entire Apennine-Maghrebian chain, from Liguria down to Sicily, even though it reaches the largest extent in the northern Apennines between Tuscany and Emilia-Romagna (e.g. Macigno fm., Marnoso-Arenacea fm.). It lays in stratigraphic continuity above the previous LCPS unit (Bosellini, 2005).

In the Alpine foothills there are Oligocenic alternations of fine-grained terrigenous sediments that formed in the continental slope and basin in front of the growing Alps (Michetti *et al.*, 2010).

In the southern Apennines and in the Maghrebian chain the turbiditic successions are less represented and they leave room for carbonate rocks from the Adriatic platform, which dates back to Oligocene and Miocene. The same rocks, but undeformed, can be found in the Apulian and Hyblean forelands (Martelli and Nardi, 2005; Carbone and Grasso, 2012; Moretti *et al.*, 2011).

The Sardinian succession goes from fluvial to coastal sandstones and conglomerates, with clasts derived from Oligocene-Miocene volcanic rocks and from the Hercynian basement; it includes platform deposits such as carbonate rocks and marls (Funedda *et al.*, 2012).

#### Statistical analysis

Table 31: descriptive statistic of EOMS unit. K<sub>2</sub>O values are expressed in wt%, U and Th values in ppm. N=number of samples. Std.Dev.=standard deviation.

	N	Mean	Median	Minimum	Maximum	25 <sup>th</sup> Percentile	75 <sup>th</sup> Percentile	Std.Dev.	Skewness	Kurtosis
K <sub>2</sub> O	62	1.7	1.5	0.3	4.0	1.0	2.2	0.9	0.6	-0.1
U	48	2.2	2.2	0.6	4.5	1.4	2.8	0.9	0.4	-0.4
Th	53	8.9	8.0	0.1	19.3	5.6	12.9	4.7	-0.1	-0.8

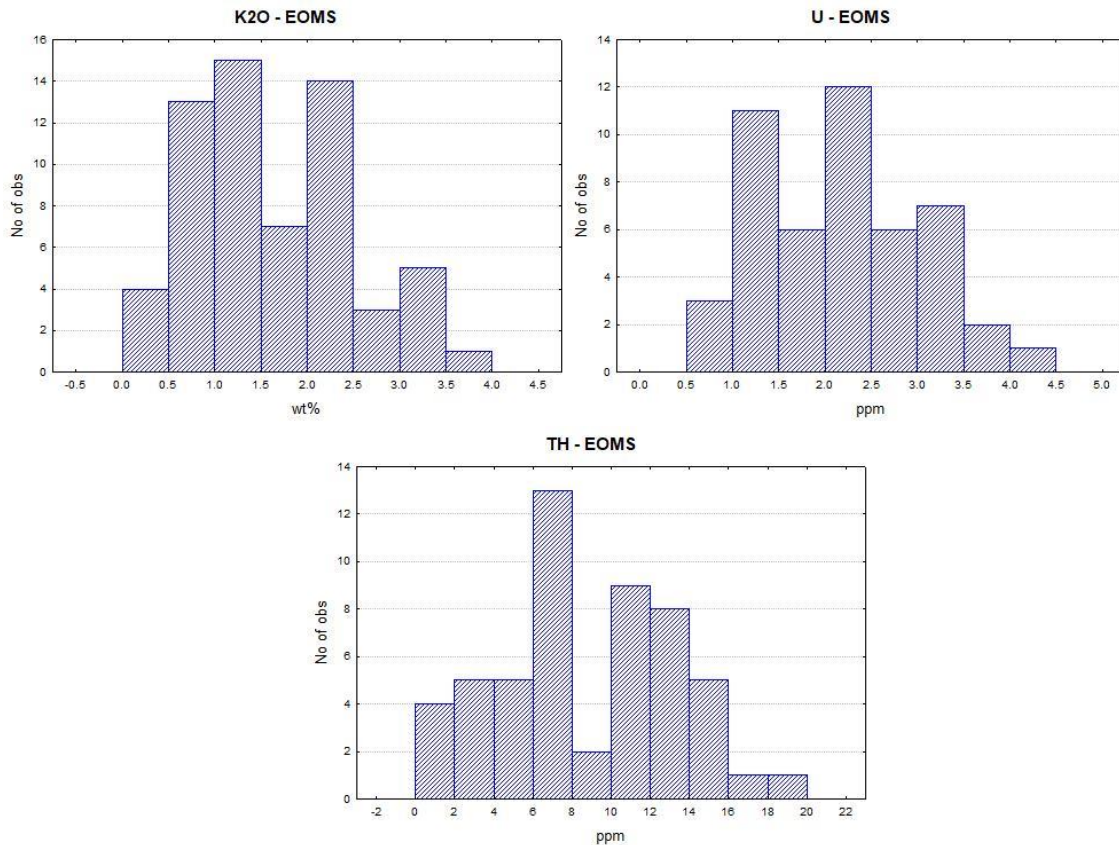


Figure 33: histograms of the K<sub>2</sub>O, U and Th distribution of the EOMS unit.

The EOMS unit has intermediate K<sub>2</sub>O, U and Th concentrations (*table 31*), that are typical of terrigenous sediments.

The distributions (*fig. 33*) are quite symmetrical and they can be assimilated to normal distributions.

#### 4.3.8 ME – Messinian sedimentary rocks

##### Description

Successions mainly composed by evaporites and products of their weathering besides of pelagic sedimentation. It is known historically as “gessoso-solfifera” group or formation, depending on the author.

Age: upper Miocene (Messinian).

Location of the main outcrops: Langhe e Monferrato (Piedmont); central Apennines, on the Adriatic side; southern Sicily; Ionian side of Calabria; middle-eastern Sardinia.

Lithology/composition: halite, gypsum, calcium carbonate and other salts as chemical precipitates; mudstone and sandstone.

Genesis/emplacement: during lower Messinian, when the Gibraltar Strait tectonically closed and the Mediterranean Sea became isolated, the basin saw its water level decrease by around 1.5 km (Christeleit *et al.*, 2015); this led to the deposition of a thick sequence of evaporitic deposits (mostly CaCO<sub>3</sub>, CaSO<sub>4</sub>×2H<sub>2</sub>O and NaCl) throughout the Mediterranean area. When the Gibraltar Strait re-opened during middle Messinian, the subaerial and subaqueous weathering of the evaporitic sequences produced clastic sediments made up of the former constituents (Deiana, 2009).

The Sardinian deposits differ from the other ones: the successions are formed by carbonates with intercalations of marls and shales, without any trace of sulphates or chlorides (Barca *et al.*, 2011).

### Statistical analysis

Table 32: descriptive statistic of ME unit. K<sub>2</sub>O values are expressed in wt%, U and Th values in ppm. N=number of samples. Std.Dev.=standard deviation.

	N	Mean	Median	Minimum	Maximum	25 <sup>th</sup> Percentile	75 <sup>th</sup> Percentile	Std.Dev.	Skewness	Kurtosis
K <sub>2</sub> O	32	2.1	2.2	1.2	2.6	2.0	2.3	0.4	-1.0	0.5
U	44	3.7	3.3	0.9	9.0	2.2	5.0	2.0	0.8	0.0
Th	44	7.5	7.0	2.3	14.3	5.3	9.5	3.1	0.5	-0.5

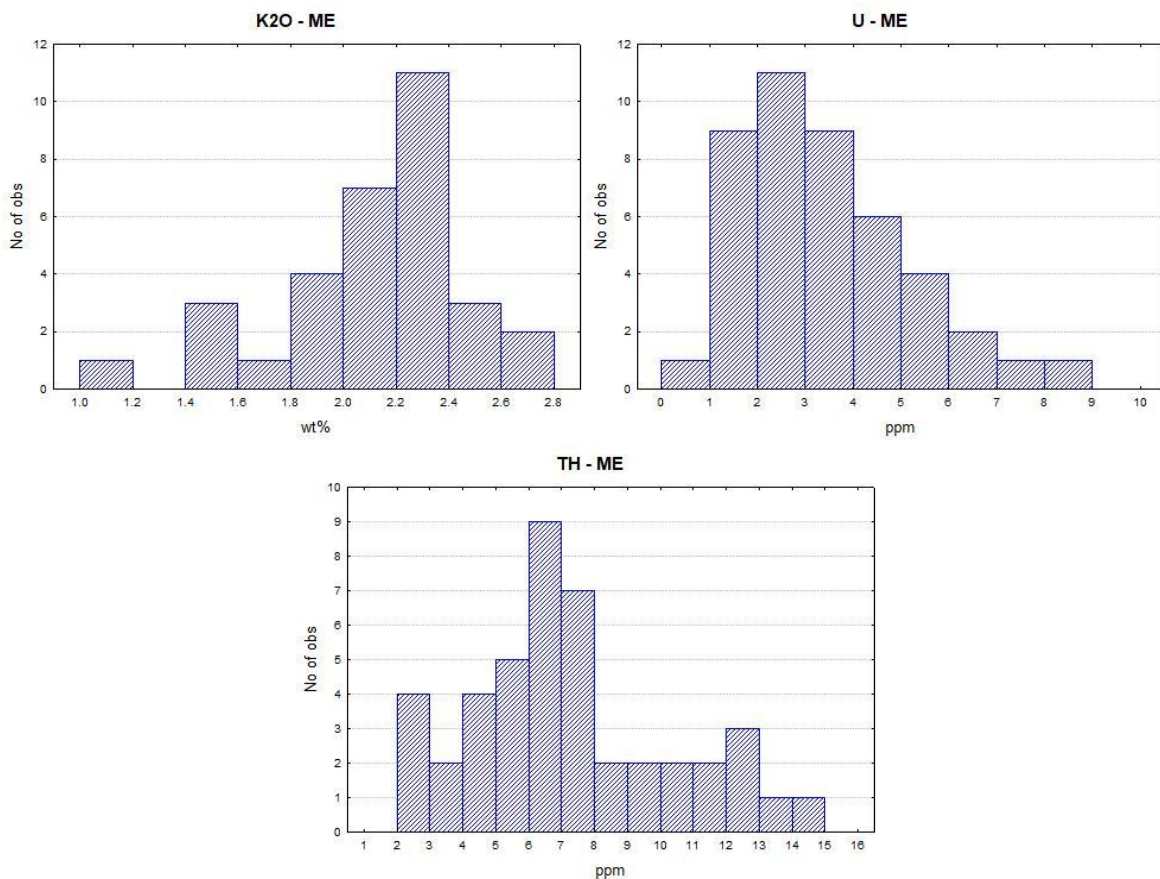


Figure 34: histograms of the K<sub>2</sub>O, U and Th distribution of the ME unit.

The ME unit has intermediate K<sub>2</sub>O, U and Th concentrations (*table 32*). These values could not be representative for the entire unit because of the low amount of analysis regarding evaporites that we found in scientific literature.

The distributions (*fig. 34*) are asymmetrical, but their body can still be assimilated to a normal distribution.

### 4.3.9 PLS – Pliocene sedimentary rocks

#### Description

Pliocene sedimentary successions of the Apennine-Maghrebian chain.

Age: lower-upper Pliocene.

Location of the main outcrops: front of the Apennine-Maghrebian chain and Ionian side of Calabria.

Lithology/composition: marl, sandstone, conglomerate.

Genesis/emplacement: terrigenous and pelagic sediments that formed in Pliocene in a coastal environment at the front of the advancing orogeny. During late Pliocene and Pleistocene these sediments have been uplifted by the orogeny and they are now part of the subaerial front of the Apennines. In Calabria, they've been uplifted by the isostatic reaction of the Calabrian-Peloritan arc to the slab detachment (Bosellini, 2005).

### Statistical analysis

Table 33: descriptive statistic of PLS unit. The values for skewness and kurtosis of the U distribution are missing because two samples were not sufficient to define them. K<sub>2</sub>O values are expressed in wt%, U and Th values in ppm. N=number of samples. Std.Dev.=standard deviation.

	N	Mean	Median	Minimum	Maximum	25 <sup>th</sup> Percentile	75 <sup>th</sup> Percentile	Std.Dev.	Skewness	Kurtosis
K <sub>2</sub> O	37	2.1	2.1	1.9	2.4	2.1	2.2	0.1	0.1	0.3
U	2	2.5	2.5	2.3	2.7	2.3	2.7	0.3		
Th	48	9.5	10.0	1.7	17.0	7.0	12.0	4.1	-0.4	-0.5

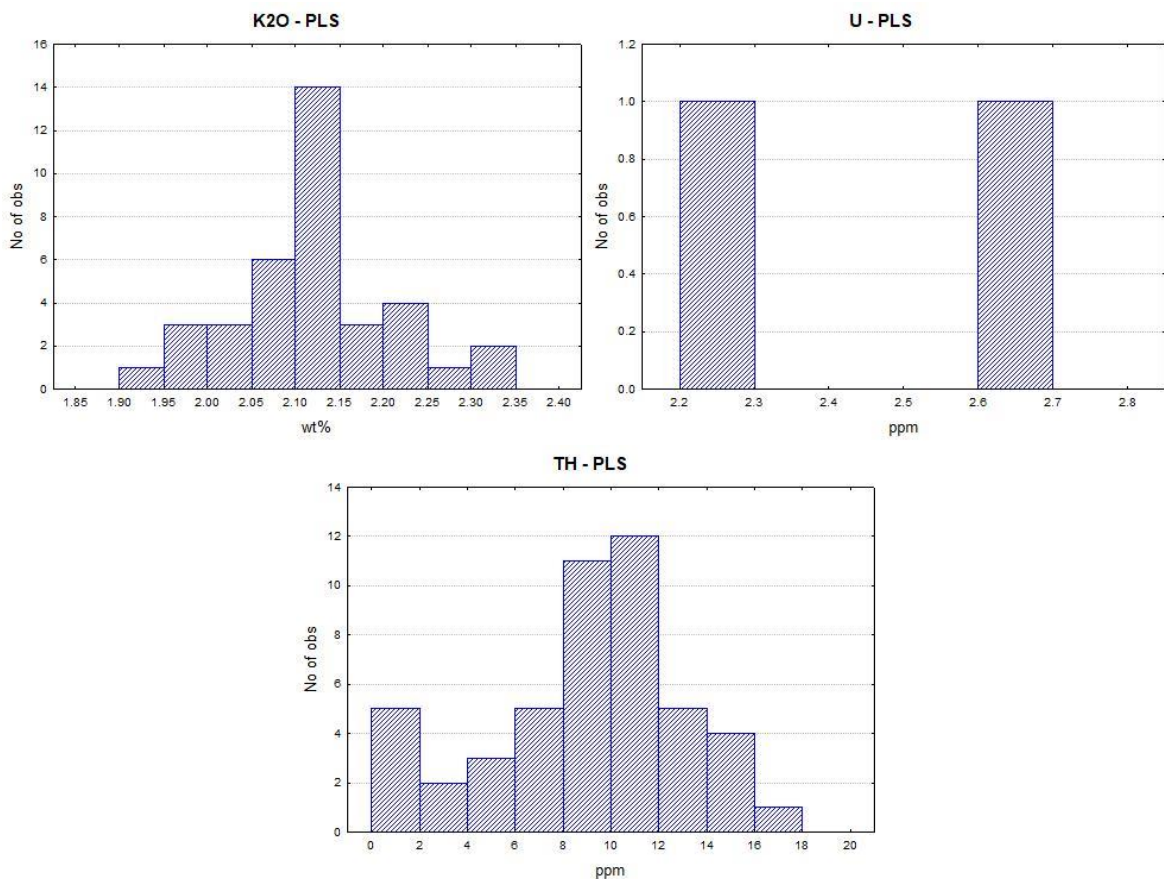


Figure 35: histograms of the K<sub>2</sub>O, U and Th distribution of the PLS unit.

The PLS unit has intermediate K<sub>2</sub>O and Th concentrations (table 33), that are typical of terrigenous sediments. The U content is probably not representative of the entire GU. The K<sub>2</sub>O and Th distributions (fig. 35) are quite symmetrical and they can be assimilated to normal distributions. There are too few U data in order to study their distribution.

#### **4.3.10 Q – Quaternary deposits**

The Q unit, which was not examined in this work, includes all the Plio-Quaternary continental and coastal unconsolidated deposits. The contribute of this unit to the natural radiation will be taking into account in the maps of  $K_2O$ , U and Th concentration in soil of the EANR.

## 5. DISCUSSION

### 5.1 Validation of the GU methodology

As we have seen before, the methodology used in this work has its disadvantages and problems. The method, consisting in creating GUs with geological knowledge and deriving the punctual data from geoscience literature, has been already tested in previous works; the maps of K<sub>2</sub>O, U and Th created so far have showed a fair resemblance with the terrestrial gamma dose rate maps, that show the measured radioactivity due to the decay of the radioisotopes of K, U and Th (Cinelli *et al.*, 2018). The relatively good agreement between them gives confidence on the reliability of the concentration maps.

In order to quantify the effects of some of the problems, the ANOVA test was used to analyse the variance of the different groupings. All the groups of data that included less than 10 samples were discarded during this testing, because the ANOVA loses too much significance when applied to smaller number of samples; so, the variables that involved small groups could not be represented in this analysis. We made the assumption that the results obtained with the bigger groups were valid for the smaller groups as well.

First, we wanted to test the variance due to the 16 different analytical techniques present in the database. They include:

- X-ray Fluorescence Spectroscopy (XRF);
- Inductively Coupled Plasma techniques (labelled as ICP if not differentiated): Mass Spectrometry (ICPMS/MC-ICPMS-ID/MC-ICPMS/LA-ICPMS) and Atomic or Optical Emission Spectrometry (ICPAES/ICPOES);
- Gamma-Ray Spectrometry (GRS);
- other types of Mass Spectrometry: Thermal Ionization and/or Isotope Dilution (TIMS/TIMS-ID/MS-ID) and Thermal Desorption (TDMS);
- Atomic Absorption Spectrometry (AAS);
- Neutron Activation Analysis (INAA/NAA).

In order to check if these methods involved strong variations in the measurements, the concentration values of some GUs lithologies represented by a high number of samples were tested with the ANOVA. We considered the concentration as the dependent variable and the analytical method as the independent one; the decision of studying the behaviour of the data included in single GUs was made with the purpose of reducing the natural variability as much as possible. The results of the testing are reported in *table 5*. The percentages of variation show that, in the worst-case scenario, the analytical method is responsible for the 27% of the total variance, although in most cases the percentage is much lower, around 1-15%. As a matter of fact, rocks with homogeneous composition, like SIP trachybasalts from Mount Etna, have really low percentage of variations. This means that the differences due to the analytical methods are not a major cause of variability between similar rocks.

Table 34: results of the ANOVA tests for the variance introduced with the analytical method. The "METHODS" rows indicate the number of different methods that was involved in that test.

K <sub>2</sub> O	PHONOLITE - CAP	TRACHYTE - CAP	TRACHYBASALT - SIP	GNEISS - PM	BASALT - AEPm
<b>METHODS</b>	2	3	3	3	5
<b>Percentage of variation</b>	1.6	3.8	2.3	0.8	12.8
U	PHONOLITE - CAP	TRACHYTE - CAP	TRACHYBASALT - SIP	GNEISS - PM	BASALT - AEPm
<b>METHODS</b>	2	NA	2	2	4
<b>Percentage of variation</b>	26.7	NA	4.7	1.0	20.7
Th	PHONOLITE - CAP	TRACHYTE - CAP	TRACHYBASALT - SIP	GNEISS - PM	BASALT - AEPm
<b>METHODS</b>	2	NA	4	2	4
<b>Percentage of variation</b>	24.1	NA	4.5	0.1	10.2

Since we proved that the analytical method has a limited influence on the variation of data composition, we studied the effect due to the variation of lithology. The GUs have, in some cases, a high lithological variability (e.g. the LTP unit, which includes from mafic to felsic magmatic terms, see *table 2*) and it was necessary to estimate its effect on the variability of the concentrations.

As a first step, we ran the ANOVA test on the entire dataset for each of the three elements, setting the concentration as the dependent variable and, as the independent one, first the lithology and then the GU. The results are shown in *table 6*.

Table 35: results of the ANOVA tests for the variance on the entire dataset based on lithological (left) and GU (right) division. The "LITHO" and "GU" rows indicate the number of different lithologies and GUs, respectively, that were involved in that test. IV: independent variable.

IV: lithology	K <sub>2</sub> O	U	Th	IV: GU	K <sub>2</sub> O	U	Th
<b>LITHO</b>	49	45	48	<b>GU</b>	28	26	27
<b>Percentage of variation</b>	77.1	60.3	45.6	<b>Percentage of variation</b>	74.3	60.2	52.2

The test pointed out that both the lithology and the GUs cause a large effect on the variability of the concentrations and this effect has approximately the same value for both of them. Therefore, the GUs created maintain a level of variability comparable to that of the lithology.

The subsequent step was to define how much variation, inside the GUs, is accounted for by lithology. We ran another ANOVA test, this time considering the GUs as separate populations, using the concentration as the dependent variable and the lithology as the independent one. The results are shown in *table 7*.

Table 36: results of the ANOVA tests for variance due to lithology in the single GUs. The "LITHO" row indicates the number of different lithologies that were involved in that test.

K <sub>2</sub> O (A)	LTP	PNVf	PNVm	EOMS	Pif	PM	AEPf	AEPm	CAP	SAPm	SIP	PV
LITHO	18	3	6	2	3	11	3	4	8	4	3	3
Percentage of variation	58.9	29.0	33.4	0.3	33.6	35.6	37.8	34.6	20.4	43.6	6.9	37.9
U (B)	LTP	PNVf	PNVm	EOMS	Pif	PM	AEPf	AEPm	CAP	SAPm	SIP	PV
LITHO	15	NA	4	NA	3	11	3	4	9	NA	3	3
Percentage of variation	28.0	NA	26.9	NA	18.8	28	54.1	17.5	28.5	NA	6.8	12.5
Th	LTP	PNVf	PNVm	EOMS	Pif	PM	AEPf	AEPm	CAP	SAPm	SIP	PV
LITHO	17	NA	6	2	3	12	3	4	9	NA	2	3
Percentage of variation	42.9	NA	29.4	3	15.0	36	54.9	23.5	31.5	NA	6.4	42.9

As the table shows, the test results state that, on average, 25-35% of the variance inside the GUs is attributable to the difference in lithology. From the initial >50% variability due to lithology, the value dropped down to ≈30%; so we can assert that the GU grouping statistically decrease the variability of rock composition.

There are some GUs, though, which shows a distinct behaviour: LTP, AEPf and SAPm have higher values than average (>40%).

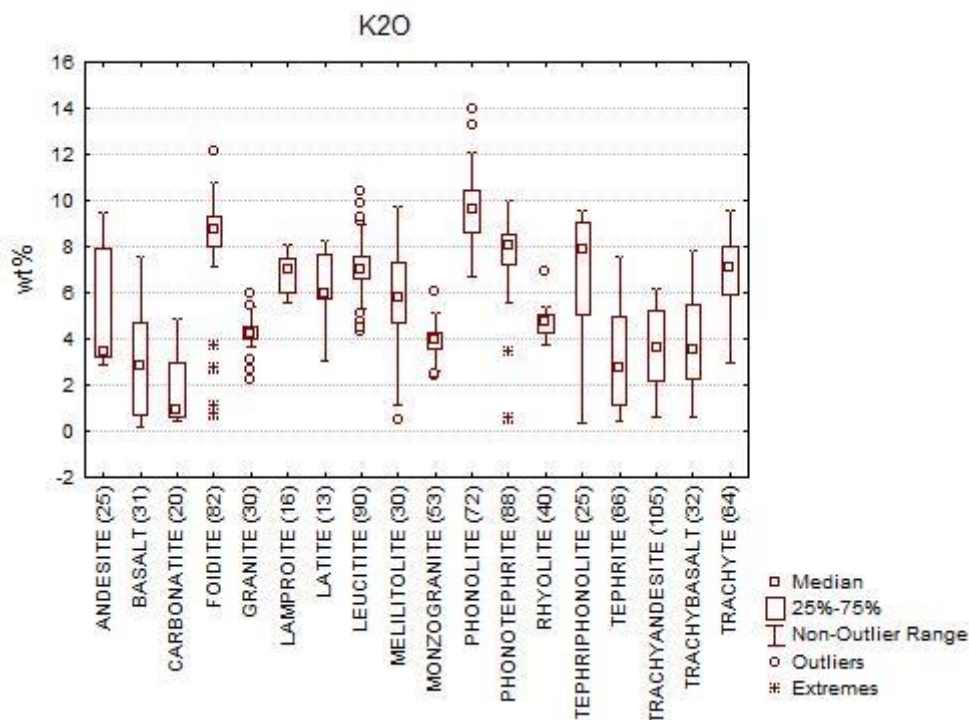


Figure 36: box plot of K<sub>2</sub>O concentration divided by lithology in LTP unit. The box plots for U and Th show a similar trend. Only lithologies with more than 10 samples are shown.

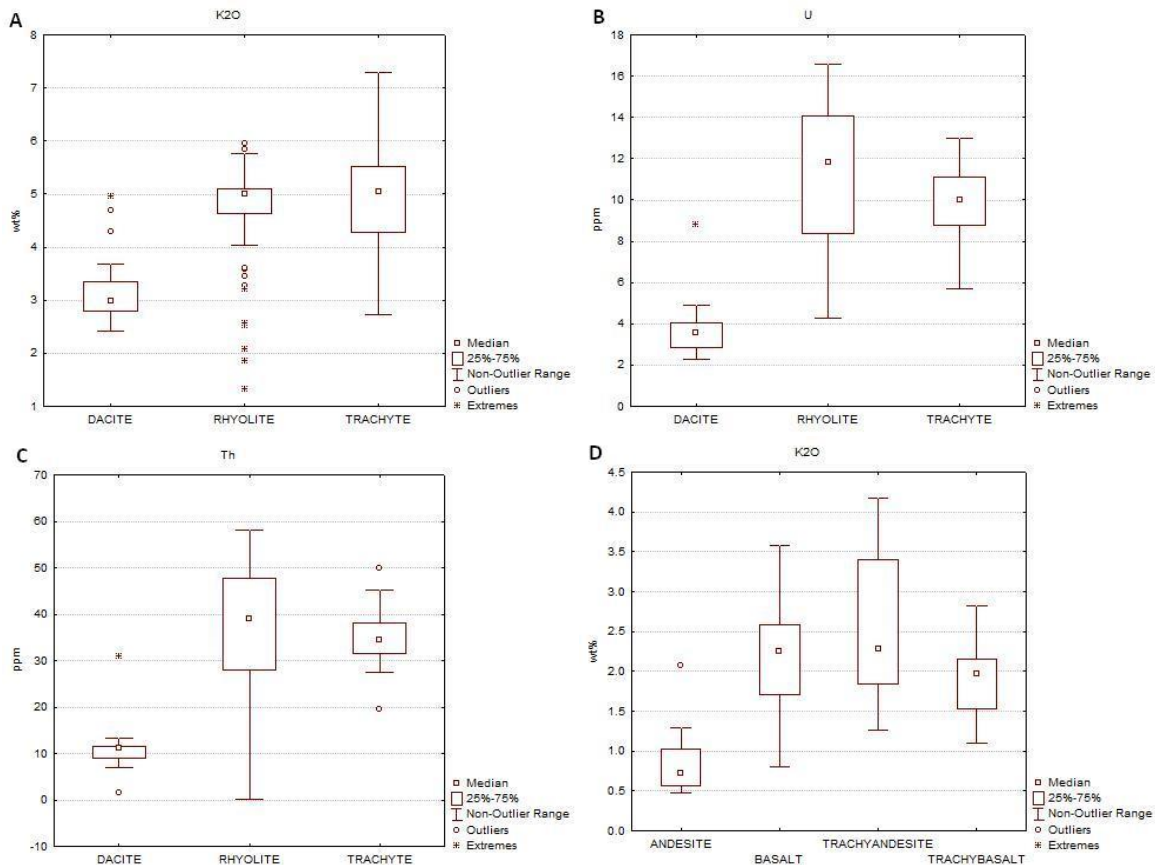


Figure 37: box plots of  $K_2O$ , U and Th concentration in AEPf (A, B, C) and SAPm (D) units. Only lithologies with more than 10 samples are shown.

For instance, LTP has the highest number of lithologies of all the GUs (*fig. 36*), since it contains rocks originated from various volcanic districts; even though these districts generated in the same large scale geotectonic context, their products can show substantial differences in  $K_2O$ , U and Th content. A way to partially solve this problem could be to divide this unit between Tuscany and Lazio region, in order to limit the great variability.

The problem with AEPf and SAPm is slightly different, because their lithological variability is small (*fig. 37*) compared to the LTP variability and so the number of lithologies cannot be the primary source of that. As it's clear from the box plots in *figure 37*, the cause of the problem is related to the discordance between the  $K_2O$ , U and Th concentration of dacite (for AEPf) and andesite (for SAPm) and the other lithologies. The dacitic and the andesitic products, respectively, are different from the other rock types due to either their real composition or the heterogeneous sampling, or a combination of the two.

Finally, we wanted to be sure that using the GUs in the map was a better, or at least equal, choice than simply using the lithologies.

A lithology can be defined with various criteria:

- For intrusive rocks, the classification is based on the modal composition of minerals, that is only partially related to the chemical composition;
- For volcanic rocks, the classification is based on the TAS diagram, so it directly depends on the chemical composition;
- For metamorphic rocks, the classification is based on visible features, usually minerals or structures due to deformation;

- For sedimentary rocks, there are several different classifications based on grain size, amount of matrix, etc., and more often than not these classifications don't take into account the chemical composition.

So the compositions related to a lithology are not always homogeneous by definition. In order to find out how much they can vary, we ran an ANOVA test considering the lithologies as single populations: we set the composition as the dependent variable and the GU as the independent one. The results are shown in *table 8*.

*Table 37: results of the ANOVA test for variance due to GU in single lithologies, considering the entire dataset. The "GU" rows indicate the number of different GUs that were involved in that test.*

<b>K2O</b>	<b>BASALT</b>	<b>MUDSTONE</b>	<b>RHYOLITE</b>	<b>SHALE</b>	<b>TRACHYANDESITE</b>	<b>TRACHYTE</b>
<b>GU</b>	7	3	6	3	5	6
<b>Percentage of variation</b>	40.7	54.9	4.2	37.2	52.4	56.2
<b>U</b>	<b>BASALT</b>	<b>MUDSTONE</b>	<b>RHYOLITE</b>	<b>SHALE</b>	<b>TRACHYANDESITE</b>	<b>TRACHYTE</b>
<b>GU</b>	7	NA	6	3	4	4
<b>Percentage of variation</b>	61.2	NA	58.8	25.7	5.6	59.7
<b>TH</b>	<b>BASALT</b>	<b>MUDSTONE</b>	<b>RHYOLITE</b>	<b>SHALE</b>	<b>TRACHYANDESITE</b>	<b>TRACHYTE</b>
<b>GU</b>	8	3	6	NA	3	3
<b>Percentage of variation</b>	59.9	16.8	33.0	NA	24.2	32.6

The test results show that, on average, the variance inside the lithology due to the GUs (35-45%) is higher than the variance inside the GUs due to the lithology (25-35%). This result supports the choice of using the Geological Units, even though the methodology remains improvable. In this work, anyway, the use of the lithology rather than the GU wasn't possible, because the geological divisions in OneGeology-Europe cartography wasn't based on single lithologies, as we saw in chapter 3.2. Obviously, using a small-scale lithology-based classification would lead to better results, but the amount of available data was not sufficient for such a detailed analysis.

## 5.2 Results and maps discussion

After validating the methodology for the creation of the database and the units, the subsequent step was to select the statistical parameter that could describe the populations in the best way. As we saw before, the data don't fit perfectly normal distributions, due to several factors:

- the natural absence of negative values that affects the left tail of the distributions;
- the different compositions of the lithologies, that could cause multi-modal distributions or a great dispersion of the values;
- the instrumental errors occurring when the concentration value is near or below the detection limit;
- the heterogeneity and the consequent unrepresentativeness of the sampling;
- and, for the least represented units, the low number of data.

Therefore, the distributions of the GUs data are affected by many uncertainties. In order to test statistically the normality of the distributions, we made a normal probability plot associated with a Shapiro-Wilk test for each of the three elements for every GU (all the graphics can be found in *appendix C*, together with the box plots of the GUs based on their different lithologies): the S-W test results showed that only 12 GUs have at least one distribution that can be considered normal. We tried the same test with the lognormal distributions, but the results were even worse.

Then we took into consideration only the normal probability plots and the forms of the distributions.

6 populations have too few samples ( $K_2O$ , U and Th of TS;  $K_2O$  and Th of DCPS; U of PLS) and their distributions can't be studied. Out of the other 81 populations, the body of the data for 68 of them fit well in a normal distribution and only the tails deviate from the trend. Since the tails suffer more from the problems listed before, we considered these as normal distributions and we chose the arithmetic mean as the better parameter to represent them for mapping purpose.

The last 13 populations are neither normal or lognormal, so we tried to understand what causes their anomaly:

- the  $K_2O$ , U and Th data of the UM unit are extremely affected by the instrumental errors due to the very low concentrations;
- the amount of U data of the MC unit is quite small and the concentration values tend to be lower than 1 ppm, so that the distribution is highly affected by the absence of negative values;
- the U data of the Plm unit can't fit well in a normal distribution due to the fact that two third of the sample's concentrations spread across only 2 values (2.0 and 3.0 ppm). Since these analyses come all from the same article, this could be due to an analytical error or a sampling bias;
- the problem of the other populations (U of CdB; Th and U of LCPS;  $K_2O$  of MVI;  $K_2O$  and U of MVP;  $K_2O$  and Th of SSDm) is related to their multi-modal distribution.

After having established the main causes of the anomalies among the distributions, we decided to consider all of them as they were normal distributions, since it seems to be the

best statistical way to represent the GUs, despite the results of the Shapiro-Wilk tests. So, the arithmetic mean was chosen as the best parameter to represent the K<sub>2</sub>O, U and Th concentrations. A schematic summary of the results is shown in *table 38* and *39*.

*Table 38: K<sub>2</sub>O, U and Th arithmetic mean and standard deviation for every GU.*

GU	K <sub>2</sub> O (wt%)	U (ppm)	Th (ppm)	GU	K <sub>2</sub> O (wt%)	U (ppm)	Th (ppm)
Pif	3.6±1.0	2.4±1.6	11.7±5.9	MVP	1.1±1.4	36.8±20.6	69.0±25.1
Plm	1.0±0.5	2.1±0.9	2.6±1.6	SIP	1.9±0.2	2.4±0.4	8.5±1.8
PV	3.6±1.9	3.4±1.1	16.9±5.2	PM	2.9±1.7	2.5±1.3	10.8±6.3
MVI	3.0±1.9	1.5±0.7	5.3±3.1	UM	0.1±0.1	0.1±0.1	0.1±0.1
PNI	1.8±0.8	3.1±1.7	11.1±6.6	TM	1.9±1.2	2.0±1.2	7.2±3.9
PNVf	4.6±1.2	5.7±2.0	23.3±7.4	COS	2.7±1.5	2.6±0.8	13.1±3.2
PNVm	1.2±0.7	1.4±1.0	6.4±3.8	DCPS	4.7±1.2	NA	23.5±3.3
LTP	5.8±2.8	11.4±7.5	56.6±38.5	TS	1.8±2.2	2.2±1.1	12.4±6.1
SAPf	5.5±1.4	4.4±1.2	21.4±7.9	MC	1.4±1.1	1.0±1.1	3.1±2.7
SAPm	1.8±0.8	0.9±0.5	4.5±2.1	CdB	3.2±1.0	2.1±1.0	9.9±4.4
CAP	7.5±1.0	8.7±4.3	29.1±14.3	LCPS	2.7±1.7	3.9±3.8	3.5±4.2
SSDf	4.5±0.2	9.6±4.4	33.2±10.0	EOMS	1.7±0.9	2.2±0.9	8.9±4.7
SSDm	1.1±0.3	1.3±0.7	3.9±2.1	ME	2.1±0.4	3.7±2.0	7.5±3.1
AEPf	4.5±1.0	8.9±3.9	29.0±14.6	PLS	2.1±0.1	2.5±0.3	9.5±4.1
AEPm	2.5±1.1	3.9±1.6	14.4±6.4				

*Table 39: distribution of the GUs based on their K<sub>2</sub>O, U and Th concentrations.*

K <sub>2</sub> O (wt%)				U (ppm)				Th (ppm)			
0-2	2-4	4-6	6-8	0-3	3-7	7-12	12-37	0-8	8-16	16-30	30-69
Plm	Pif	PNVf	CAP	Pif	PV	LTP	MVP	Plm	Pif	PV	LTP
PNI	PV	LTP		Plm	PNI	CAP		MVI	PNI	PNVf	SSDf
PNVm	AEPm	SAPf		MVI	PNVf	SSDf		PNVm	AEPm	SAPf	MVP
SAPm	PM	SSDf		PNVm	SAPf			SAPm	SIP	CAP	
SSDm	COS	AEPf		SAPm	AEPm			SSDm	COS	AEPf	
MVP	CdB	DCPS		SSDm	LCPS			UM	TS	DCPS	
SIP	LCPS			SIP	ME			MC	CdB		
UM	ME			PM				LCPS	EOMS		
TM	PLS			UM				TM	PLS		
TS	MVI			TM				ME			
MC				COS							
EOMS				TS							
				MC							
				CdB							
				EOMS							
				PLS							

The results show that the standard deviation is almost always high and, apart from some cases, it varies from 20% to even more than 100% of the arithmetic mean.

K<sub>2</sub>O data seem to be the most precise and least variable: this is probably due to the higher development in detecting K<sub>2</sub>O and to its lower variability inside a lithology. U and especially Th data show a higher relative error, which is often above 50%.

The higher values of K<sub>2</sub>O, U and Th concentrations belong to the CAP, MVP and LTP unit, together with SSDf, SAPf and AEPf. As it was expected, the GUs with the higher concentration values are magmatic units with felsic and/or ultra-alkaline products (*table 39*). The mafic units have, on average, low concentration values, except for AEPm. Sedimentary and metamorphic units have low or intermediate values, apart from DCPS (but this is probably due to the low representativeness of its dataset).

The maps (*fig. 38, 39, 40*) show how the highest natural radioactivity contributions locate in the central Italy volcanic provinces, followed by the other felsic magmatic units of Sardinia, Veneto and southern Italy islands. The other lower but still important contributions come from the metamorphic units of the Alps, Sardinia and Calabria.

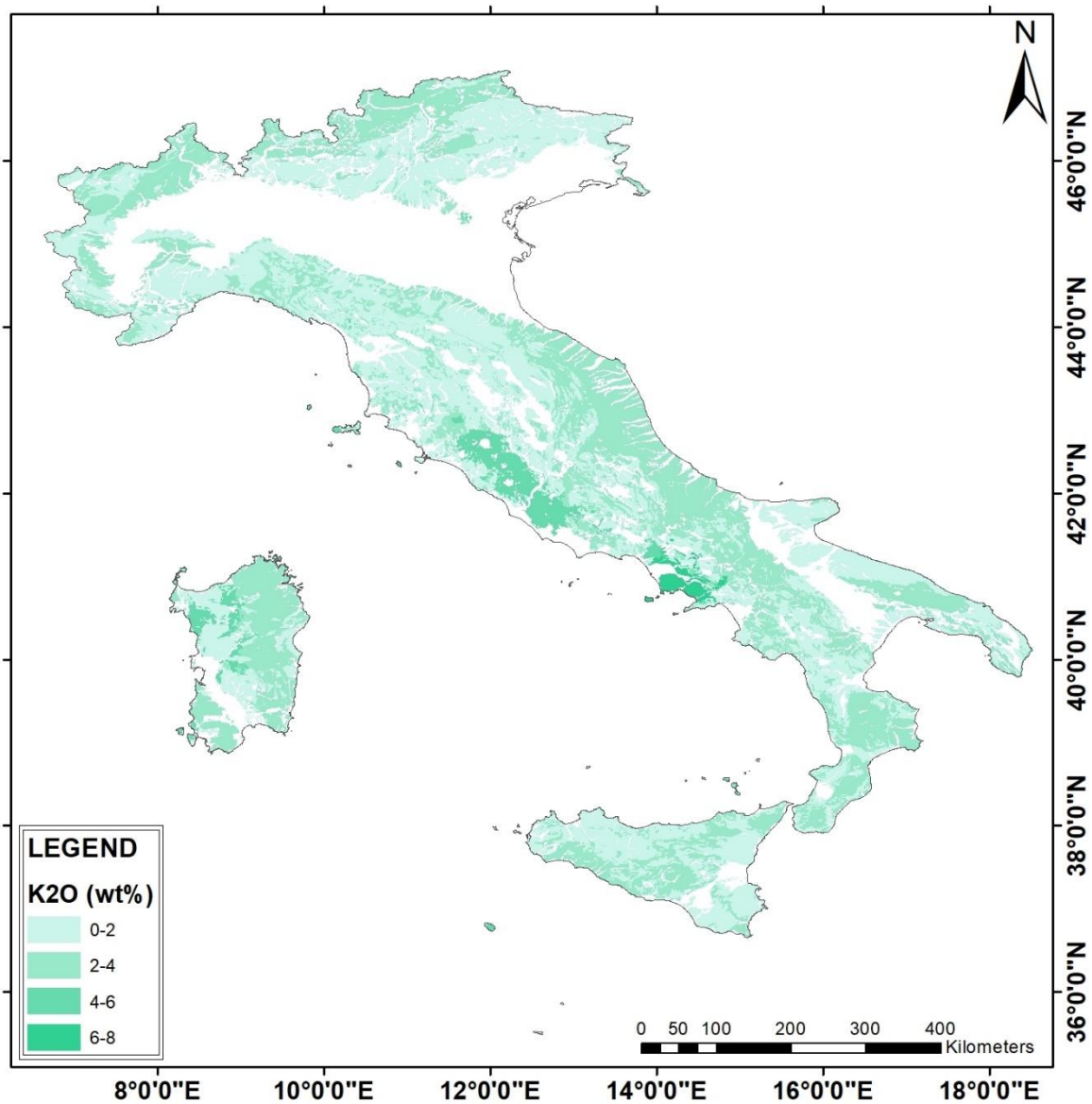


Figure 38: map of K<sub>2</sub>O concentration in bedrock in Italy expressed with the arithmetic mean.

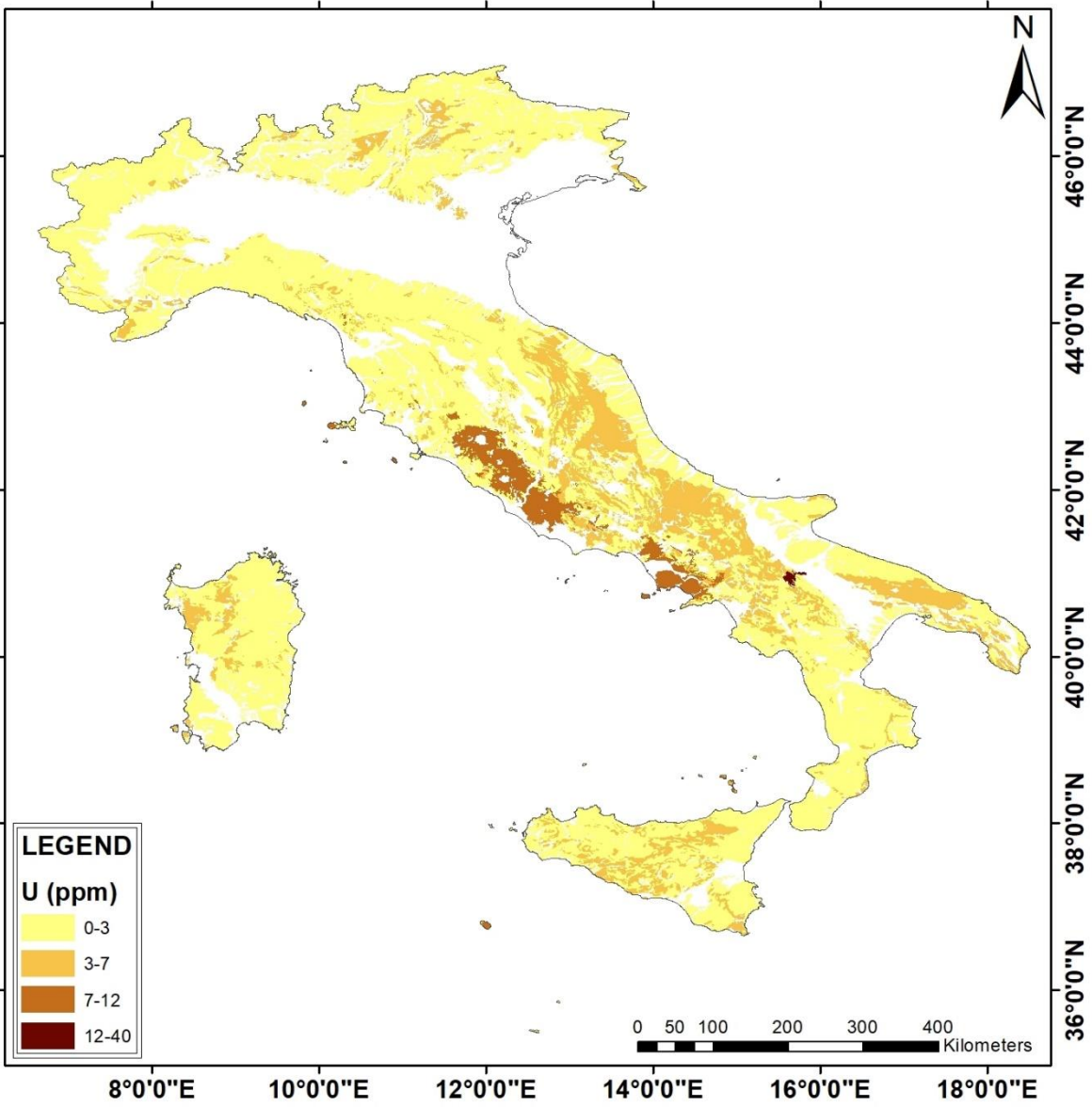


Figure 39: map of U concentration in bedrock in Italy expressed with the arithmetic mean

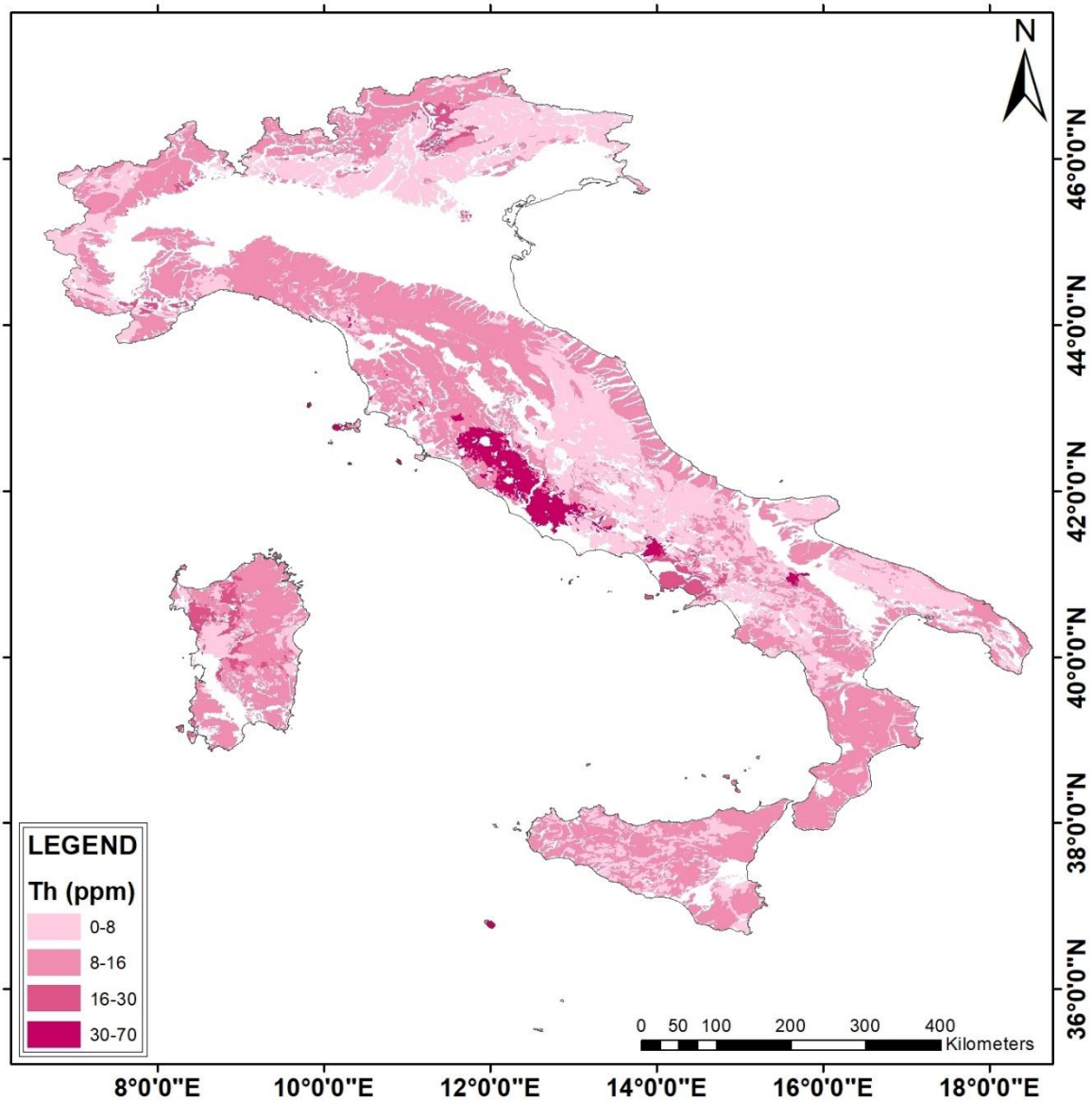


Figure 40: map of Th concentration in bedrock in Italy expressed with the arithmetic mean.

## 6. CONCLUSIONS

In the context of the European Atlas of Natural Radiation the present work focused on studying the methodology to develop and create maps of K<sub>2</sub>O, U and Th concentration in bedrock considering Italy as country study.

More than 15000 geochemical data from scientific literature and global databases have been collected, regarding K<sub>2</sub>O, U and Th concentration of bulk rocks from the Geological Units (GUs), which were identified on a litho-, chrono- and tectonostratigraphic basis using the OneGeology-Europe cartography as the starting point. The descriptive statistic performed on the data population produced, for each GU, average K<sub>2</sub>O, U and Th values. The GU division was tested through a series of ANOVAs, with the purpose of validating the methodology and understanding its limitations.

The results of the statistical analysis show that: the average K<sub>2</sub>O content is 1-4 wt%, with a minimum of 0.1 wt% (UM unit) and a maximum of 7.5 wt% (CAP unit); the average U and Th contents are 2-5 ppm and 5-15 ppm respectively, with a minimum of 0.1 ppm (UM unit) and a maximum of 36.8 ppm and 69.0 ppm (MVP unit; as pointed out previously, these values are probably overestimated due to high number of carbonatitic samples in the dataset).

Felsic and ultrapotassic volcanic rocks of central and southern Italy have the highest K<sub>2</sub>O, U and Th contents, followed by the other magmatic products. Metamorphic rocks have slightly higher than average K<sub>2</sub>O and Th contents. Ultramafic rocks have the lowest concentration values, because of their geochemical and mineralogical characteristics. Sedimentary rocks mostly lie within average values, but the number of data referred to them is far from representative considering their surface extension; in order to characterise them better, a sampling campaign would be necessary.

As we proved, there are many problems related to the creation of a database for the realisation of the K<sub>2</sub>O, U and Th concentration map in bedrock: the lack of representativeness of some samples, the poor coverage of some units and the complexity in finding data, especially regarding sedimentary rocks, are difficult to deal with and unfortunately there are no simple solutions to these problems.

Nonetheless, the approach that was used in this work has been tested and the advantages exceed the disadvantages: by simply researching and classifying data from scientific literature, it's possible to create quite accurate concentration maps, after the establishment of a coherent geological subdivision. The current approach aims to reduce the number of units to the lowest possible though maintaining a geological coherence, since the more units you have to consider, the more you need a homogeneous and precise database with a good coverage; the nowadays available databases still have too few data to realise small-scale projects. This leads to the issues of identifying the large-scale GUs that we addressed in this work. But since the realisation of these maps is essential in order to study the natural radioactivity across the different countries, this methodology, even with its cons, can prove itself to be of primary importance in the developing of the European Atlas of Natural Radiation.

An obvious continuation and improvement of this work could be divided in three steps:

- firstly, the comparison of these maps with a radiometric map of Italy, like the one of the Italian Radioactivity Project (ITALRAD; <http://www.fe.infn.it/italrad/>) of the National Institute of Nuclear Physics (INFN). This could help verify how much the two kinds of maps differ from one another; the disparity will be due to both the uncertainties related to the different methods used and the natural difference between bedrock contribution and total terrestrial contribution, which involves soil and other geological aspects;
- secondly, the developing of smaller-scale maps, involving a sampling campaign for the less represented terrains and the collection of other data from literature, both from future geochemistry works and from past published articles that we could not use because of their unavailability;
- lastly, the realisation of concentration maps using georeferenced data, in order to interpolate the values using a GIS software, so that the value displayed in an area will directly depend on the neighbourhood values, rather than on an assigned average value applied to a geological unit.

## 7. BIBLIOGRAPHY

- Abbate E., Fanucci F., Benvenuti M., Bruni P., Cipriani N., Falorni P., Fazzuoli M., Morelli D., Pandeli E., Papini M., Sagri M., Reale V., Vannucchi P., 2005. Note illustrative della carta geologica d'Italia alla scala 1:50000: foglio 248, La Spezia. Servizio geologico d'Italia, 204 pp.
- Barca S., Patta E.D., Murtas M., Pisanu G., Serra M., Lecca L., De Muro S., Pascucci V., Carboni S., Tilocca G., Andreucci S., Pusceddu N., 2011. Note illustrative della carta geologica d'Italia alla scala 1:50000: foglio 528, Oristano. Servizio geologico d'Italia, 260 pp.
- Beccaluva L., Siena F., Coltorti M., Di Grande A., Lo Giudice A., Macciotta G., Tassinari R., Vaccaro C., 1998. Nephelinitic to tholeiitic magma generation in a transtensional tectonic setting: an integrated model for the Iblean volcanism, Sicily. *Journal of Petrology* 39: 1547-1576.
- Beccaluva L., Bianchini G., Bonadiman C., Coltorti M., Milani L., Salvini L., Siena F., Tassinari R., 2007. Intraplate lithospheric and sublithospheric components in the Adriatic domain: Nephelinite to tholeiite magma generation in the Paleogene Veneto volcanic province, southern Alps. *Geological Society of America Special Paper* 418: 131-152.
- Bosellini A., 2005. *Storia geologica d'Italia*. Zanichelli, Bologna, 183 pp.
- Braga R., Cinelli G., Tollefsen T., De Cort M., 2015. Bedrock U-Th-K signatures in the ongoing European Atlas of Natural Radiation. *International Workshop on the European Atlas of Natural Radiation*, Verbania, 2015.
- Branca S., Coltelli M., Groppelli G., 2004. Geological evolution of Etna volcano. In: Bonaccorso A., Calvari S., Coltelli M., Del Negro C., Falsaperla S. (Eds), *Mt. Etna: Volcano Laboratory*, American Geophysical Union, pp. 49-64.
- Brondi A., Mittempergher M., Panizza M., Rossi D., Sommovilla E., Vuillermin F., 1977. Note esplicative del F° 028 La Marmolada, *Carta Geologica d'Italia alla scala 1:50000*. Servizio geologico d'Italia, 30 pp.
- Callegari I., Bezzon G.P., Brogginì C., Buso G.P., Cacioli A., Carmignani L., Colonna T., Fiorentini G., Guastaldi E., Xhixha M.K., Mantovani F., Massa G., Menegazzo R., Mou L., Pirro A., Alvarez C.R., Strati V., Xhixha G., Zanon A., 2013. Total natural radioactivity, Tuscany, Italy. *Journal of Maps* 9:3: 438-443.
- Carbone S., 2011. Note illustrative della carta geologica d'Italia alla scala 1:50000: foglio 641, Augusta. Servizio geologico d'Italia, 247 pp.
- Carbone S., Grasso M., 2012. Note illustrative della carta geologica d'Italia alla scala 1:50000: fogli 597, 610, Cefalù - Castelbuono. Servizio geologico d'Italia, 199 pp.
- Chelazzi L., Bindi L., Olmi F., Menchetti S., Peccerillo A., Conticelli S., 2006. A lamproitic component in the high-K calc-alkaline volcanic rocks of the Capraia Island, Tuscan Magmatic Province: evidence from clinopyroxene crystal chemical data. *Periodico di Mineralogia* 75: 75-94.
- Christeleit E.C., Brandon M.T., Zhuang G., 2015. Evidence for deep-water deposition of abyssal Mediterranean evaporites during the Messinian salinity crisis. *Earth and Planetary Science Letters* 427: 226-235.
- Cicchella D., Albanese S., Birke M., De Vivo B., De Vos W., Dinelli E., Lima A., O'Connor P., Salpeteur I., Tarvainen T., 2014. Natural radioactive elements uranium, thorium and

- potassium in European agricultural and grazing land soil. In: Reimann C., Birke M., Demetriades A., Filzmoser P., O'Connor P. (Eds), *Chemistry of Europe's Agricultural soils, Part B*, Geologisches Jahrbuch, Heft, pp. 145-159.
- Cinelli G., Tositti L., Capaccioni B., Brattich E., Mostacci D., 2015. Soil gas radon assessment and development of a radon risk map in Bolsena, Central Italy. *Environmental Geochemistry and Health* 37: 305-319.
- Cinelli G., Gruber V., De Felice L., Bossew P., Hernandez-Ceballos M. A., Tollefsen T., Mundigl S., De Cort M., 2017. European annual cosmic-ray dose: estimation of population exposure. *Journal of Maps* 13:2: 812-821.
- Cinelli G., Tollefsen T., Bossew P., Gruber V., Bogucarskis K., De Felice L., De Cort M., 2018. Digital version of the European Atlas of natural radiation. *Journal of Environmental Radioactivity*, in press. DOI: <https://doi.org/10.1016/j.jenvrad.2018.02.008>.
- Cortosogno L., Cassinis G., Dallagiovanna G., Gaggero L., Oggiano G., Ronchi A., Seno S., Vanossi M., 1998. The Variscan post-collisional volcanism in Late Carboniferous-Permian sequences of Ligurian Alps, Southern Alps and Sardinia (Italy): a synthesis. *Lithos* 45: 305-328.
- Damiani A.V., 2011. Note illustrative della carta geologica d'Italia alla scala 1:50000: foglio 336, Spoleto. Servizio geologico d'Italia, 176 pp.
- De Cort M., Gruber V., Tollefsen T., Bossew P., Janssens A., 2011. Towards a European Atlas of natural radiation: goal, status and future perspectives. *Radioprotection* 46: 737-743.
- Deiana G., 2009. Note illustrative della carta geologica d'Italia alla scala 1:50000: foglio 302, Tolentino. Servizio geologico d'Italia, 113 pp.
- Ditz R., Sarbas B., Schubert P., Töpfer W., 1990. *Gmelin Handbook of Inorganic Chemistry, Thorium, Supplement Volume A1a*. Springer-Verlag Berlin Heidelberg GmbH, Berlin, 392 p.
- EC (European Commission), (1996). Council Directive 96/29/Euratom of 13 May 1996, laying down basic safety standards for the protection of the health of workers and the general public against the dangers arising from ionizing radiation. Official Journal L-159 of 27/06/96. European Commission, Bruxelles.
- EC (European Commission), (1997). Radiation Protection 88, Recommendations for the implementation of title VII of the European Basic Safety Standards Directive (BSS) concerning significant increase in exposure due to natural radiation sources.
- EC (European Commission), (2013). Council Directive 2013/59/Euratom of 5 December 2013 laying down Basic Safety Standards for Protection against the Dangers Arising from Exposure to Ionising Radiation. Official Journal L13 of 17/01/2014 European Commission, Bruxelles.
- Elter P., Lasagna S., Marroni M., Pandolfi L., Vescovi P., Zanzucchi G., 2005. Note illustrative della carta geologica d'Italia alla scala 1:50000: foglio 215 Bedonia. Servizio geologico d'Italia, 117 pp.
- Filipponi A., 2018. Modellizzazione petrogenetica dell'origine e dell'evoluzione dei complessi magmatici di Predazzo-Monzoni. Unpublished thesis, BIGEA, Università di Bologna, 88 p.
- Funedda A., Carmignani L., Pertusati P.C., Forci A., Calzia P., Marongiu F., Pisanu G., Serra M., 2012. Note illustrative della carta geologica d'Italia alla scala 1:50000: foglio 548, Senorbì. Servizio geologico d'Italia, 196 pp.

- Gasparini D., Blichert-Toft J., Bosch D., Del Moro A., Macera P., Albarède F., 2002. Upwelling of deep mantle material through a plate window: evidence from the geochemistry of Italian basaltic volcanics. *Journal of Geophysical Research* 107: 1-19.
- Gelati R., Gnaccolini M., Polino R., Mosca P., Piana F., Morelli M., Fioraso G., 2010. Note illustrative della carta geologica d'Italia alla scala 1:50000: foglio 211, Dego. Servizio geologico d'Italia, 111 pp.
- Ielsch G., Cuney M., Buscail F., Rossi F., Leon A., Cushing M.E., 2017. Estimation and mapping of uranium content of geological units in France. *Journal of Environmental Radioactivity* 166: 210-219.
- Kapferer N., Mercolli I., Berger A., Ovtcharova M., Fügenschuh B., 2012. Dating emplacement and evolution of the orogenic magmatism in the internal Western Alps: 2. The Biella Volcanic Suite. *Swiss Journal of Geosciences* 105: 67-84.
- Lavecchia G., Stoppa F., 1996. The tectonic significance of Italian magmatism: An alternative view to the popular interpretation. *Terranova* 8: 435-446.
- Lustrino M., Morra V., Melluso L., Brotzu P., D'Amelio F., Fedele F., Franciosi L., Lonis R., Petteruti-Liebercknecht A.M., 2004. The Cenozoic igneous activity of Sardinia. *Periodico di Mineralogia* 73: 105-134.
- Martelli L., Nardi G., 2005. Note illustrative della carta geologica d'Italia alla scala 1:50000: foglio 503, Vallo della Lucania. Servizio geologico d'Italia, 82 pp.
- Michetti A.M., Livio F., Pasquare F.A., Vezzoli L., Bini A., Bernoulli D., Sciunnach D., 2010. Note illustrative della carta geologica d'Italia alla scala 1:50000: foglio 075, Como. Servizio geologico d'Italia, 206 pp.
- Moretti M., Pieri P., Ricchetti G., Spalluto L., 2011. Note illustrative della carta geologica d'Italia alla scala 1:50000: foglio 396, San Severo. Servizio geologico d'Italia, 145 pp.
- Morini D., 2006. Carta geologica d'Italia alla scala 1:50000: foglio 273, Pisa.
- Pasci S., Carmignani L., Pisanu G., Sale V., Ulzega A., Orrù P., Pintus C., Deiana G., 2011. Note illustrative della carta geologica d'Italia alla scala 1:50000: foglio 564, Carbonia. Servizio geologico d'Italia, 272 pp.
- Peccerillo A., 1998. Relationships between ultrapotassic and carbonate-rich volcanic rocks in central Italy: petrogenetic and geodynamic implications. *Lithos* 43: 267-279.
- Peccerillo A., 2005. Plio-Quaternary Volcanism in Italy: Petrology, Geochemistry, Geodynamics. Springer, Berlin-New York, pp. 365.
- Pertusati P.C., Sarria E., Cherchi G.P., Carmignani L., Barca S., Benedetti M., Chighine G., Cincotti F., Oggiano G., Ulzega A., Orrù P., Pintus C., 2000. Note illustrative della carta geologica d'Italia alla scala 1:50000: foglio 541, Jerzu. Servizio geologico d'Italia, 169 pp.
- Principi G., Bortolotti V., Fanucci F., Benvenuti M., Chiari M., Dini A., Fazzuoli M., Menna F., Morelli D., Moretti S., Nirta G., Reale V., 2010. Note illustrative della carta geologica d'Italia alla scala 1:50000: foglio 316, 317, 328, 329, Isola d'Elba. Servizio geologico d'Italia, 263 pp.
- Rudnick R.L., Gao S., 2003. Composition of the continental crust. In: Rudnick R.L., Holland H.D., Turekian K.K. (Eds), *Treatise on geochemistry*, Volume 3, Elsevier, Amsterdam.
- Taylor S.R., McLennan S.M., 1985. The continental crust: its composition and evolution. Blackwell Scientific Publication, Carlton, 312 p.
- Tositti L., Cinelli G., Brattich E., Galgaro A., Mostacci D., Mazzoli C., Massironi M., Sassi R., 2017. Assessment of lithogenic radioactivity in the Euganean Hills magmatic district (NE Italy). *Journal of Environmental Radioactivity* 166: 259-269.

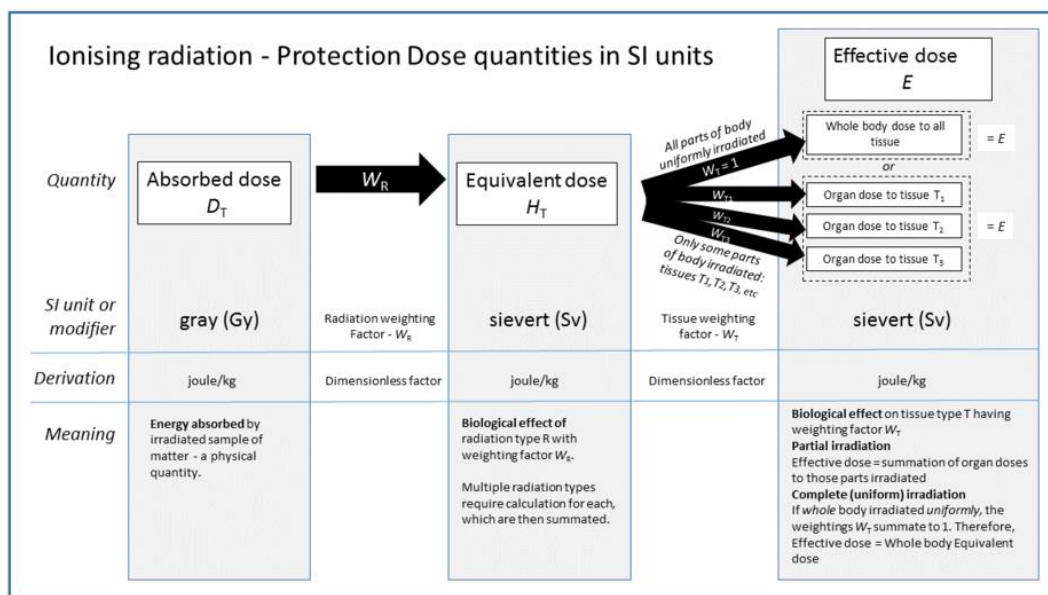
- UNSCEAR (United Nations Scientific Committee on the effects of Atomic Radiation), 2000. Sources and effects of ionizing radiation. Report to General Assembly, Volume I: sources, United Nations, New York, 76 p.
- UNSCEAR (United Nations Scientific Committee on the effects of Atomic Radiation), 2008. Sources and effects of ionizing radiation. Report to General Assembly, Annex B, United Nations, New York, 249 p.
- Venturini C., 2009. Note illustrative della carta geologica d'Italia alla scala 1:50000: foglio 031, Ampezzo. Servizio geologico d'Italia, 232 pp.
- von Blanckenburg F., Davies J.H., 1995. Slab breakoff: A model for syncollisional magmatism and tectonics in the Alps. *Tectonics* 14: 120-131.

## 8. APPENDIX

### 8.1 Appendix A – The dose

The total dose depends on the activity of the radionuclides involved, which measures the amount of radioactive decay in a second of a certain radionuclide and therefore is expressed by  $s^{-1}$  (named becquerel, Bq).

The impact of radiation on an object is represented by the absorbed dose, that is the energy received per unit mass, measured in joules per kilogram (named gray, Gy); in order to estimate the effects of radiation on a human body, the equivalent and the effective doses were introduced: they both have joules per kilogram (named sievert, Sv) as unit of measure, but while the former is only weighted depending on the radiation type, the latter is weighted depending on the tissue or organ interested too.



from [https://en.wikipedia.org/wiki/Equivalent\\_dose#/media/File:SI\\_Radiation\\_dose\\_units.png](https://en.wikipedia.org/wiki/Equivalent_dose#/media/File:SI_Radiation_dose_units.png)

The limits and recommendations of the national and international organizations for radiation protection are based on the definition of the different doses, in order to prevent the potential hazards and to lower the risk of being exposed to ionising radiation for a too long period, especially for various categories of workers.

## 8.2 Appendix B – Sardinian samples

Description and geographical coordinates of the three samples collected in Sardinia.

### **OMS**

Polygenic conglomerate with mostly granitoid, rhyolitic and metamorphic clasts, with a grain size from few centimetres to half a meter. The texture is mainly clastic, with low amount of reddish matrix. There is evidence of cementation, mainly of carbonatic composition. There are no visible preferential orientations of the clasts, even though the sediment deposited in a fluvial environment.

Age: Oligocene-Miocene (Ussana formation).

Coordinates: 39.961N; 8.830E.

GU: EOMS.

### **CS**

Highly foliated and altered micashist (metapelite), with little or none sedimentary feature preserved. The foliation follows a local orientation of 30/30 (expressed as dip and dip direction).

Age: Precambrian-early Paleozoic.

Coordinates: 39.958N; 8.834E.

GU: COS.

### **SS**

Highly foliated metasandstone with little sedimentary features preserved. The foliation follows a local orientation of 15/90 (expressed as dip and dip direction).

Age: late Ordovician (Genna Mesa metarkose formation).

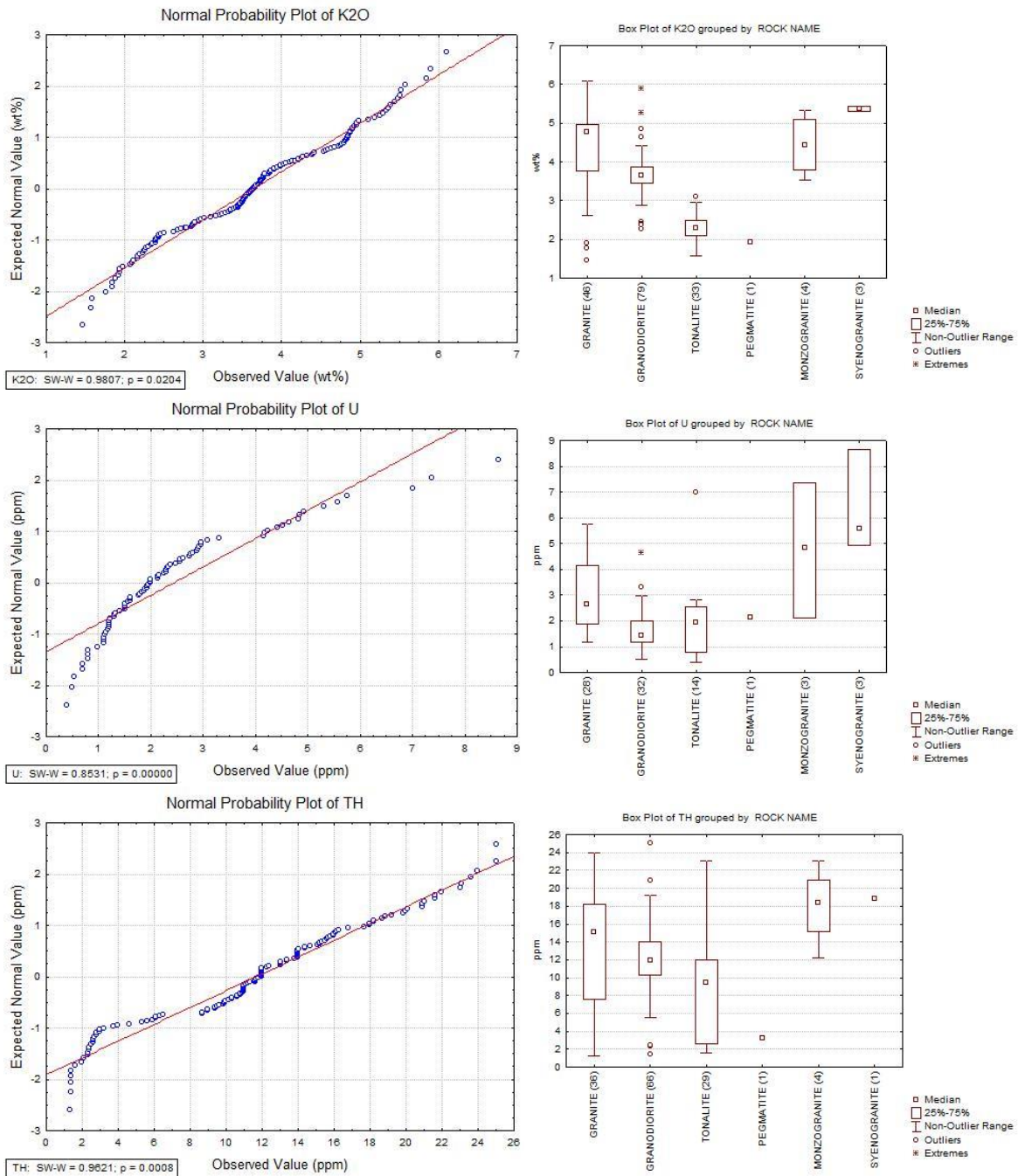
Coordinates: 39.895N; 8.931E.

GU: DCPS.

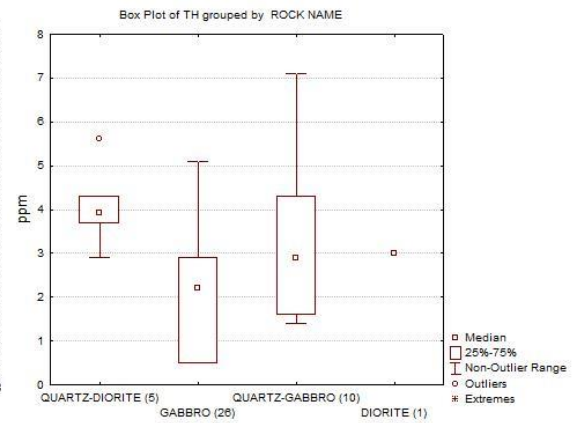
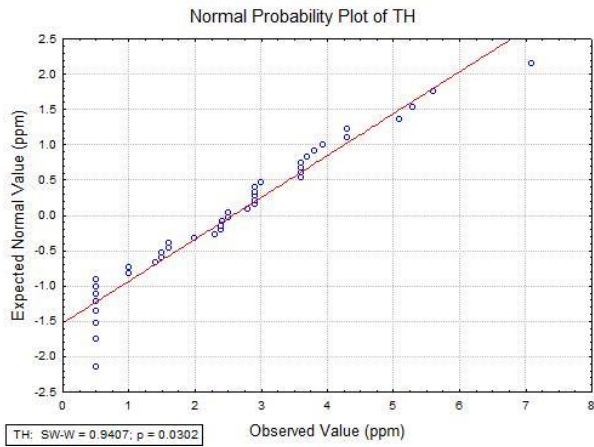
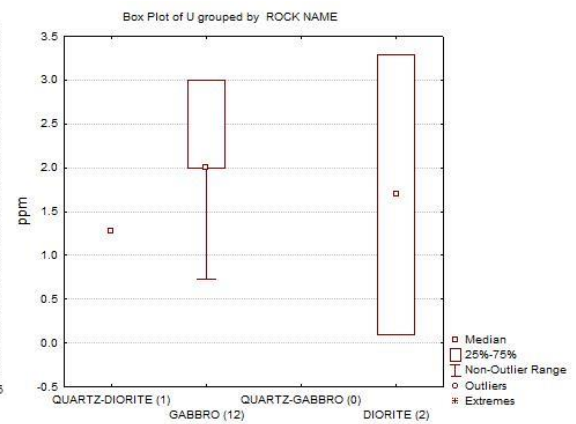
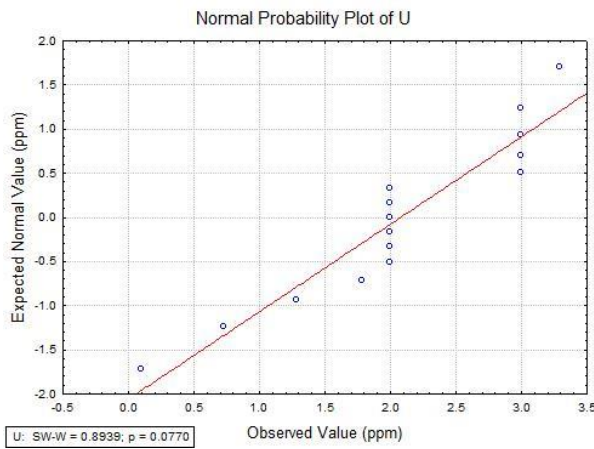
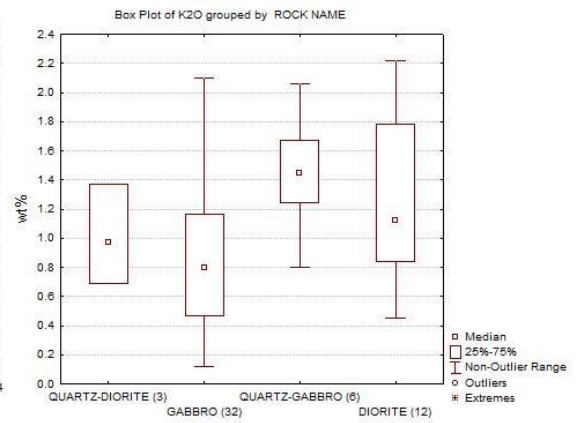
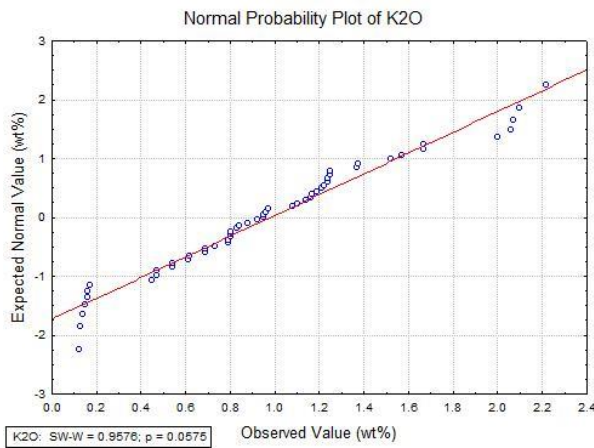
### 8.3 Appendix C – Statistical graphs

Here the normal probability plots and the box plots referred to all the GUS are reported. The missing graphics were not representative because of the very low number of data.

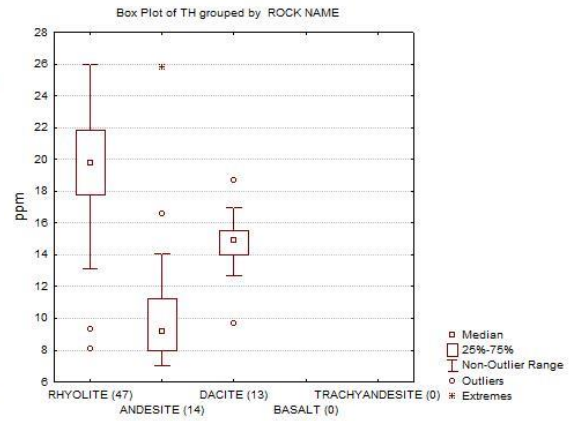
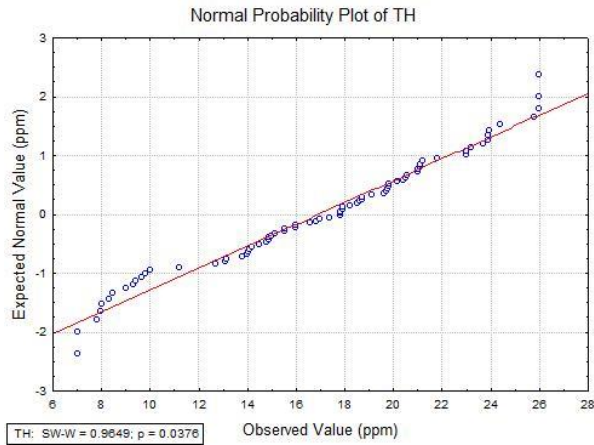
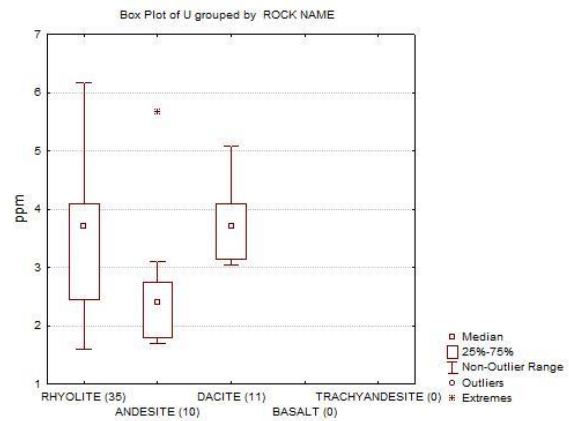
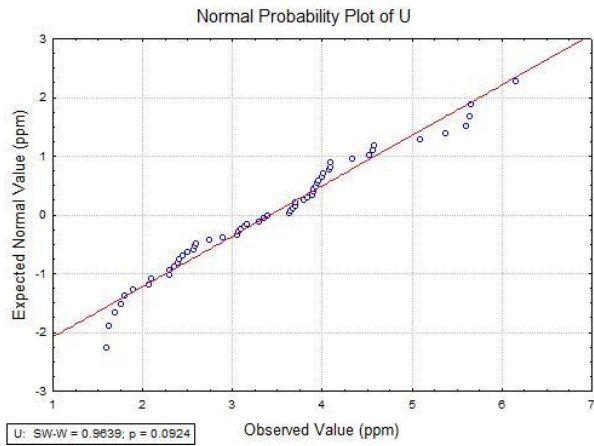
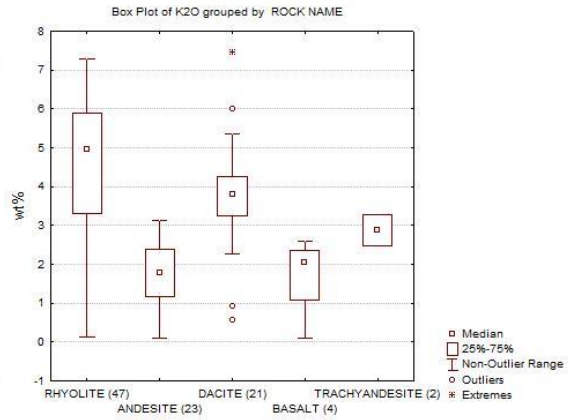
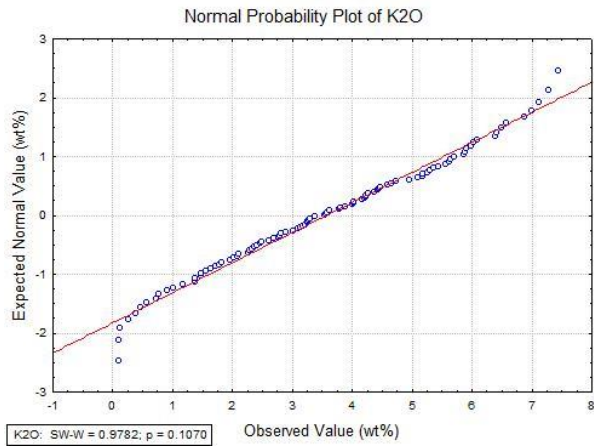
#### PIf



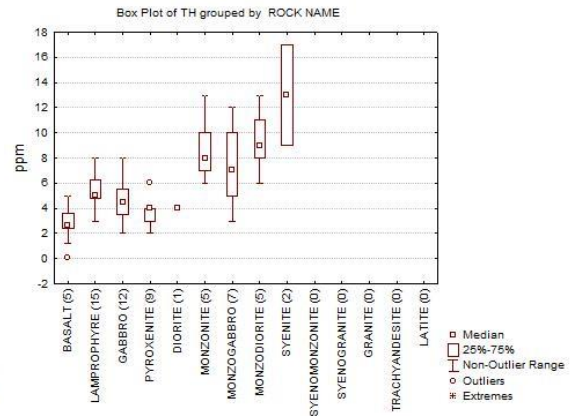
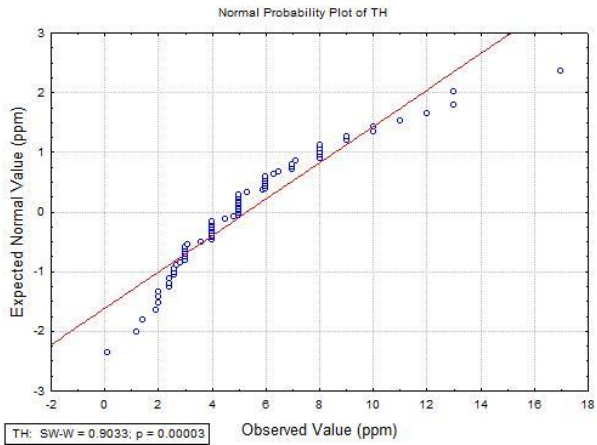
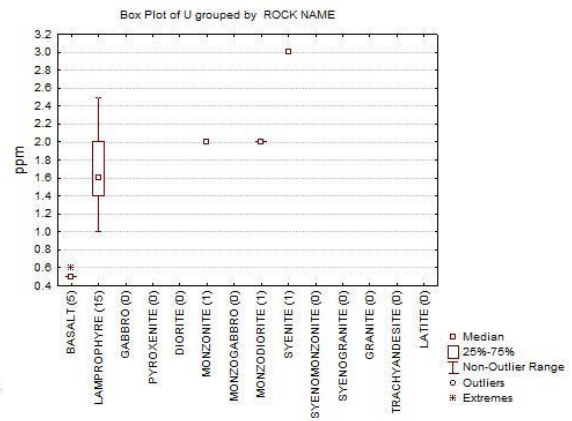
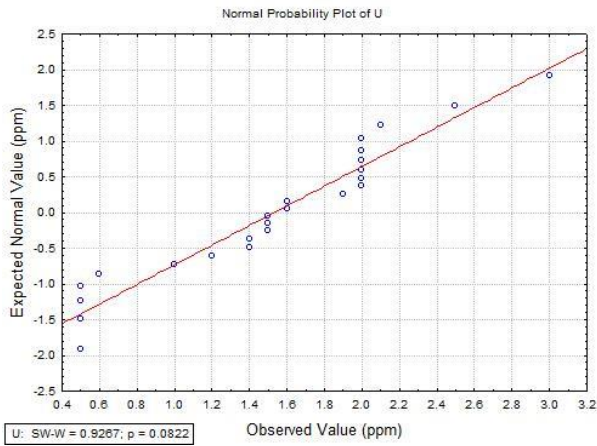
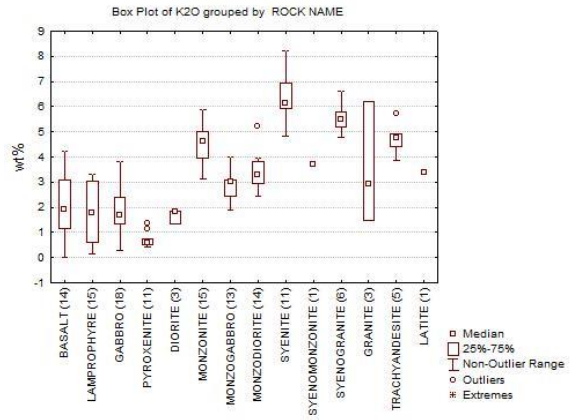
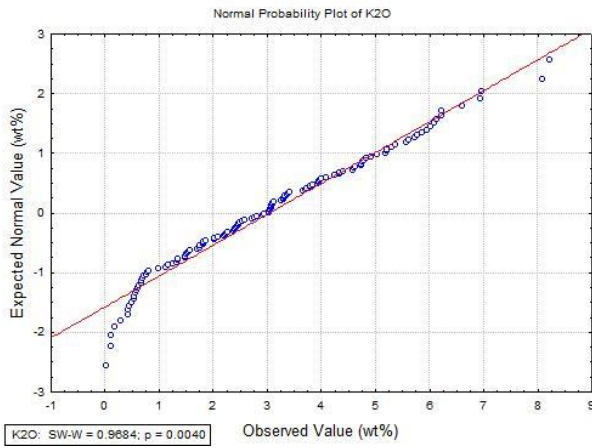
# Plm



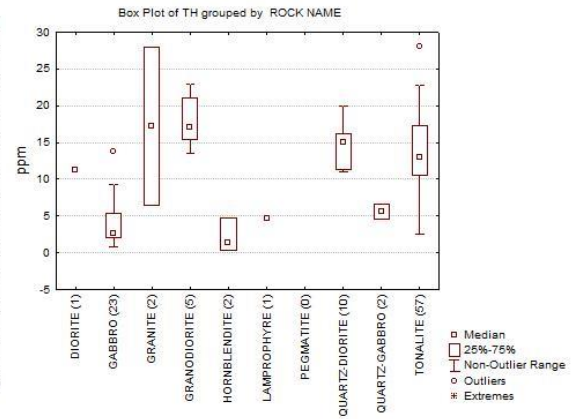
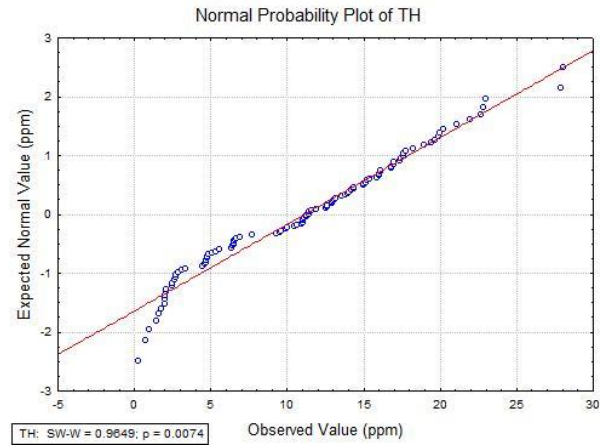
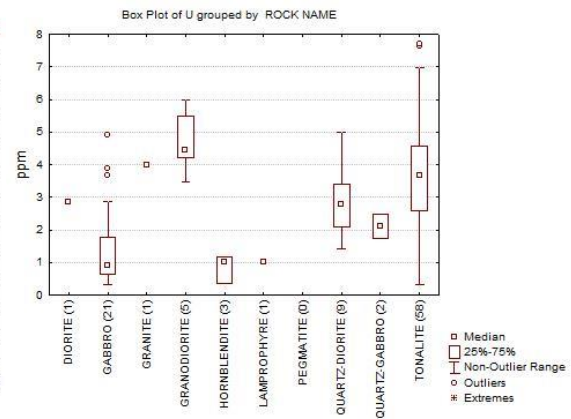
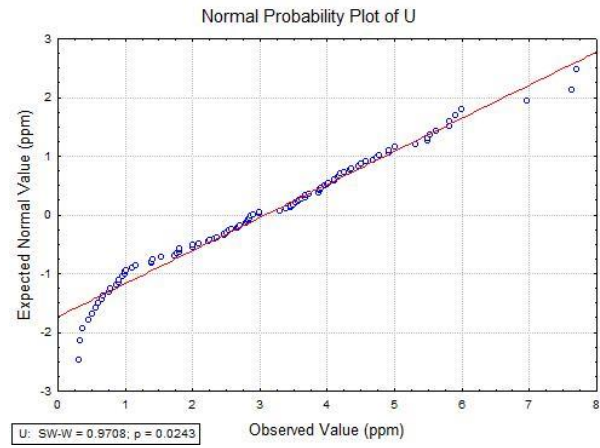
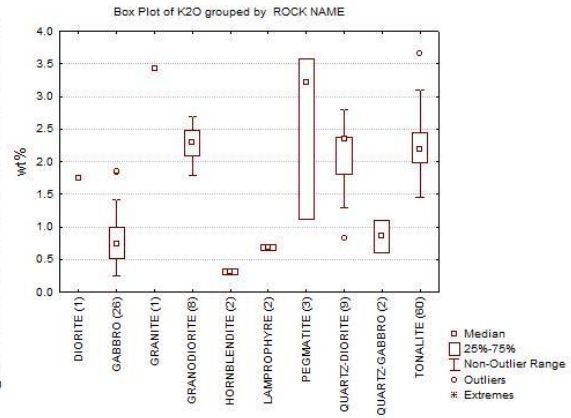
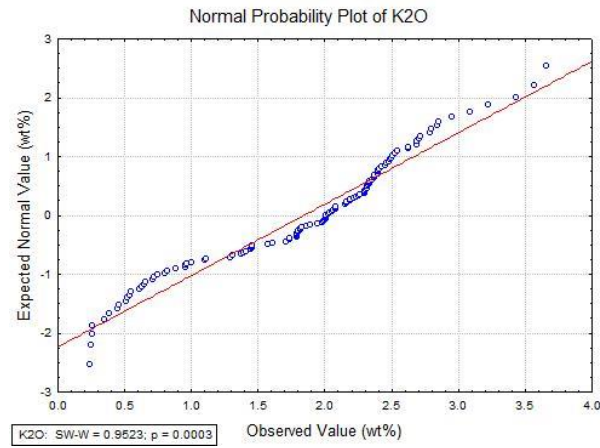
# PV



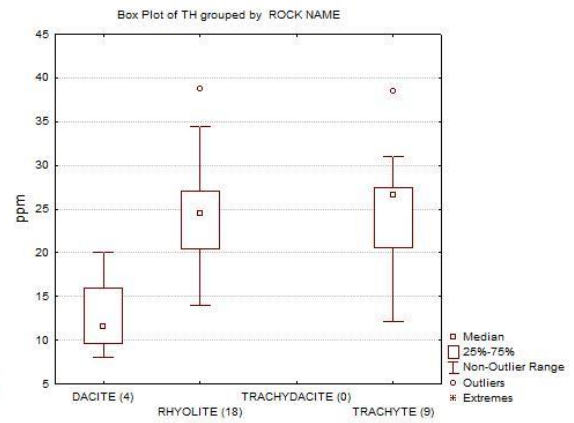
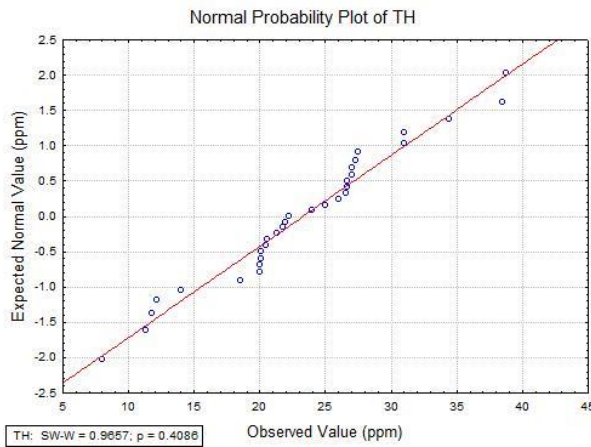
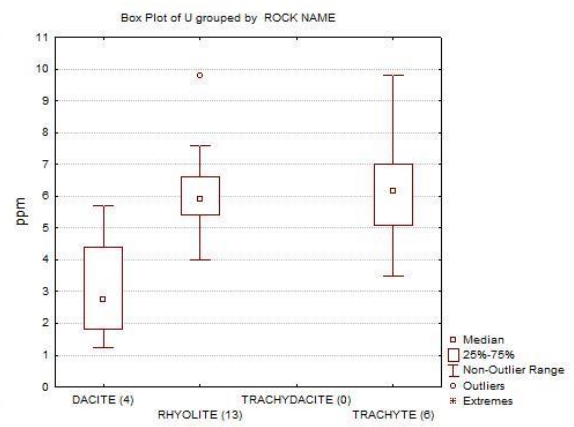
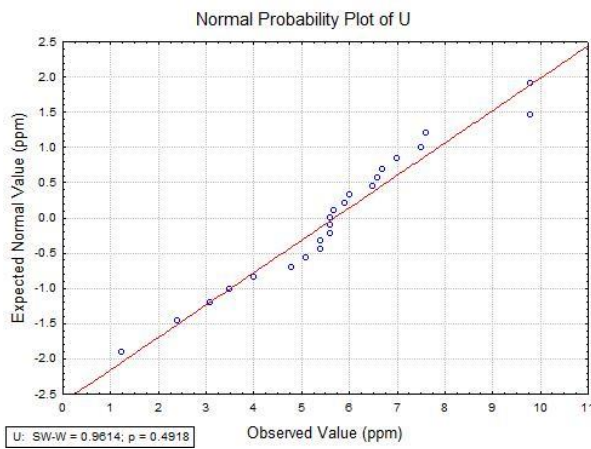
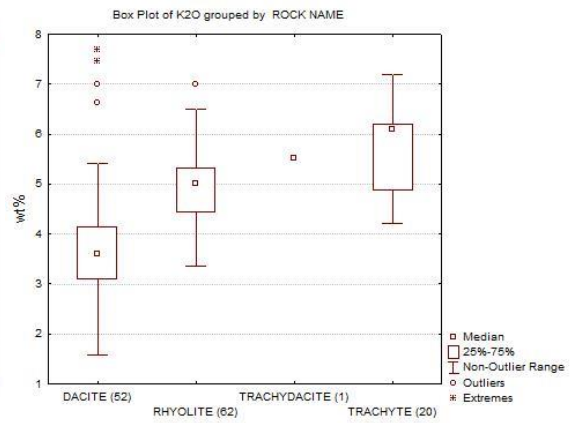
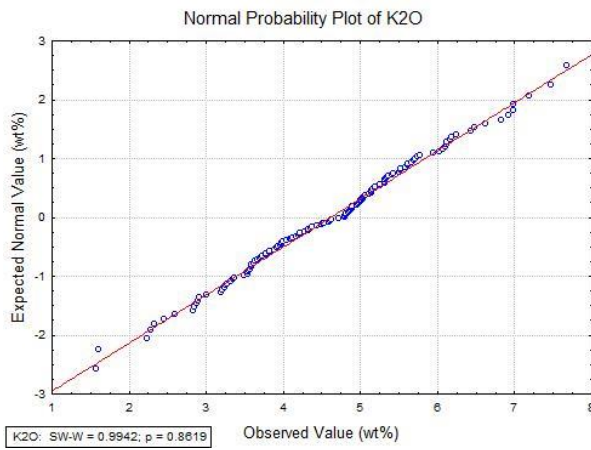
# MVI



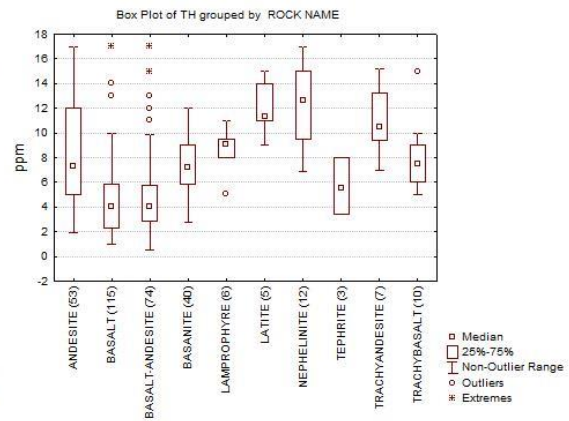
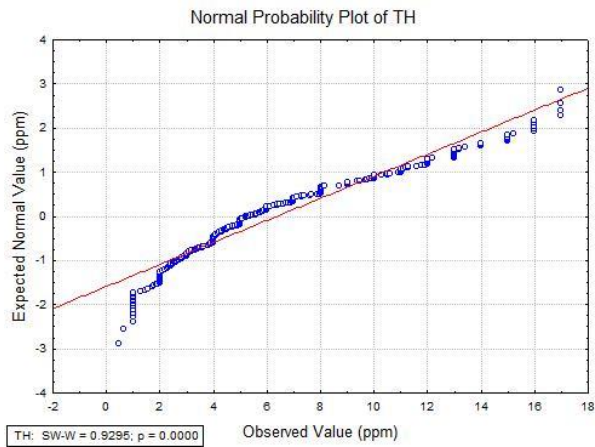
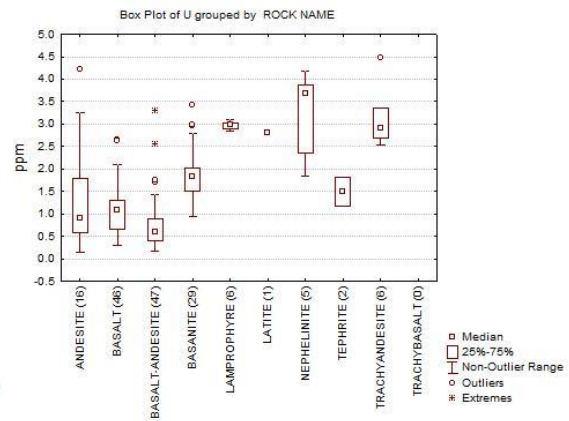
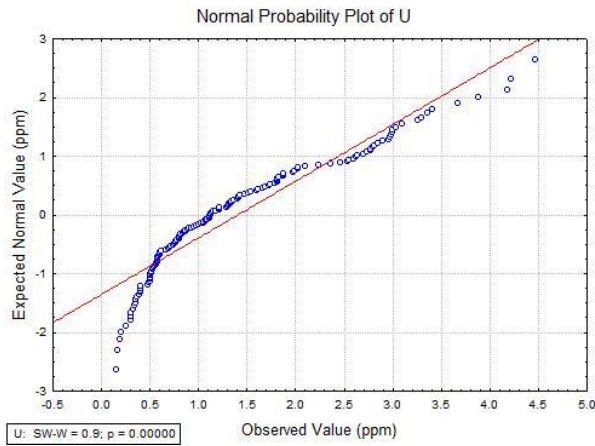
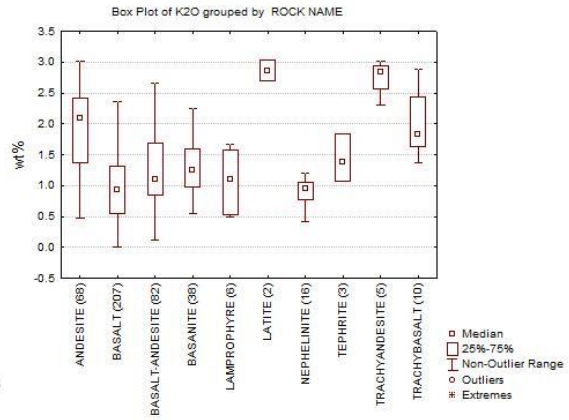
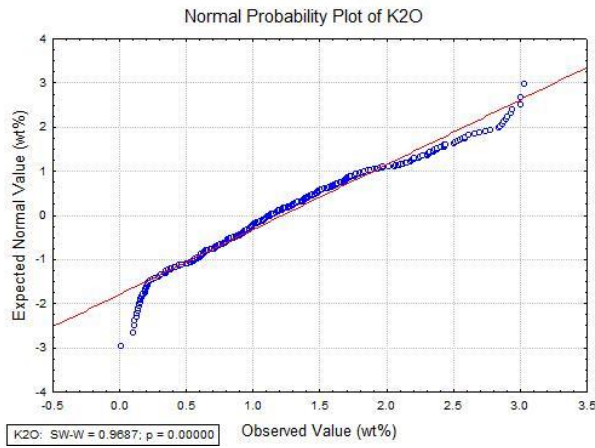
# PNI



# PNVf

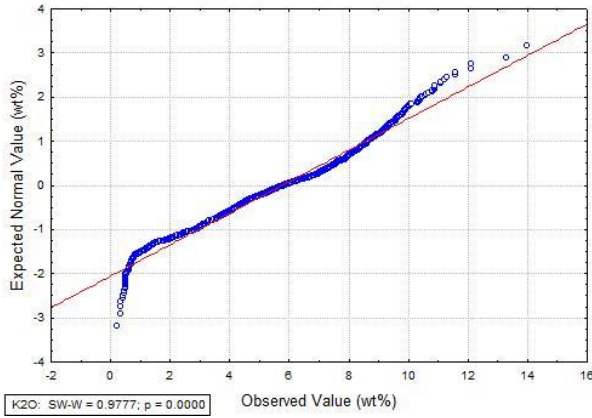


# PNVm

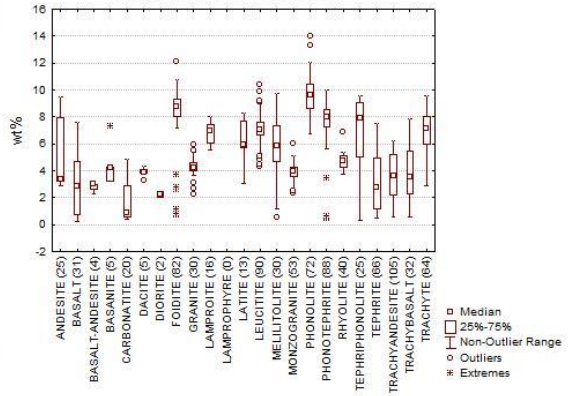


LTP

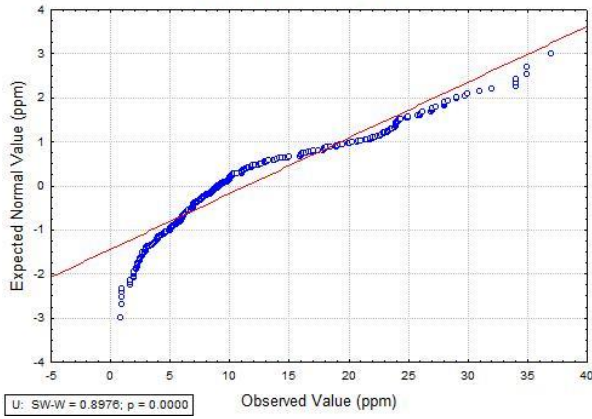
Normal Probability Plot of K2O



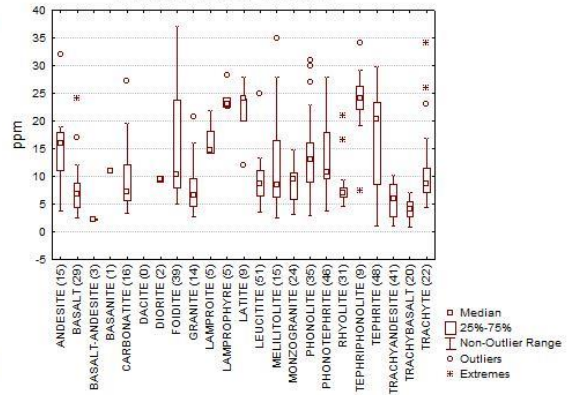
Box Plot of K2O grouped by ROCK NAME



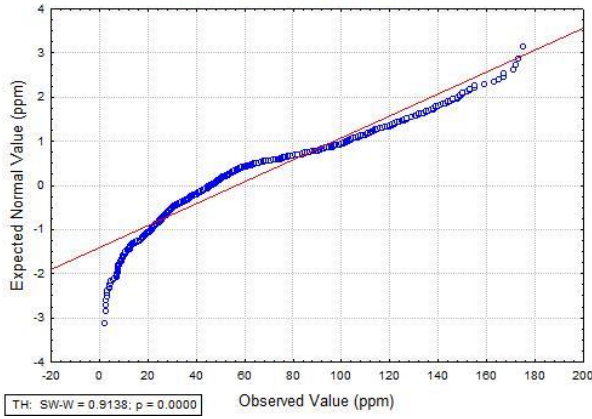
Normal Probability Plot of U



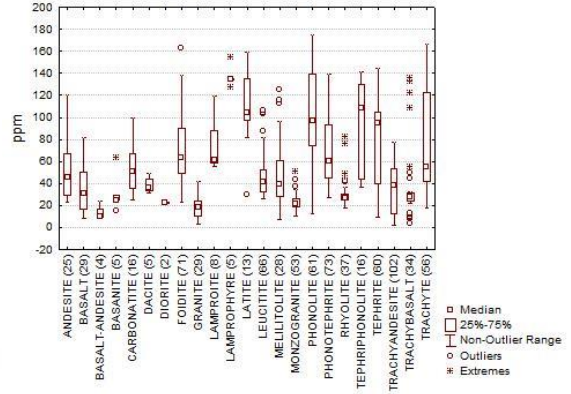
Box Plot of U grouped by ROCK NAME



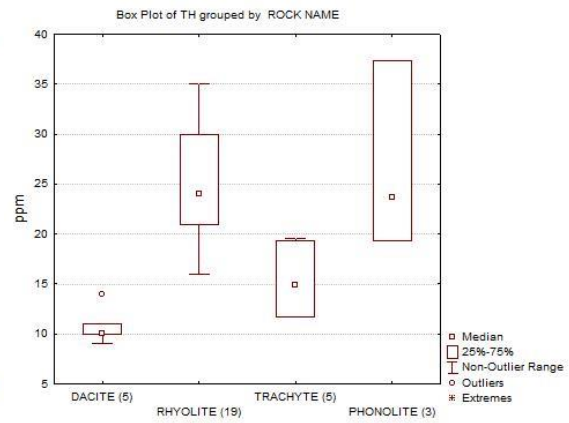
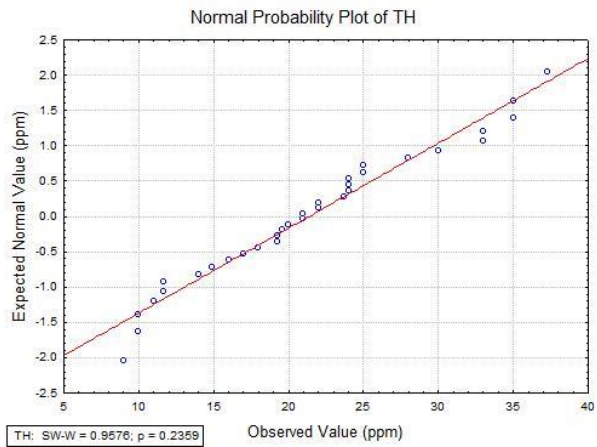
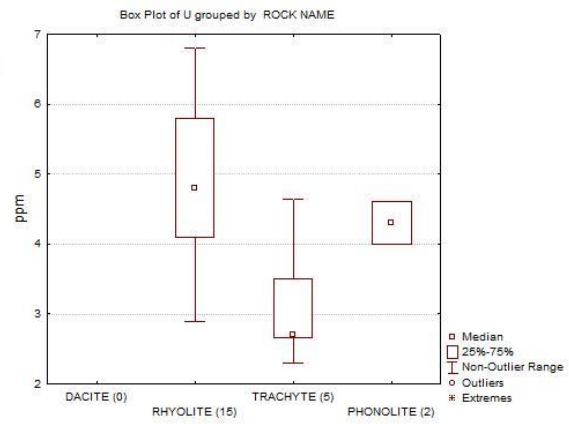
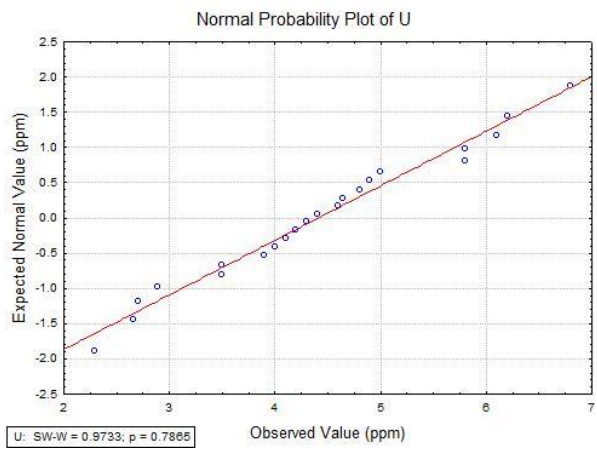
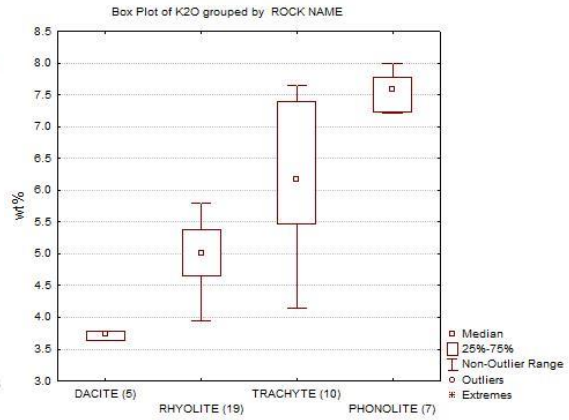
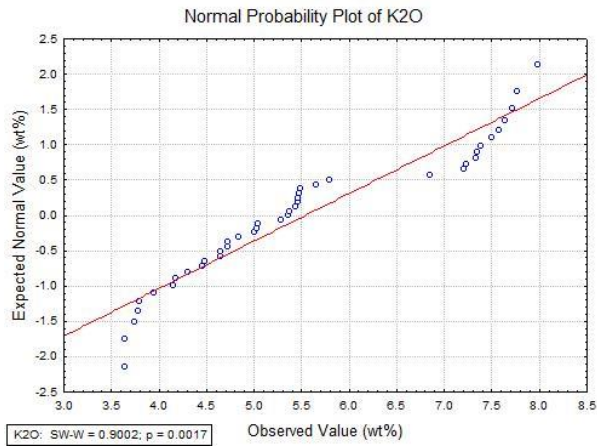
Normal Probability Plot of TH



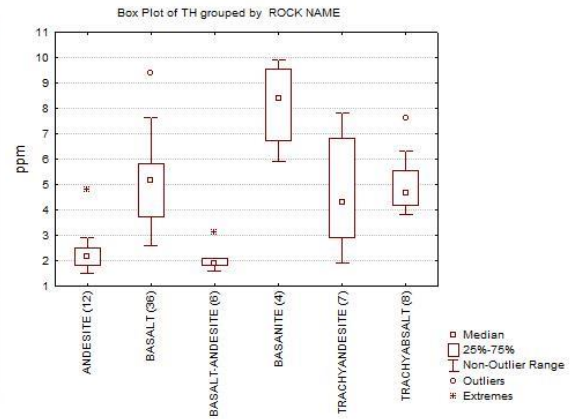
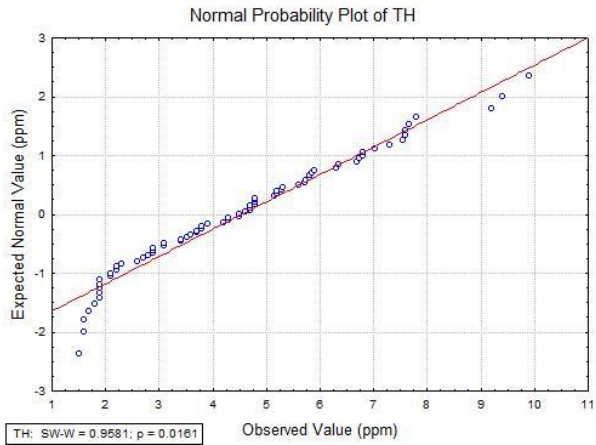
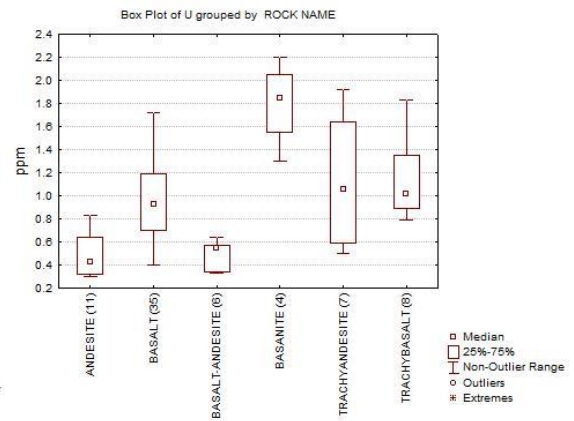
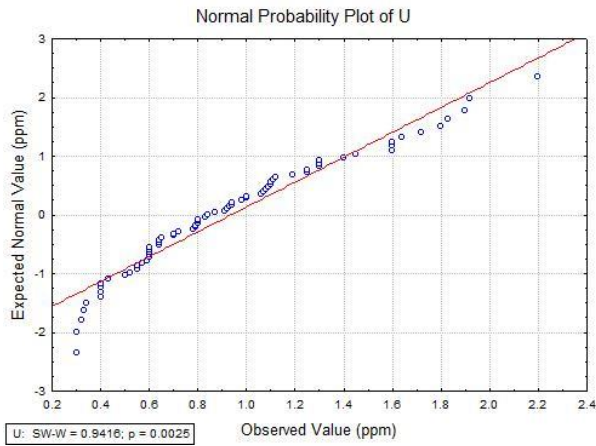
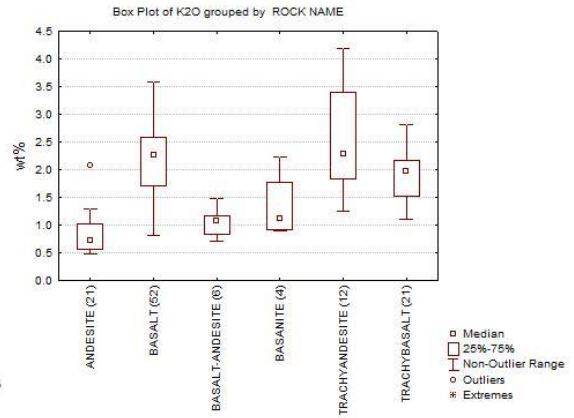
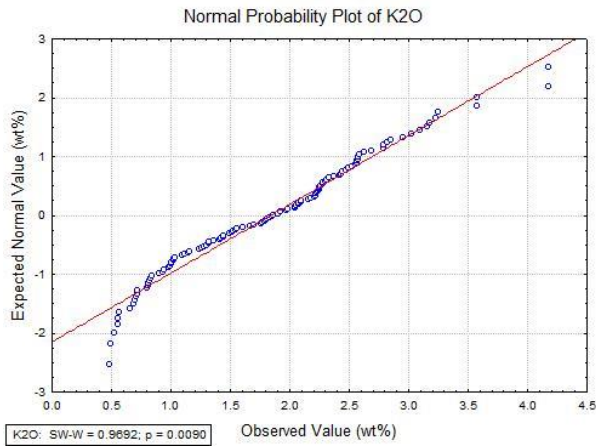
Box Plot of TH grouped by ROCK NAME



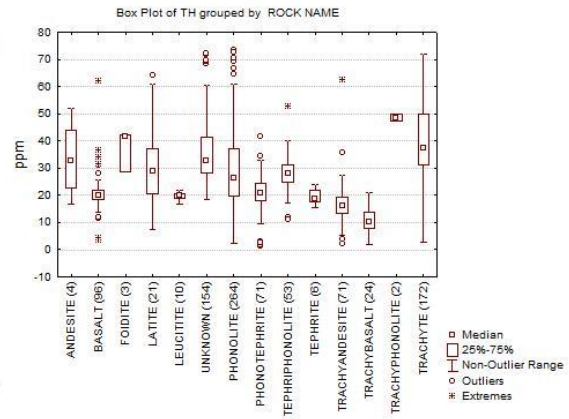
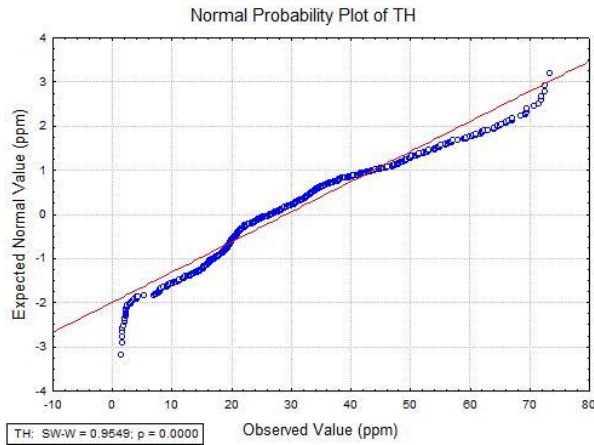
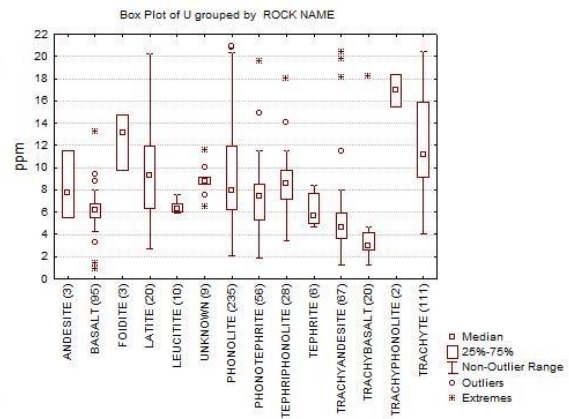
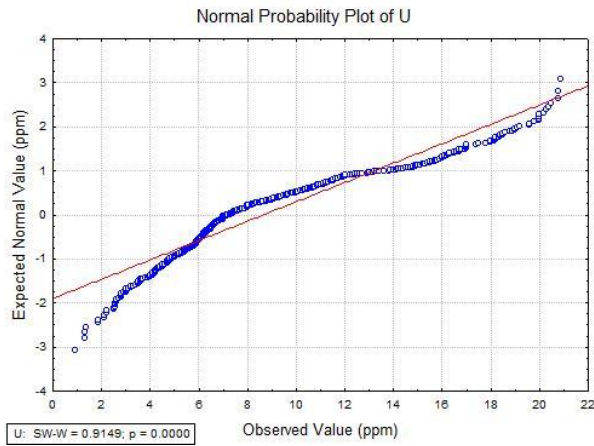
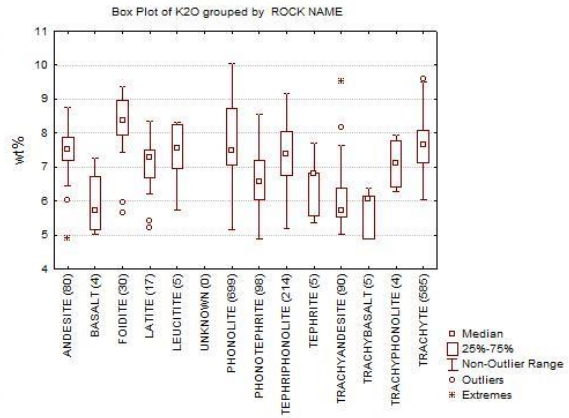
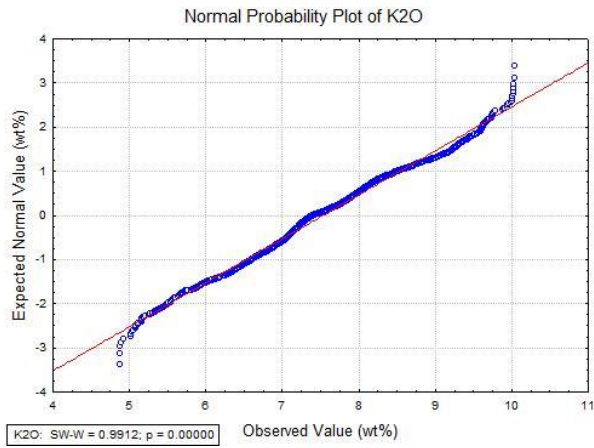
# SAPf



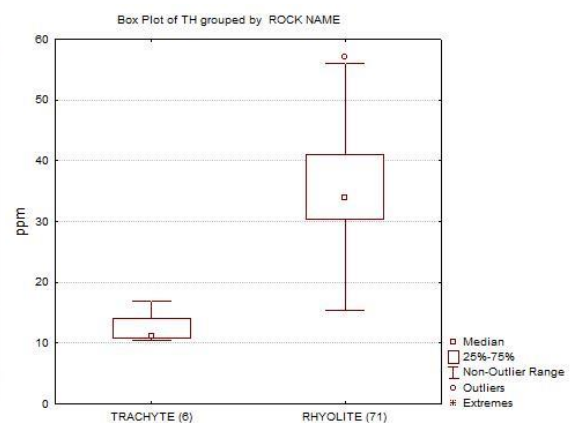
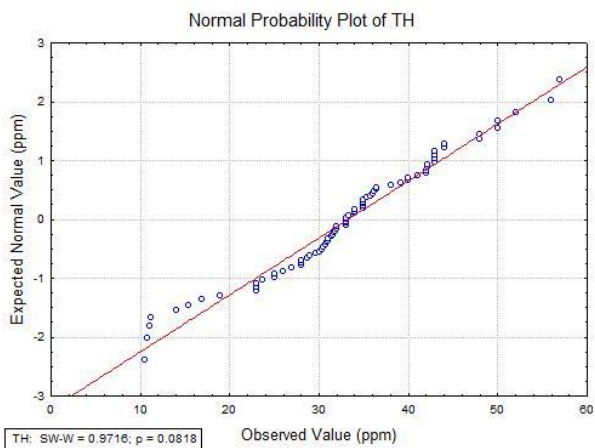
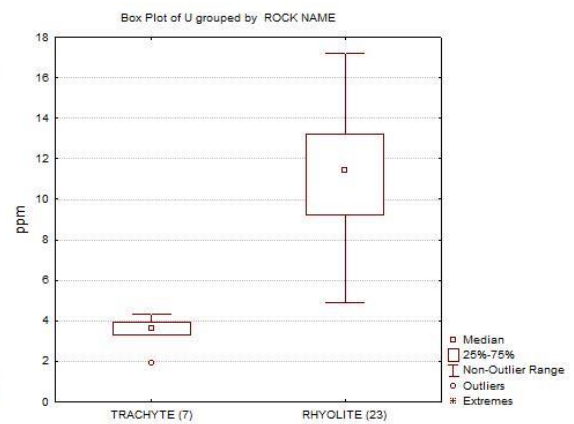
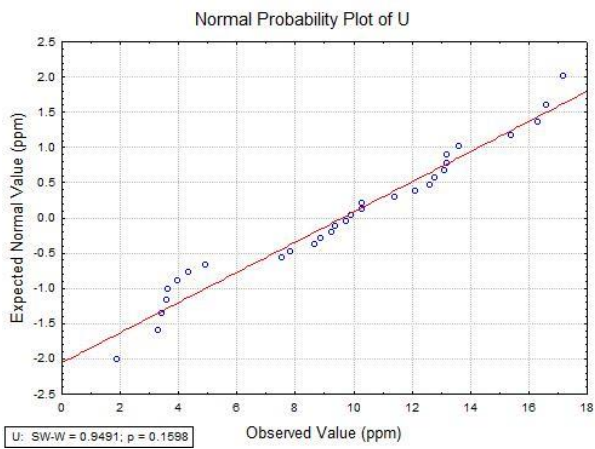
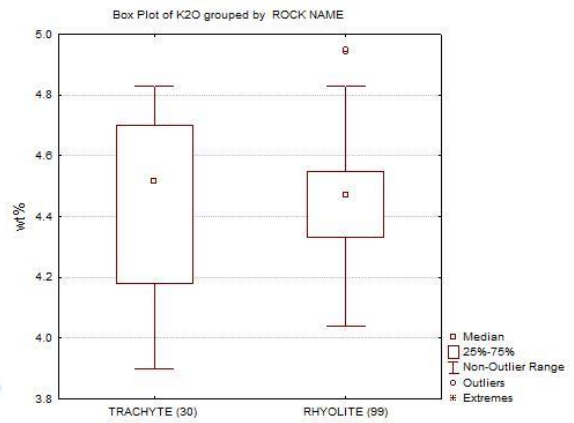
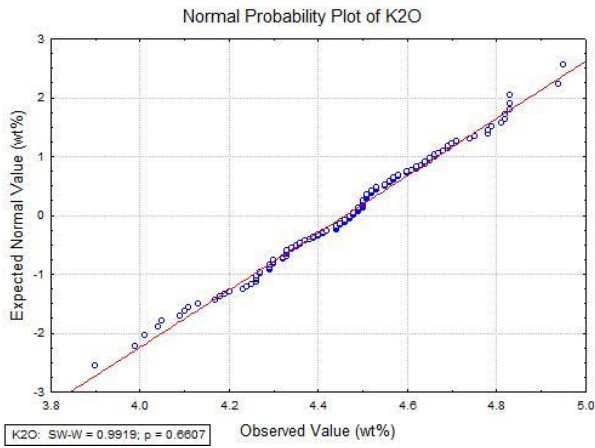
# SAPm



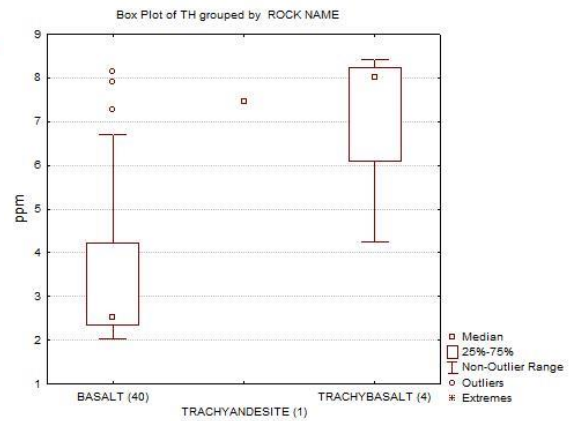
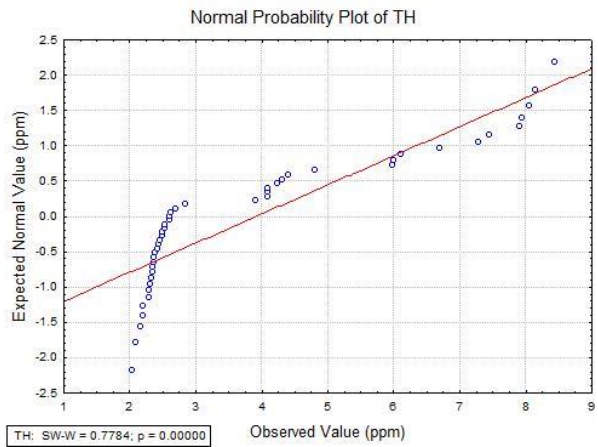
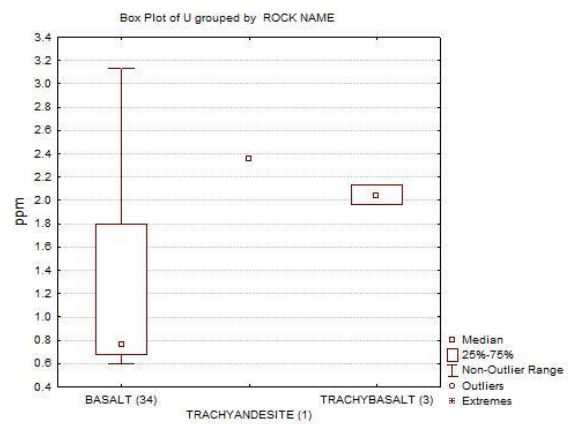
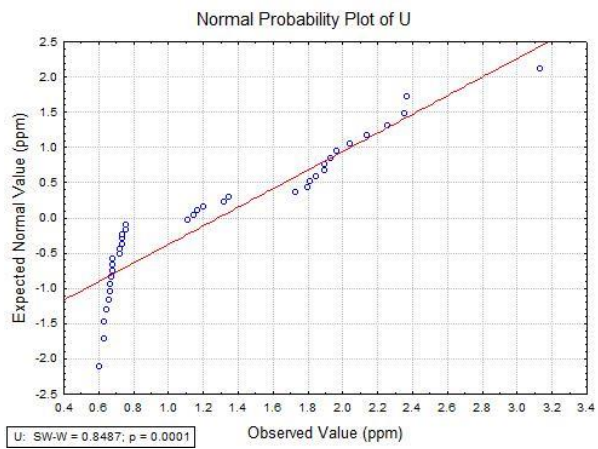
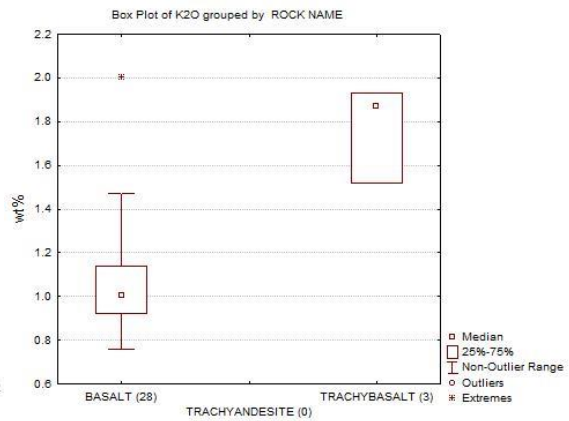
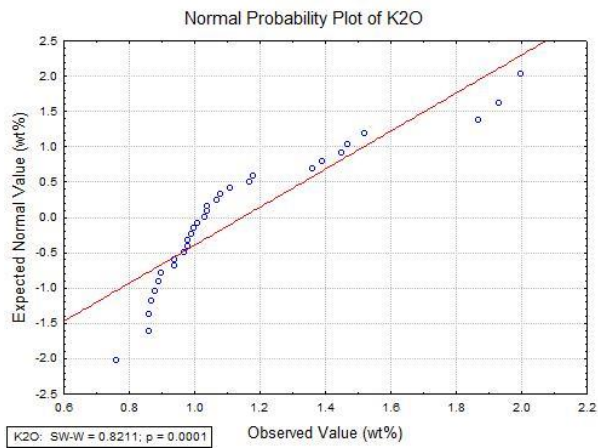
# CAP



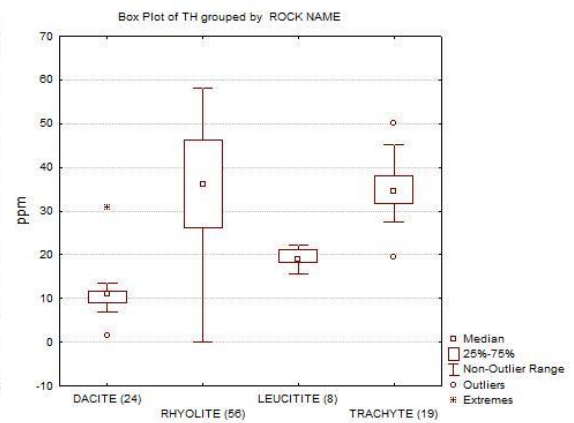
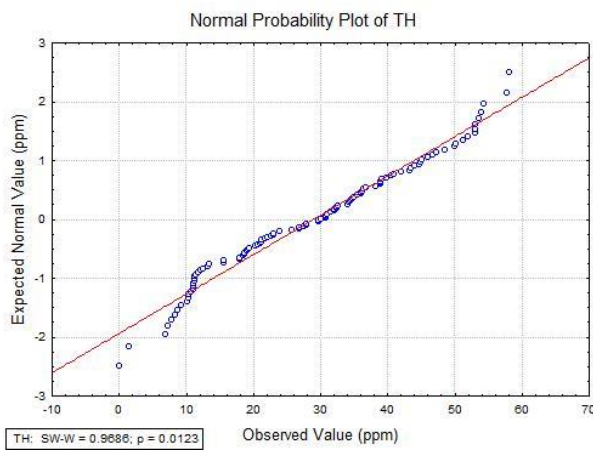
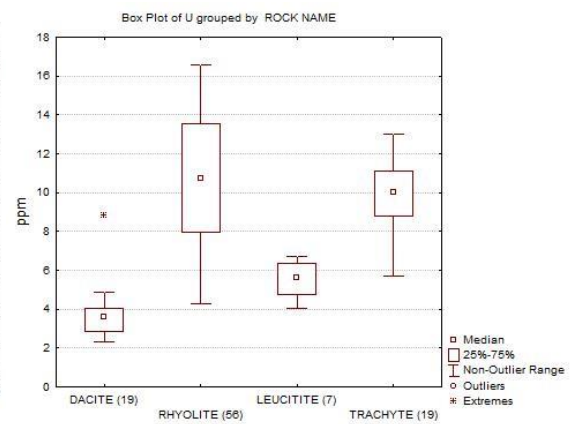
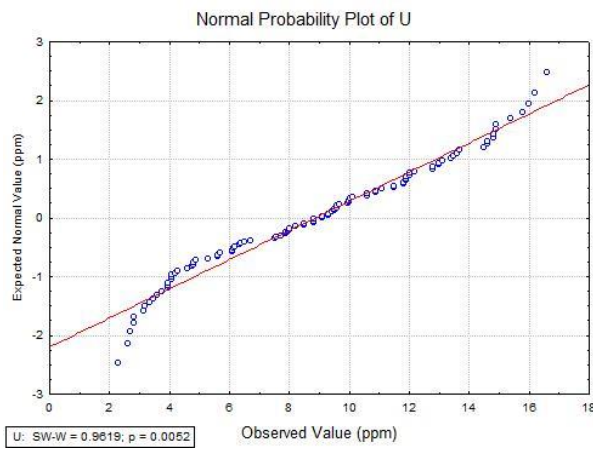
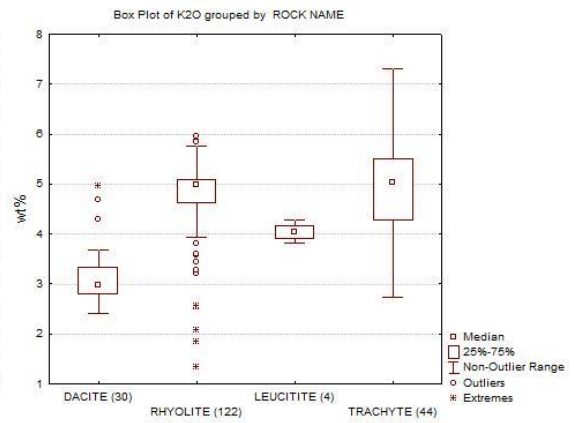
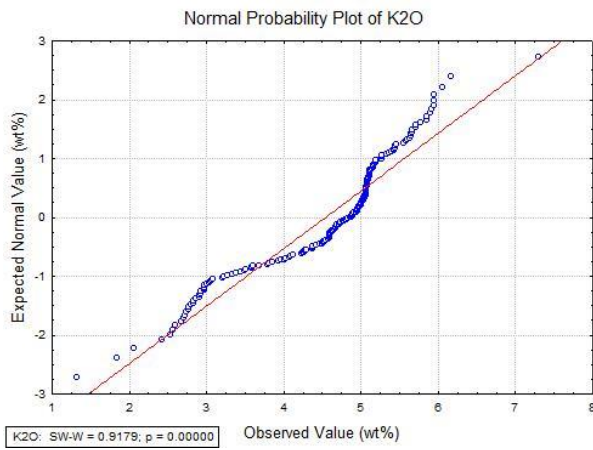
# SSDf



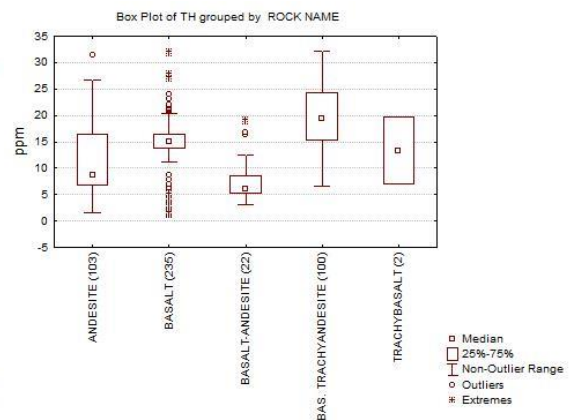
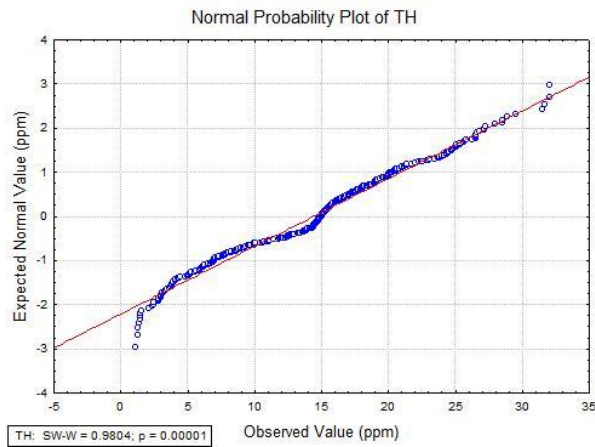
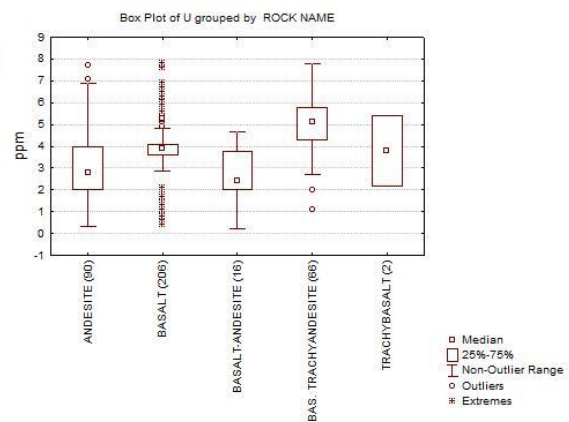
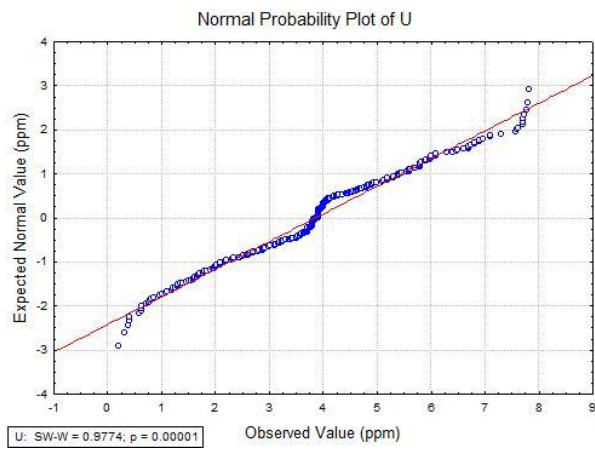
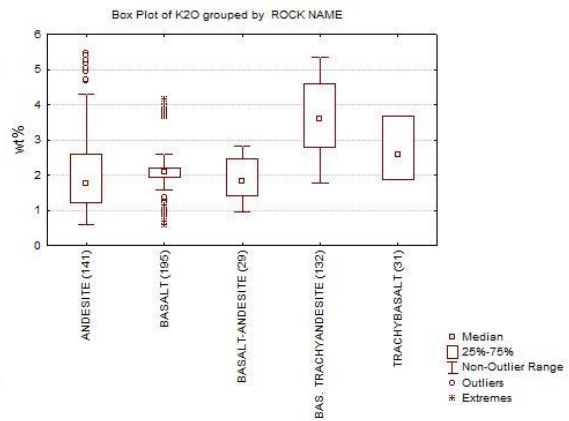
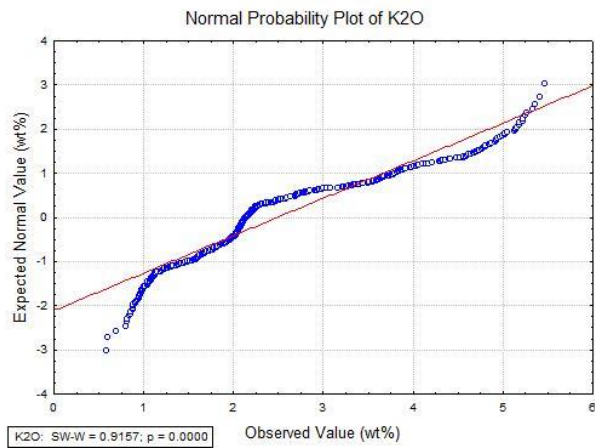
# SSDm



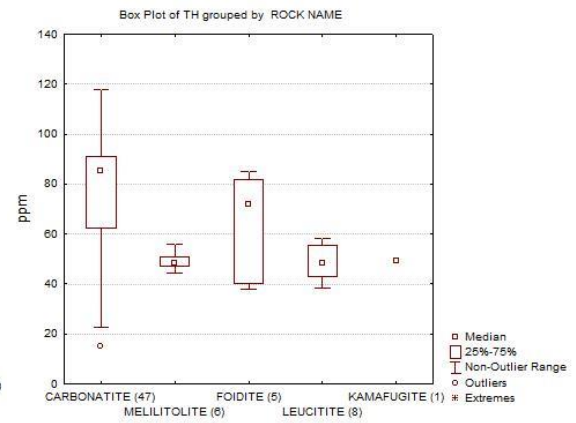
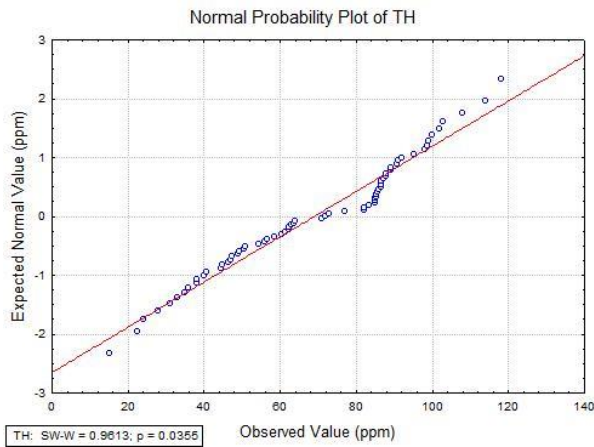
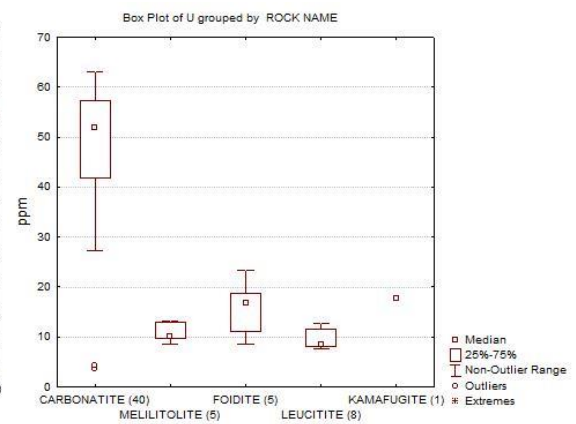
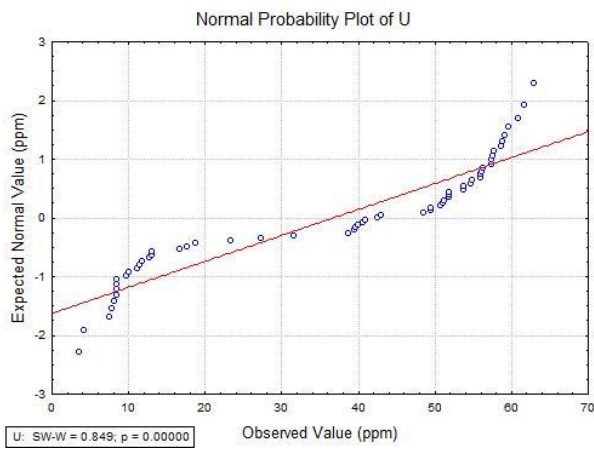
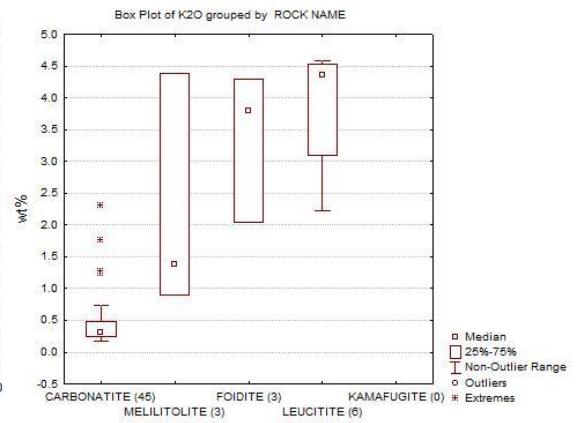
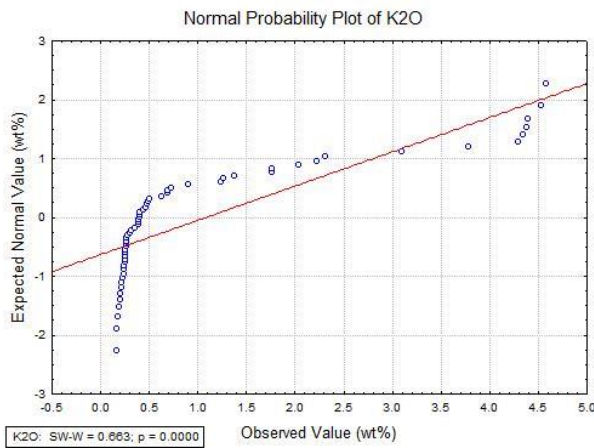
# AEPf



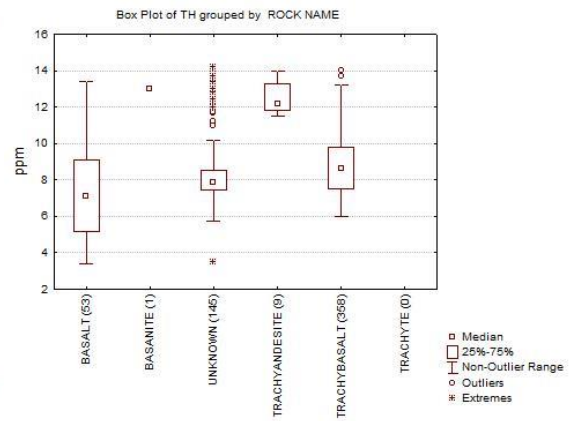
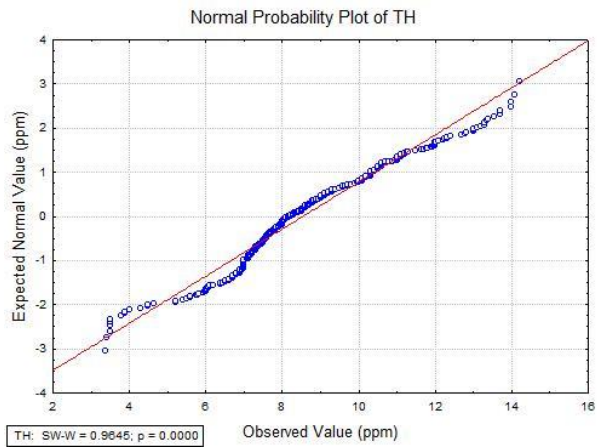
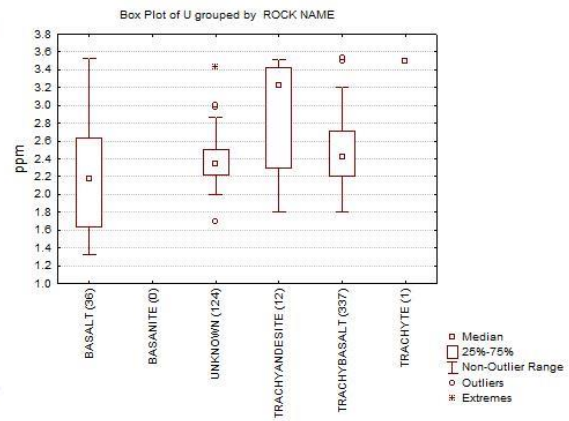
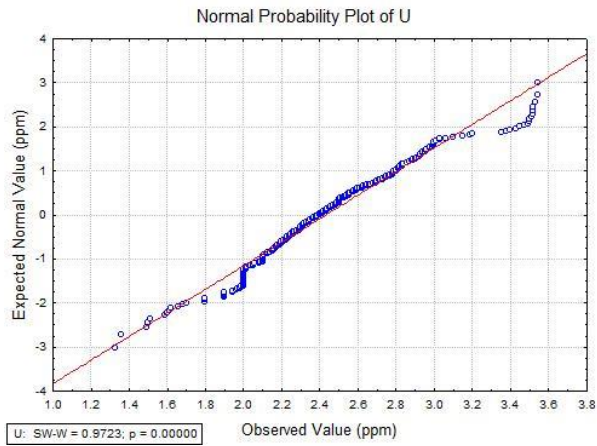
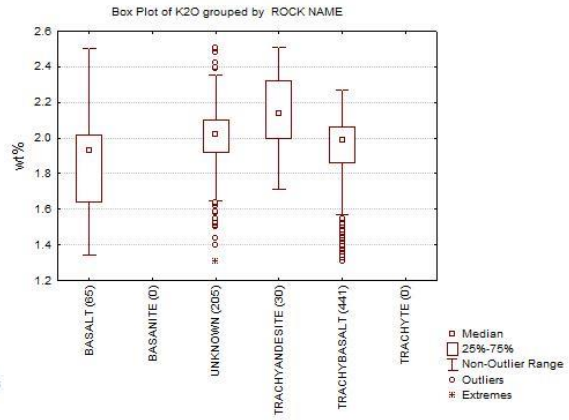
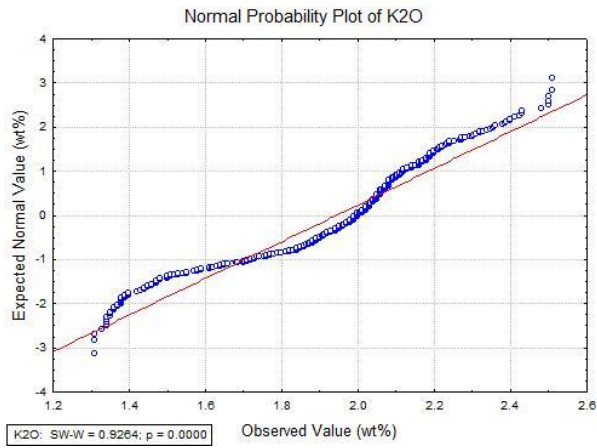
# AEPm



# MVP

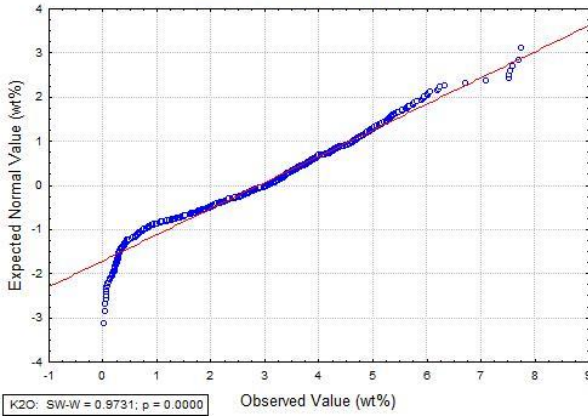


# SIP

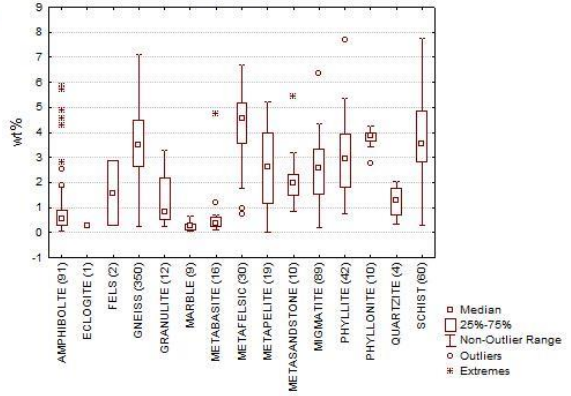


PM

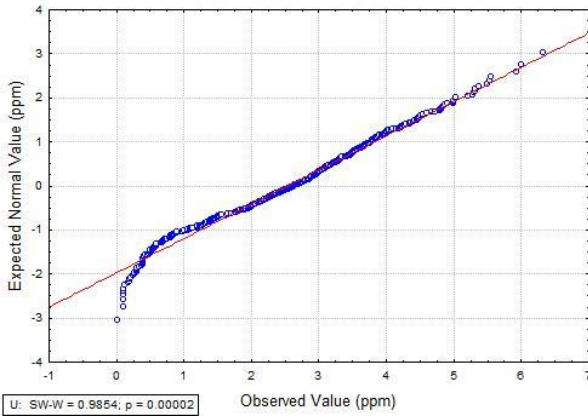
Normal Probability Plot of K2O



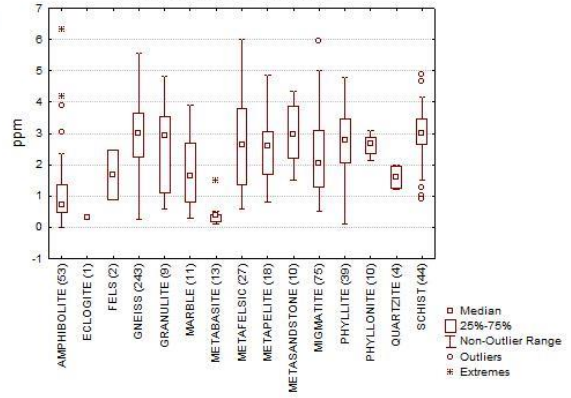
Box Plot of K2O grouped by ROCK NAME



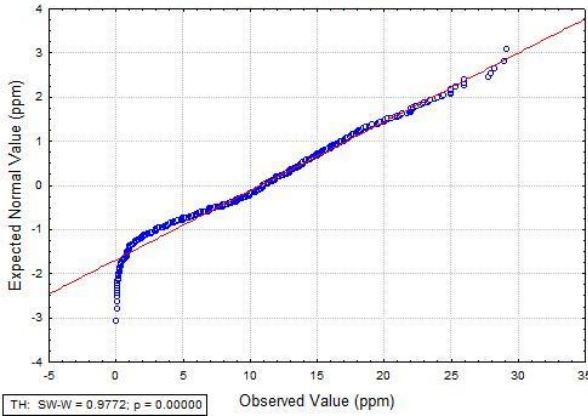
Normal Probability Plot of U



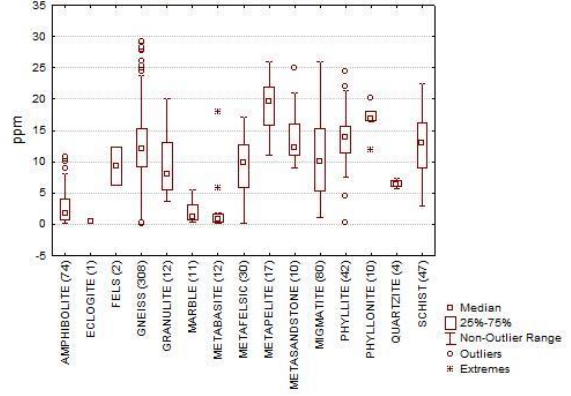
Box Plot of U grouped by ROCK NAME



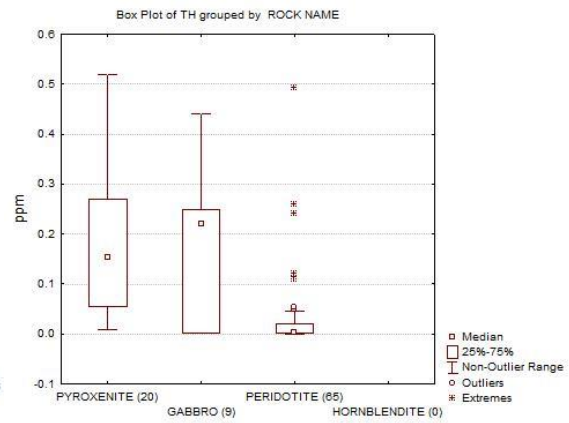
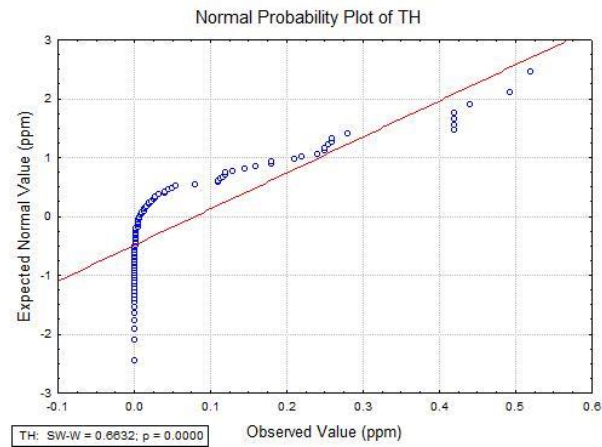
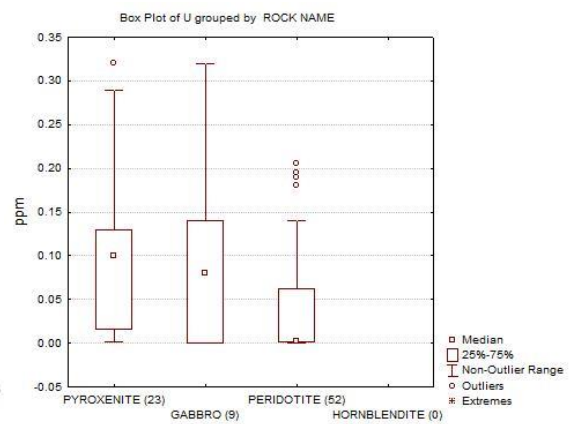
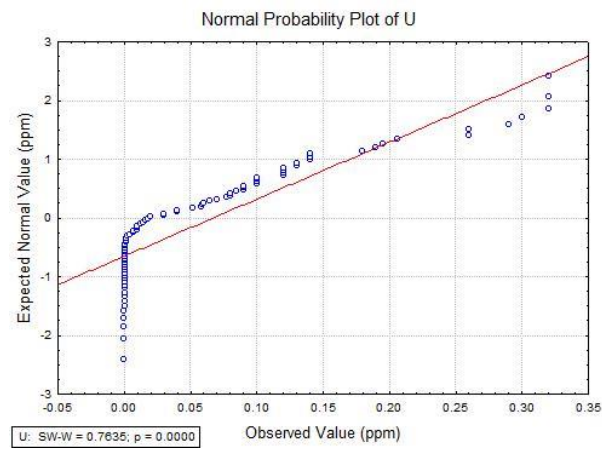
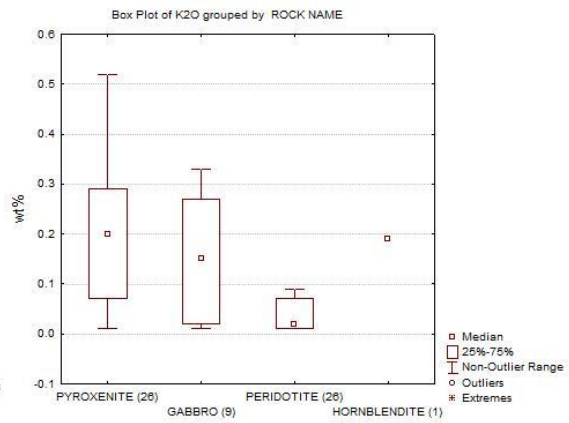
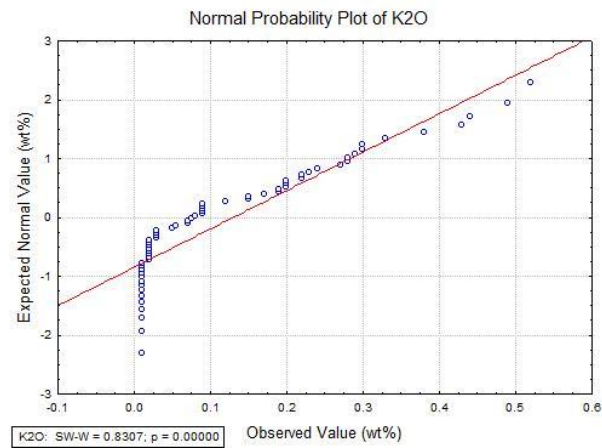
Normal Probability Plot of TH



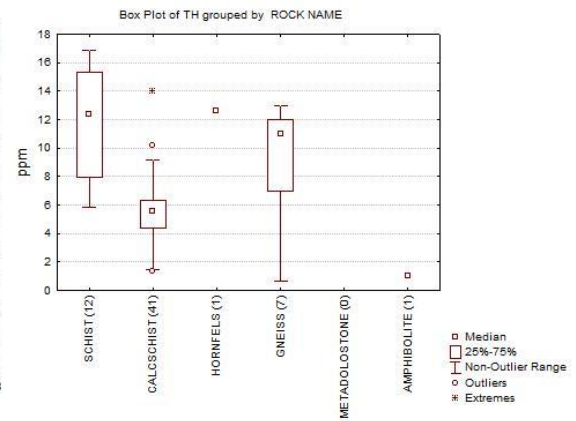
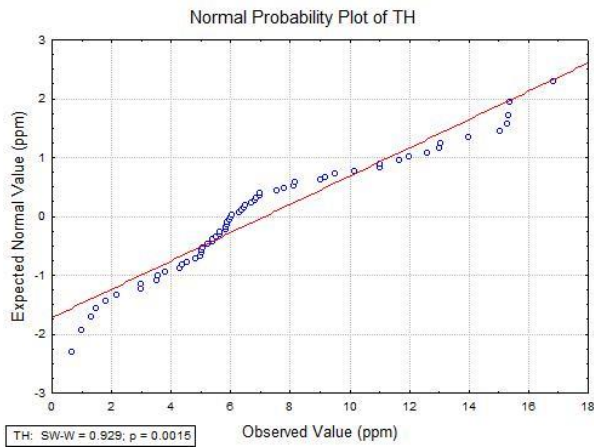
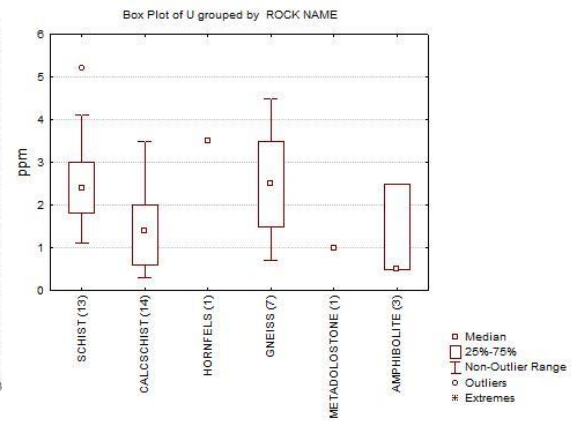
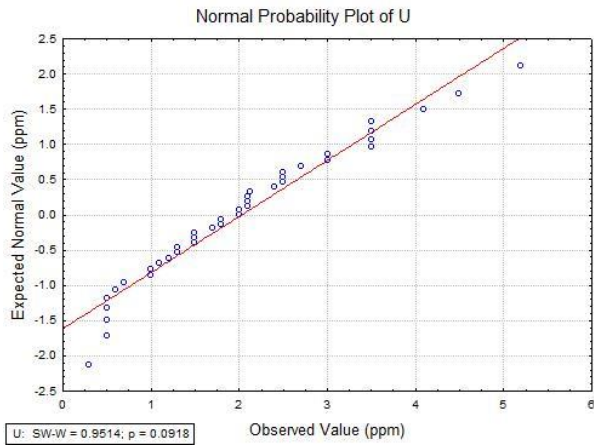
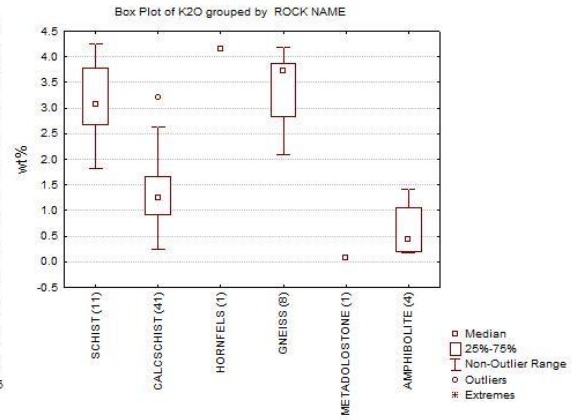
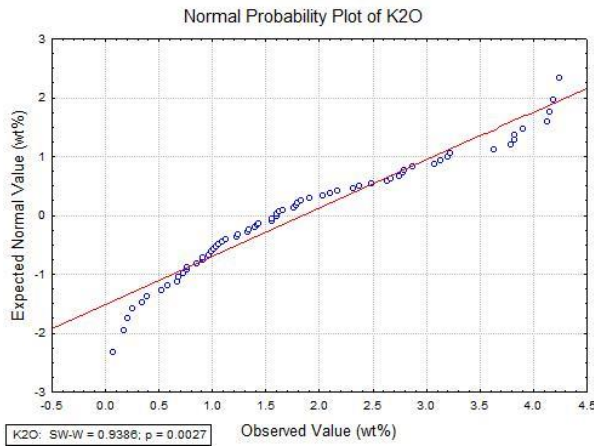
Box Plot of TH grouped by ROCK NAME



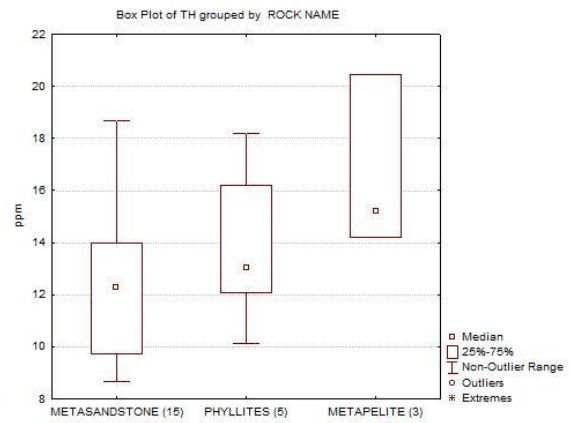
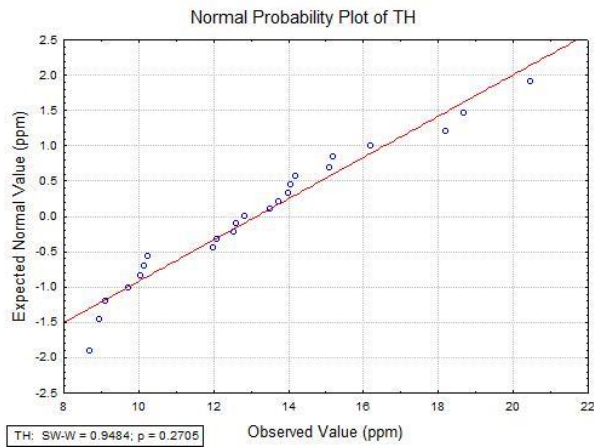
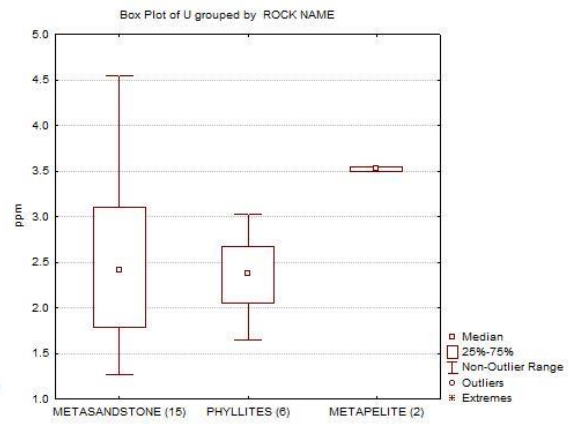
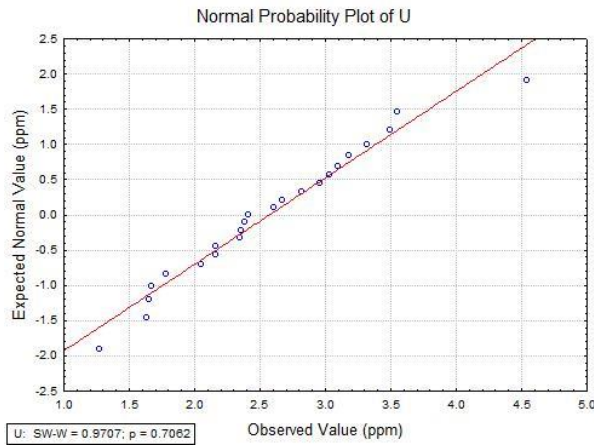
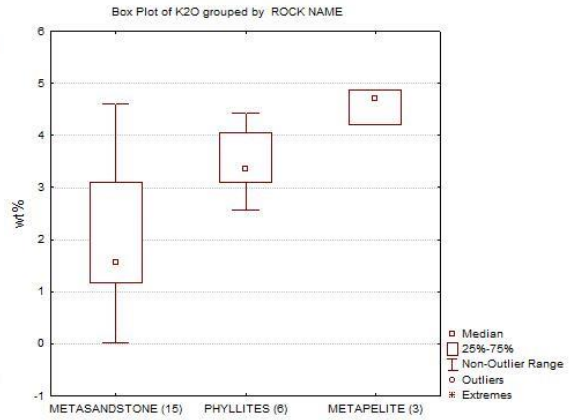
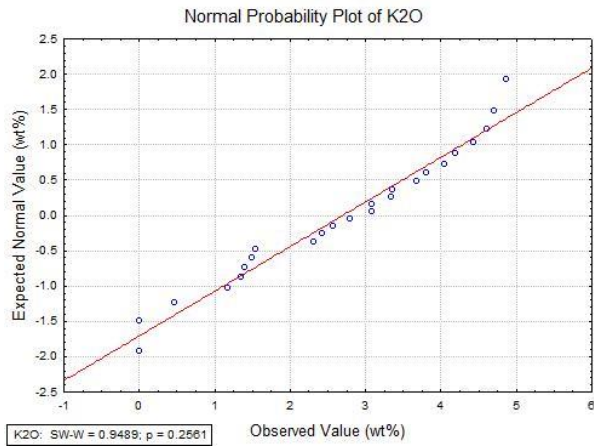
# UM



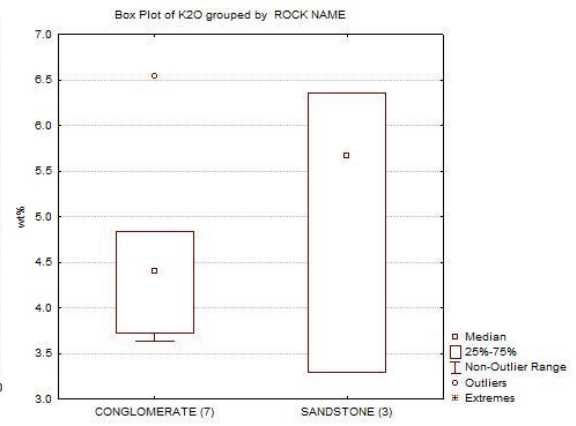
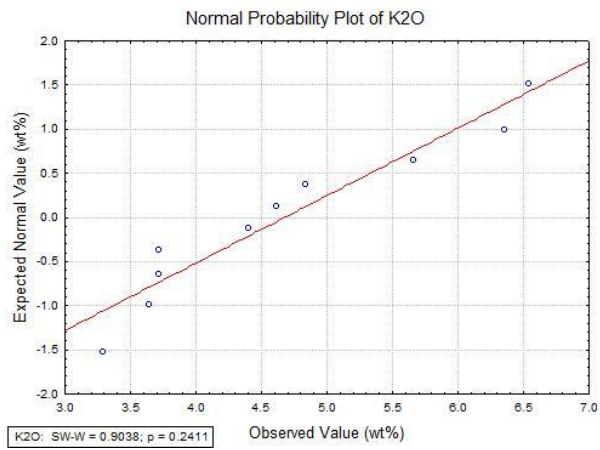
TM



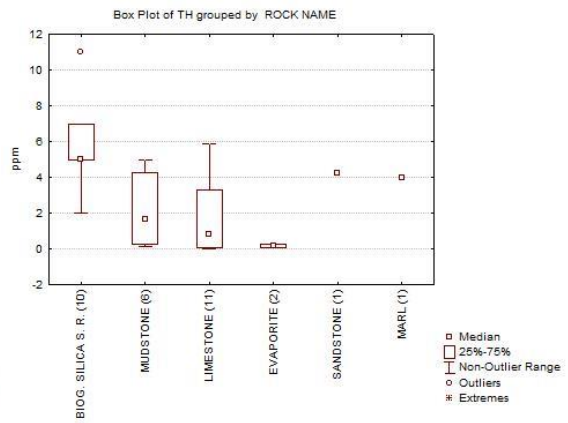
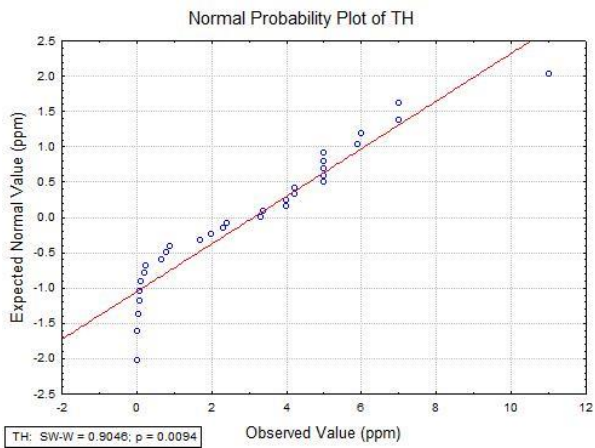
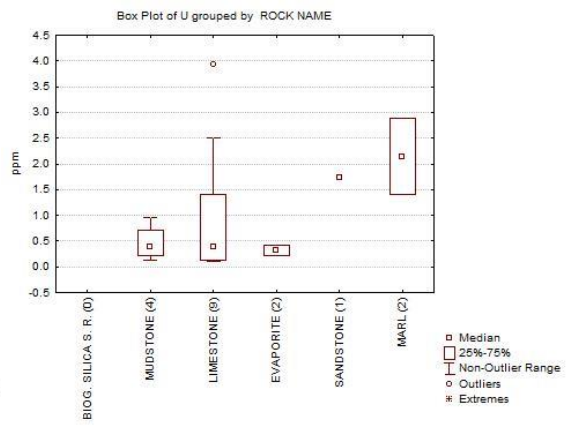
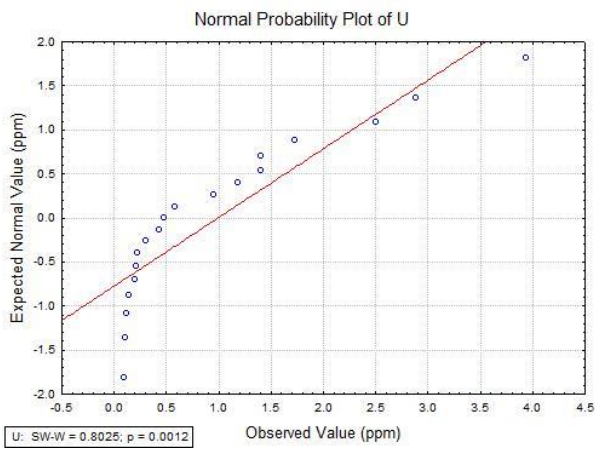
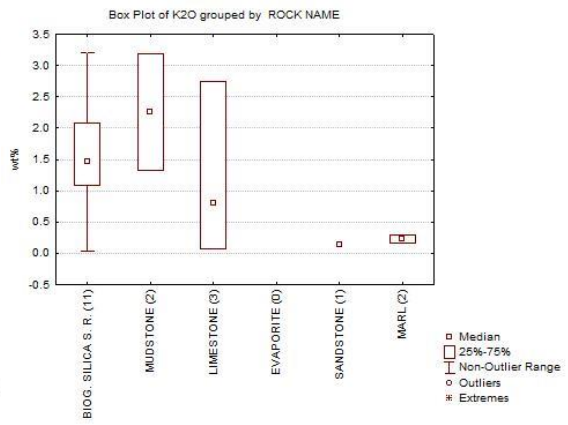
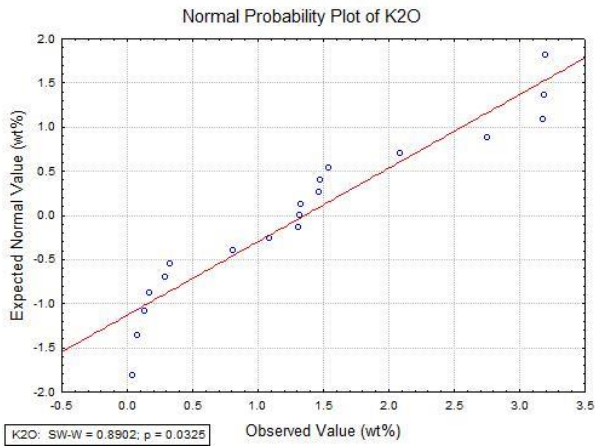
# COS



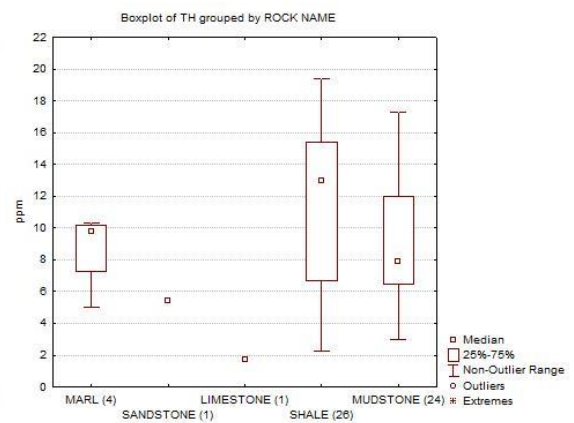
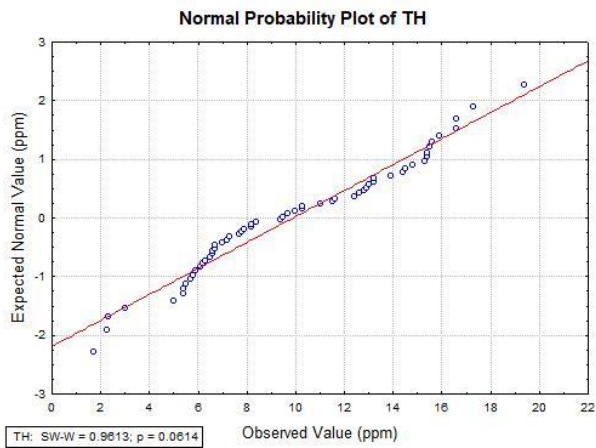
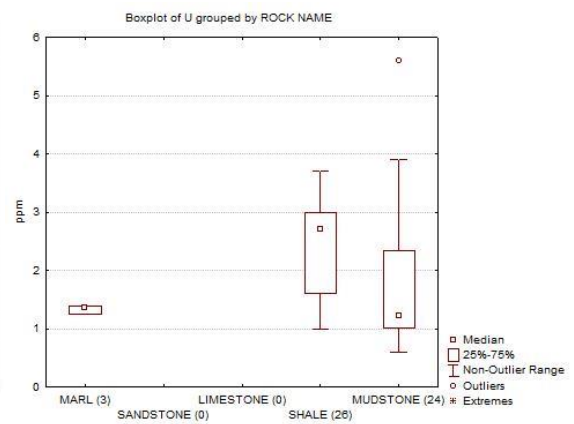
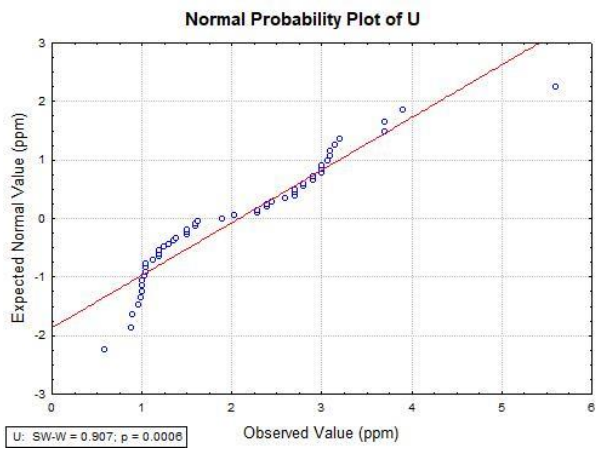
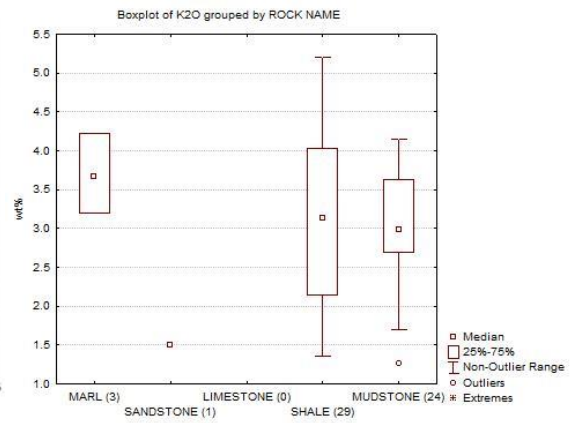
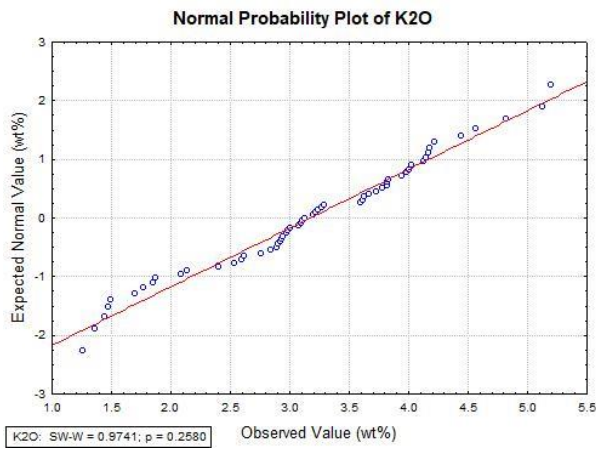
# DCPS



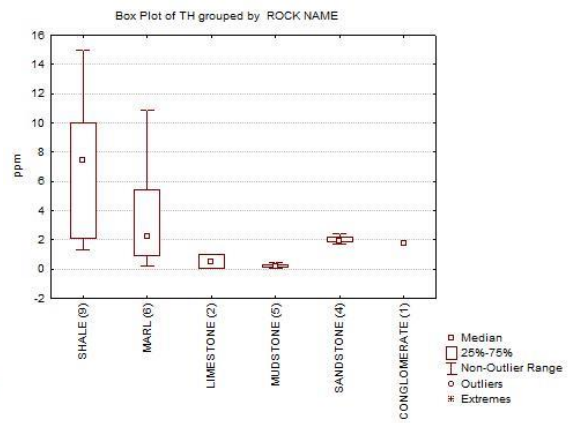
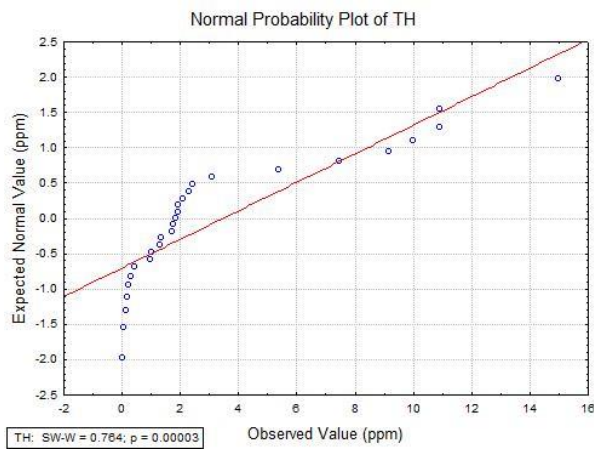
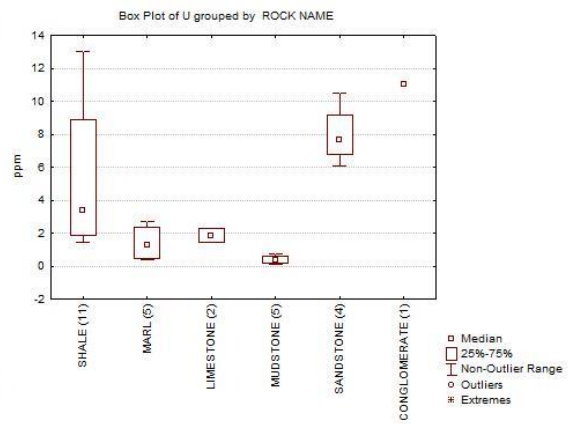
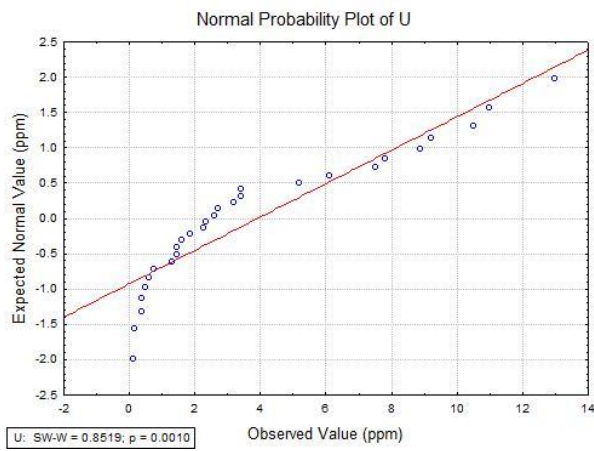
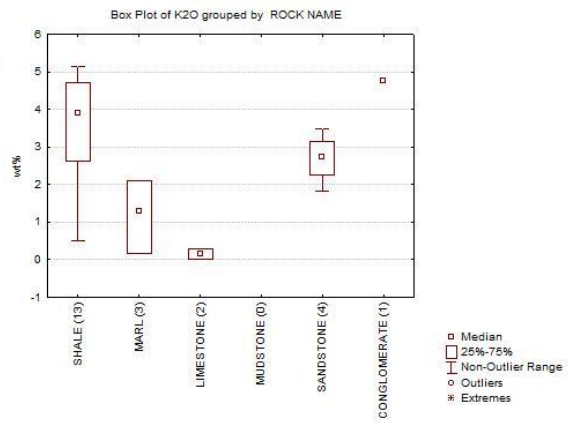
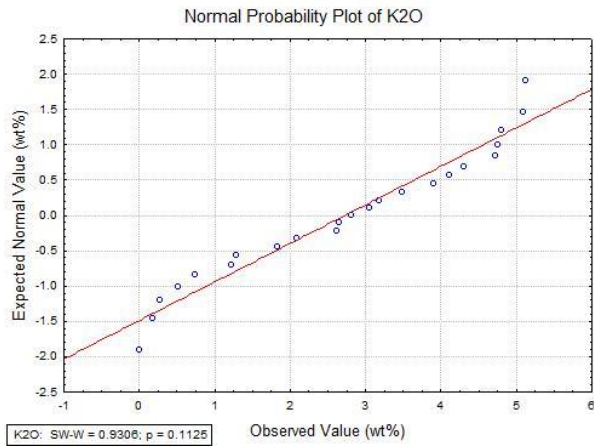
# MC



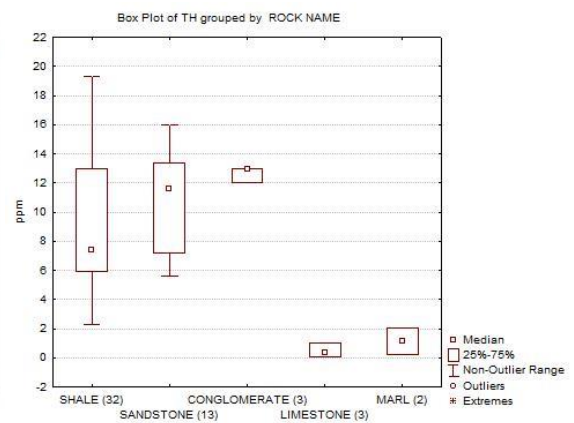
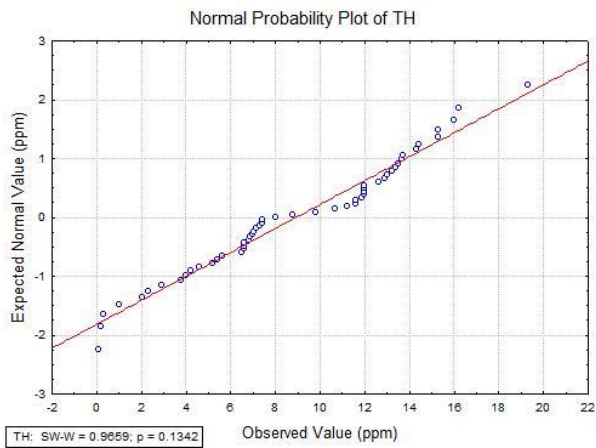
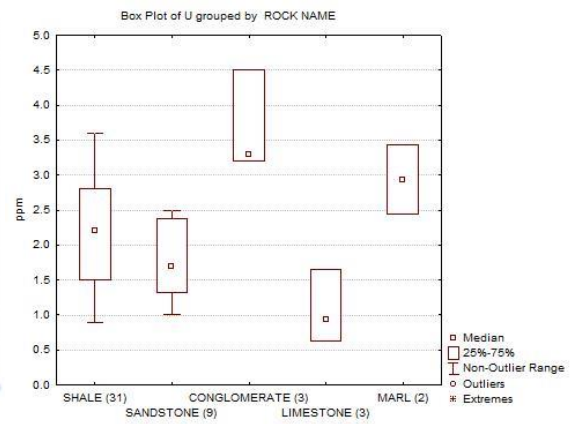
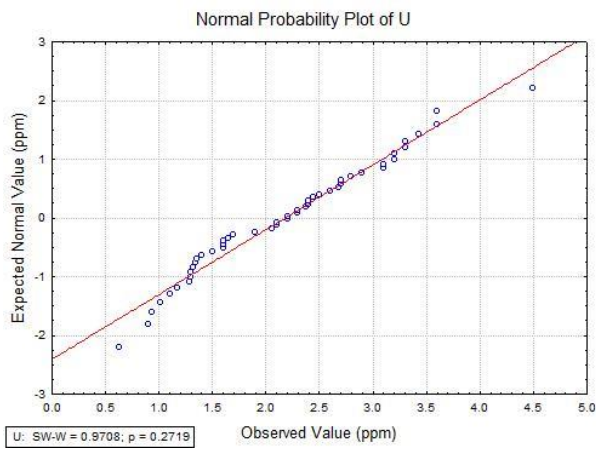
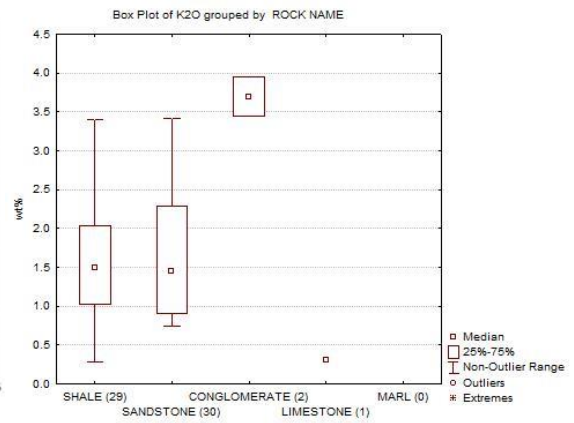
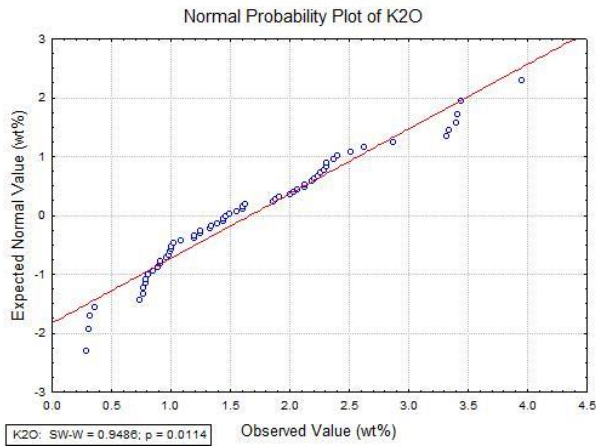
# CdB



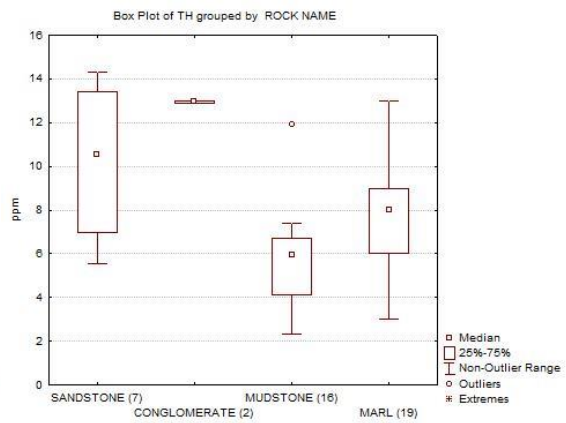
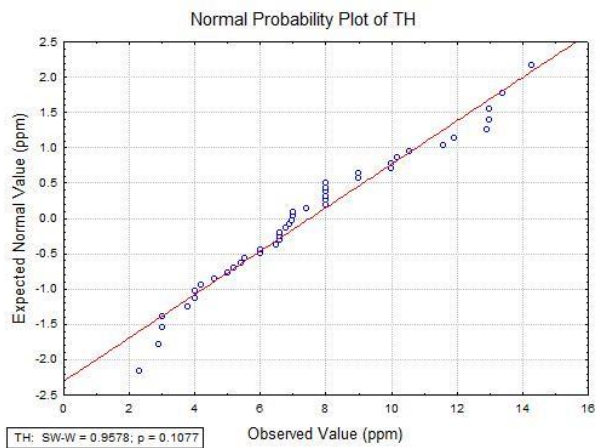
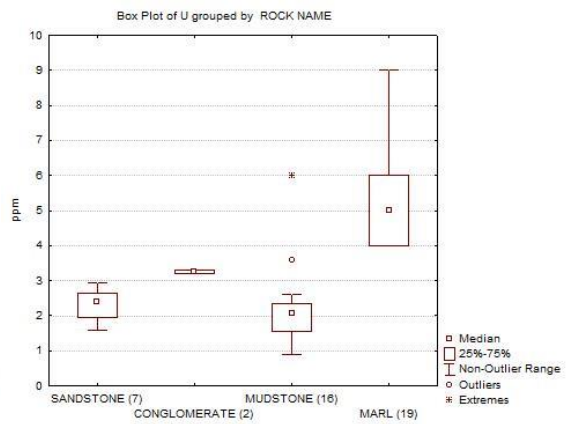
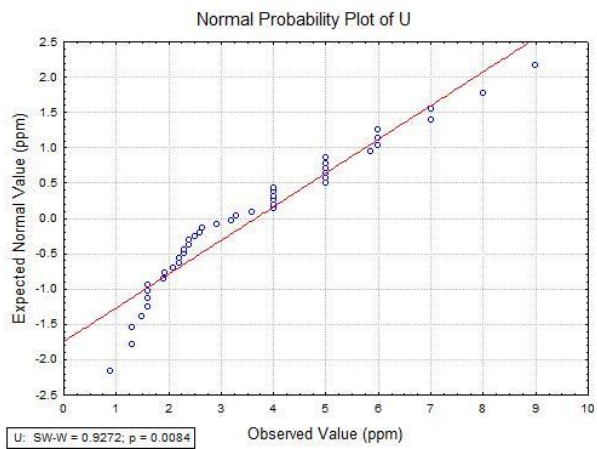
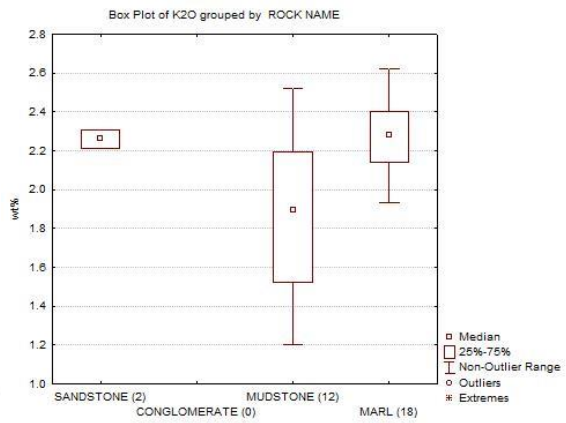
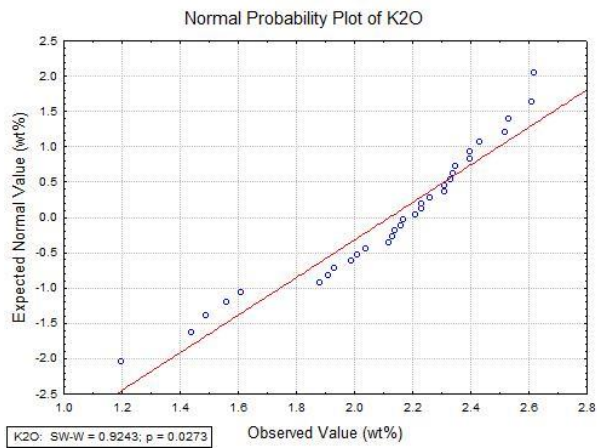
# LCPS



# EOMS



# ME



# PLS

